Retrospective Theses and Dissertations

Iowa State University Capstones, Theses and Dissertations

2008

A static analysis of maximum wind penetration in Iowa and a dynamic assessment of frequency response in wind turbine types

Eknath Vittal
Iowa State University

Follow this and additional works at: https://lib.dr.iastate.edu/rtd

Part of the Electrical and Electronics Commons, Energy Systems Commons, Oil, Gas, and Energy Commons, and the Power and Energy Commons

Recommended Citation

A static analysis of maximum wind penetration in Iowa and a dynamic assessment of frequency response in wind turbine types

by

Eknath Vittal

A thesis submitted to the graduate faculty

in partial fulfillment of the requirements for the degree of

MASTER OF SCIENCE

Major: Electrical Engineering

Program of Study Committee:
James McCalley, Co-major Professor
Venkataramana Ajjarapu, Co-major Professor
Fred Haan

Iowa State University

Ames, Iowa

2008

UMI Number: 1453053

Copyright 2008 by
Vittal, Eknath

All rights reserved.

UMI®

TABLE OF CONTENTS

CHAPTER 1: INTRODUCTION

As the energy industry moves into the 21st century the use and research into renewable resources has expanded significantly. Whether it is wind, biomass, or solar, the industry is seeking ways to breakthrough and integrate the newest technologies into their power systems. Wind energy, in particular, has seen significant expansion since the 1980's, with generating capability of wind turbines increasing dramatically from 50 kW to nearly 5 MW presently. Currently, the United States has over 11,699 MW of installed wind generation spread across the country with 932 MW installed in Iowa. As the price fuel and environmental concerns grow, wind generation has proven to be an efficient and fiscally sound alternative for the energy industry.

Seeking to introduce larger levels of wind generation in the Iowa electricity system, the goal of this thesis was to:

- First, determine the maximum wind penetration level of the existing transmission system in Iowa based on thermal loading limitations.
- Second, identify effects of increased wind penetration on system frequency response.

This integration process is broken down into six chapters that provide a systematic approach to determining the maximum wind penetration level in an existing transmission system. Chapters 2 and 3 discuss the static issues and identification of regions that are suitable for the integration of new wind generation in order to determine a maximum wind penetration level. The term "static" is used to refer steady-state (i.e., power-flow based) reliability criteria that are necessary for transmission planning. Specifically, Chapter 2 provides a literature review of the static analyses processes developed around the world as well as the criteria required within a region to support wind generation. By studying techniques developed outside of the United States, in particular Europe, where wind generation is already well established, the basic steps required to determine the maximum penetration level in an existing transmission system are described. The application of these steps to the Iowa electricity system are discussed in Chapter 3. Using the criteria established in Chapter 2, Chapter 3 describes how regions suitable for wind generation were identified

throughout Iowa and details the power flow simulations and resulting contingency analyses that were run in order to determine the initial maximum wind penetration level for the state.

In order to achieve the second goal set forth in this thesis, the dynamic characteristics of wind turbines needed to be study. As a result, Chapter 4 examined the modeling concepts of wind turbines necessary to represent wind farms in time domain simulations. It focused on the control systems and generator modeling concepts associated with the doubly-fed induction generator (DFIG) and the fixed speed generator (FSG) wind turbine. Chapter 5 detailed the issues associated with system frequency response and using the modeling concepts from Chapter 4, provided a series of dynamic simulations that showed the effects of wind generation on system frequency. In particular Chapter 5 described the effects on a power system's frequency response to a loss of generation event as the penetration level of wind generation increased from 15% to 30% within the system.

Next, Chapter 6 described the effects of these penetration levels on a system's dynamic voltage stability through another series of dynamic simulations. The goal behind these simulations was to explore consequences of improving system frequency response and the effects it had on the dynamic voltage stability of the transmission system. In an ancillary effort, Chapter 6 also provided a brief assessment of two software platforms, PSS/E and Eurostag, and their ability to model and simulate power systems with wind generation. Finally, Chapter 7 will conclude this thesis and examine the future prospects of interconnecting wind into the Iowa power system.

CHAPTER 2: LITERATURE REVIEW – SITING AND STATIC APPROACHES

This section will present a review of the materials pertinent to determining the maximum wind penetration of a region. It will examine the characteristics and features that determine a region's ability to support wind generation and the different analysis methods that help in determining a maximum penetration level based on thermal limitations.

Wind Speed Distribution and Analysis

The first issue in integrating any level of wind generation into a power system is siting suitable locations for new wind farms. Due to the inherent variability of the resource, wind farm sites need to be planned very carefully. The first step in determining these locations is to compare the wind patterns with the seasonal loading trends of the selected region. This is first completed on a monthly average level. An example of this can be seen in the Figure 2.1. Prepared by E.ON.Netz for a study of wind integration into the German system [1], Figure 2.1, shows the relationship between seasonal wind speed variation and electric consumption.
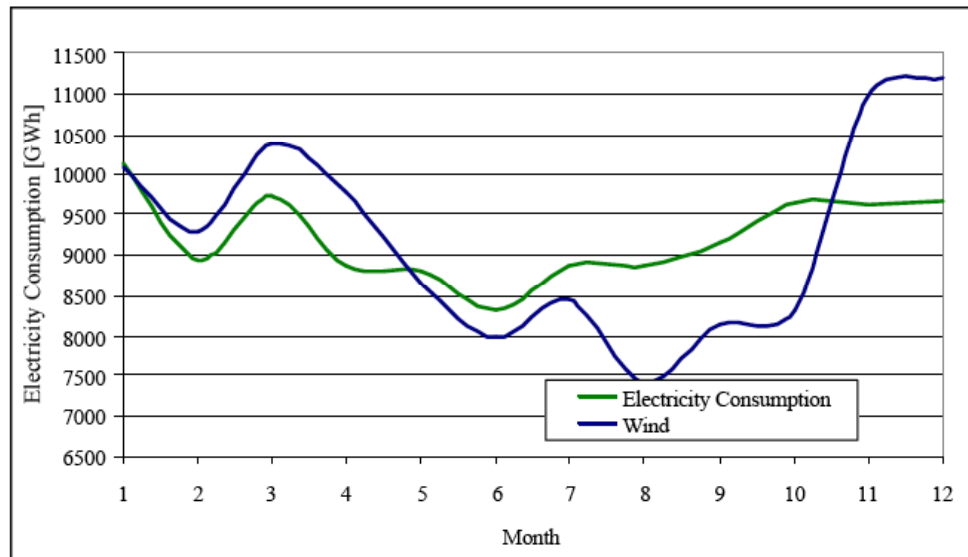
Figure 2.1: Monthly analysis of wind speed variation and electric consumption [2]

This allows for the selection of the study period and loading scenario. Selecting December as the study period would serve as a peak loading study. During this period, the

transmission system would be the most congested, as electrical consumption is at a maximum, and provide the allowable penetration level based on the constraints of the existing system. Using August would provide an alternative study, where wind speeds are at a minimum and the loading is less. This study would yield the necessary level of wind penetration to support the electrical consumption level of the region. The selection of the loading scenario is crucial in the development of a study case. Based on this selection, decisions on the determining appropriate locations for new wind farms can begin.

By conducting a detailed examination of the average wind speeds of a region, appropriate sites for wind farms can be selected. Studying wind speeds is not only essential to the location determination process, but when economics and market issues are discussed, the forecasting of wind speeds is a crucial element in the day-ahead and planning markets [2]. A good example of detailed wind forecasting is seen in the 2006 Minnesota Wind Integration Study Final Report. By synthesizing three years of data from, 2003-2005, the study was able to develop a map that identified the most favorable sites for new wind farms. The results of this process can be seen in Figure 2.2. By assessing the capacity factor and the ratio of mean power production versus installed capacity of each county the study was able to determine a geographically beneficial dispersion of wind farm sites in the state. In particular this selection was based on three criteria:

- The presence of existing wind farms in favorable locations
- Proposed locations of future wind farms already in development
- Favorable locations for new wind farms based on the most beneficial geographic locations
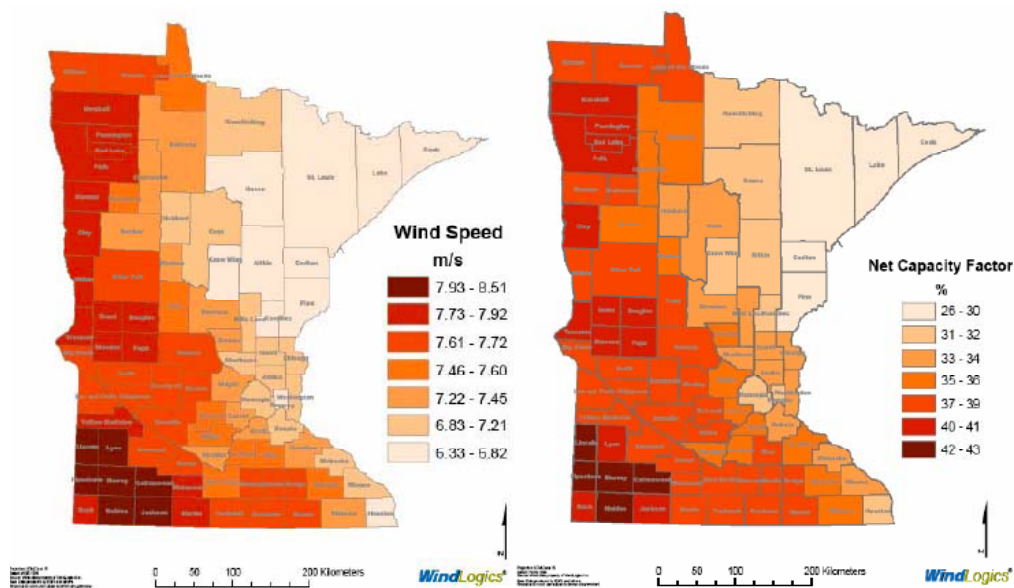
Figure 2.2. Wind distribution plots for the Minnesota Wind Integration Study [2]

The decision of site is not only based on looking at the average speed of the region, but needs to broken down further and examined on a diurnal basis. A site should not only have high average wind speeds, but should trend with daily electrical consumption. This is an important factor in determining a site's viability as a location to support wind generation. It is desirable to have wind farms produce power at times when consumption levels are higher. This is to maximum the use of the wind energy when it is produced. Figure 2.3, provides an example of a diurnal study once again from the E.ON Netz study of the German system.
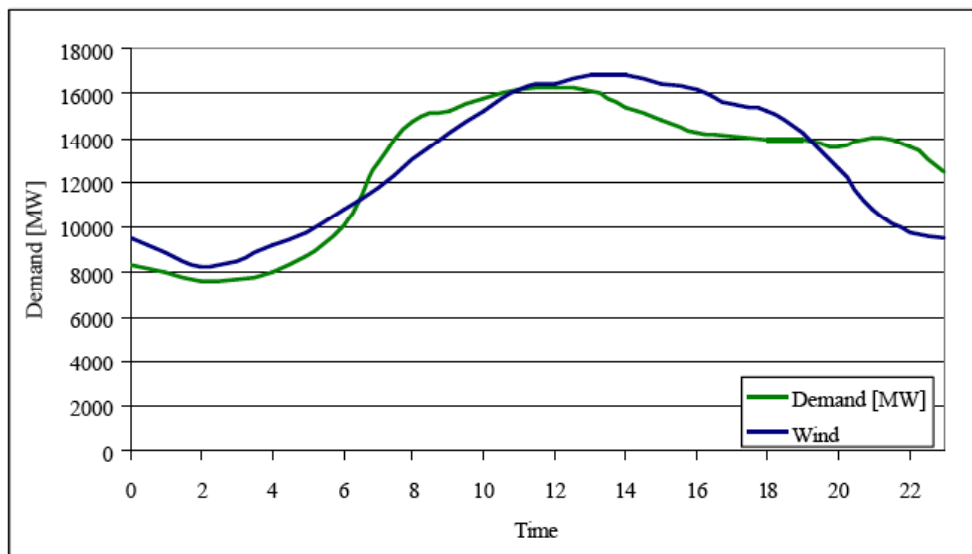
Figure 2.3. Diurnal comparison of wind speeds and electrical consumption [2]

As seen in Figure 2.3, the trends of the proposed site follow the demand curve of the region fairly closely. Completing such studies will help in determining a site's potential to support a wind farm. By taking all the necessary steps to conduct a complete and thorough wind study, the next step in integrating wind into the power system can begin.

Interconnection to the Grid

The ability of a site to sufficiently accommodate wind generation not only depends on wind speeds but its ability to interconnect to the transmission system. The entity installing the wind generation must decide the most efficient method to integrate the new generation into the system including the ability to increase the capacity of the transmission system, or need to install new generation based on the limits of the existing transmission system. Included in this decision will be the interconnection voltage level. If a utility is planning to export the wind generation it will be desirable to interconnect at relatively high voltages, however if it chooses to utilize the new generation within the system, interconnecting at lower voltages may be beneficial.

Several studies have been completed worldwide at interconnecting wind generation at various voltage levels. Ireland has large levels of wind energy connected at the 110 kV level and below [1]. This is due to the small size of the country and little need to transport power

over long distances. Also, a key issue in the addition of wind generation at this level is a policy adopted in the study that wind interconnections are not required to be "firm", i.e., in the event of a fault, wind generation can be dropped from the system. Ireland avoids the issue of system reinforcement through the use of this policy. Minnesota, citing a desire to send much of its generation to the east coast of the United State [2], performed its study by interconnecting at the extra high voltage level, 345 kV and above. Germany has approached wind integration in a very different manner. Between April 2002 and December 2003, Germany experienced a dramatic surge in the introduction of wind generation into its power system. During this period of 20 months, 3984 wind turbines with a capacity of 4686 MW, were installed into the medium-voltage, high-voltage, and extra-high-voltage systems throughout the country. This large level of integration required significant transmission reinforcement commitment from the utilities in the country [4]. This level of wind integration in such a short period of time is rare, and utilities are often reluctant to commit to the task of building expensive new transmission systems. As a result, it is often a goal to accommodate wind generation to the existing transmission system.

There are two critical issues that determine the capacity of an existing transmission system; the thermal and the voltage stability limitations of the system. The thermal limit of a transmission line is reached when the current flowing in the line begins to exceed the manufacturer ratings and the material begins to soften. The thermal limit is not only associated with the transmission line, but can be based on the limitations of other network components such as breakers or transformers. The lowest rating of the all equipment in the system is defined as the thermal rating of the system. As a result, the new generation added to the system must follow these limitations.

Voltage stability issues arise as a result of disturbances in a system. The system must maintain acceptable voltage levels at all buses in the system following a disturbance. Voltage instability could lead to loss of load or synchronism in the system. To avoid voltage instability, the level of power transmitted as well as the power factor of the system must be carefully monitored during the integration process.

Utilizing these two limits, a level for the transmission capacity of a system can be determined as per the following procedure [1][2][4][5][6][7].

1. Prepare a base case load flow model of the network.

2. Maintain appropriate interchange levels between regions. This means as the generation in the exporting region is increased by ΔP, the importing region must incur a decrease in generation by the same amount. This simulates a transfer of power between regions

3. Following the transfer of power, the new network conditions must satisfy the required security conditions. If it meets the security criteria, the change in power is added to the base case exchange value.

By following this pattern, a value for the maximum transmission capacity can be determined. This is a very general method, and will vary based on the regional security requirements and selection of the base case as discussed previously. However, tailoring the process to meet all of the security criteria, will allow for the determination of a maximum power injection level for a system. This value can be used as a limit during short-term studies for planning day-ahead forecasts of wind generation.

CHAPTER 3: STATIC ANALYSIS OF WIND INTEGRATION IN IOWA

Locating New Wind Farms in Iowa

To begin a discussion of wind generation potential in Iowa it is important to provide a brief summary of the current state of wind generation in the state. Based on data from the American Wind Energy Association, Iowa has 1273 MW of installed wind capacity, ranking behind Texas, California and Minnesota, as the fourth largest producer of wind energy in the country [3]. This is approximately a 3% penetration level for the state. As discussed earlier, one of the objectives of this project is to complete a static study to determine a maximum penetration level based on the constraints of the existing transmission system. The first step in determining this level is to identify where wind generation can be added to the state. The following section identifies sites with the highest potential to accommodate new generation throughout the state.

The concepts and techniques discussed in Chapter 2 provided a foundation to determine the maximum penetration level in Iowa. This first issue was to determine the appropriate loading situation, namely, whether to select system loading conditions corresponding to peak loading conditions or corresponding to peak wind generation levels. The first situation would correspond to summer loading scenario, while the latter would be a winter scenario when there are significantly higher wind speeds across the state. Figures 3.1 and 3.2, from the Iowa Energy Center [8], show the average wind speeds for the months of July and December. The green, yellow, orange, and red areas represent high average wind, from 15.7 mph to speeds greater than 19.0 mph. The blue, cyan, purple, and pink regions represent average wind speeds less than 15.7 mph.

Estimated Average July Wind Speeds
Typical average wind speeds on well exposed sites at 50 m above ground
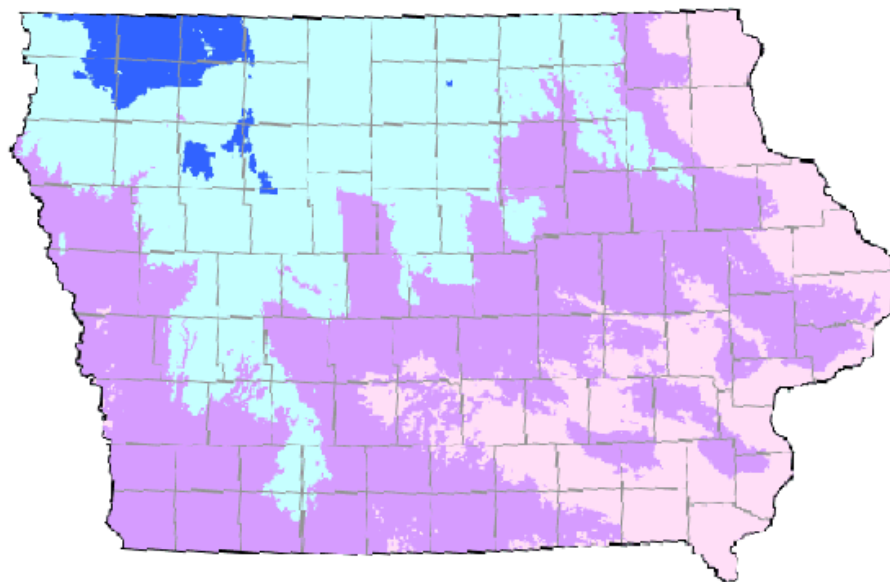
Figure 3.1: Average wind speeds in July [8]

Estimated Average December Wind Speeds
Typical average wind speeds on well exposed sites at 50 m above ground
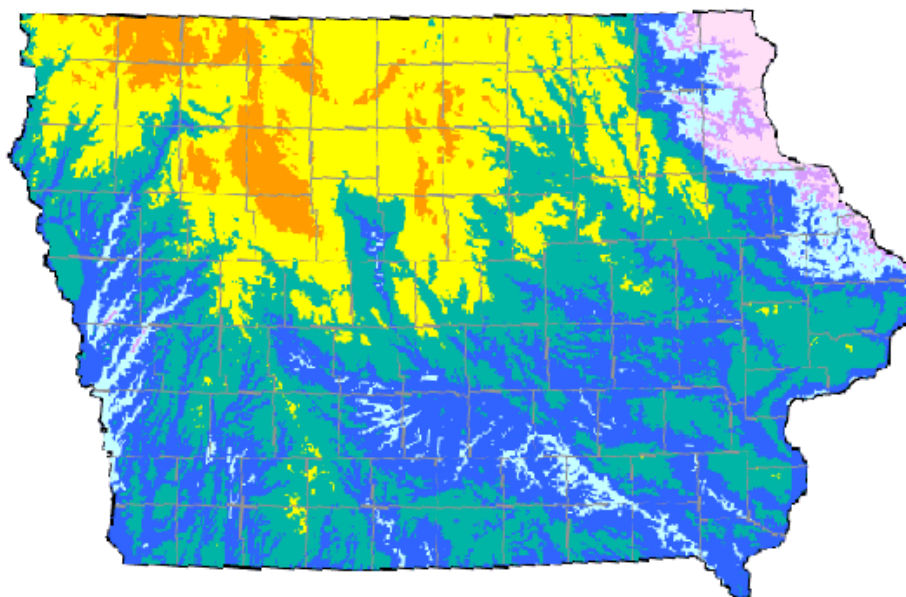
Figure 3.2: Average wind speeds in December [8]

From these maps it was concluded that the use a peak loading case that corresponds to a summer scenario would provide the most viable result for the maximum level of wind penetration. There are two reasons behind this selection: First, the transmission system is most stressed during the summer months, thus providing a more accurate result in terms of transmission capability. Secondly, although the average wind speeds are lower, high summer loads and high wind speeds can occur simultaneously. The diurnal wind speeds can be seen in Figure 3.3. As seen in the plot, wind speeds peak during the evening hours when loading levels are generally considered at maximum. To determine the average wind speeds a conversion was required. The data provided by the Iowa Energy Center, from weather stations in the study region, is gathered at an altitude of 50 m. In order to estimate the wind speeds at the standard turbine height of 80 the following conversion was used [9]:

$$Estimated\ Wind\ Speed = (Measured\ Wind\ Speed) * \left(\frac{Desired\ Height}{Measured\ Height} \right)^{.18} = (X\ m/s) * \left(\frac{80m}{50m} \right)^{.18} \quad (3.1)$$

Diurnal July Wind Speeds
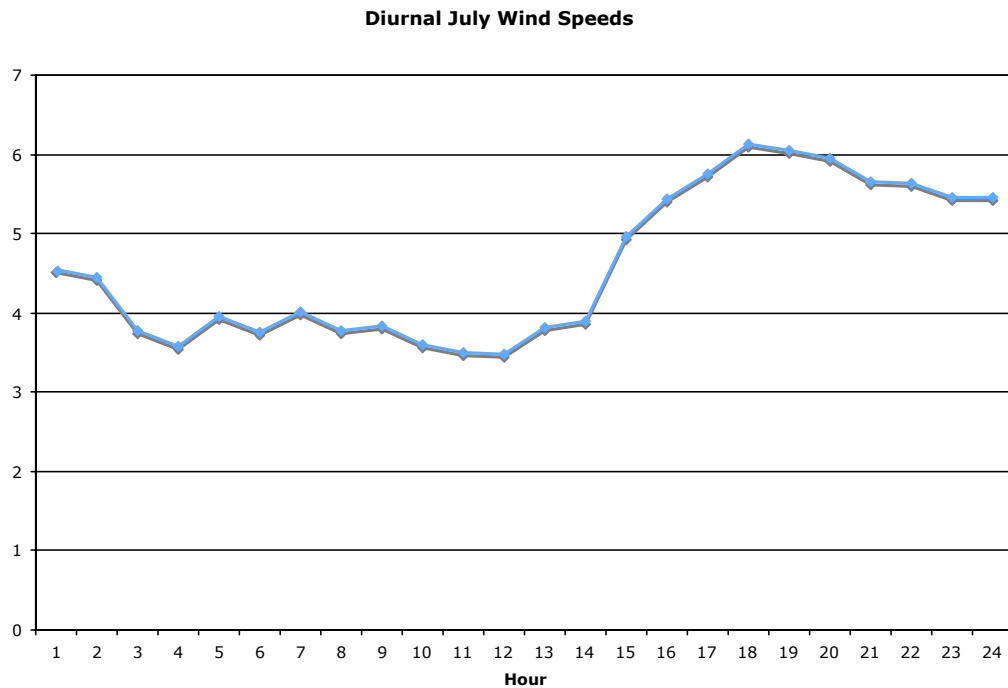
Figure 3.3: Diurnal July Wind Speeds

Based on these assumptions, a power flow case was provided by MidAmerican Energy (MEC) and Alliant Energy (AE). The case represents a summer 2008 peak case, with the following changes made by MEC:

- CB4 unit transmission, which is scheduled to be in service in 2007 has been added

- CB4 has been redispatched to its expected gross output, compensating by reducing peaking generation in the MEC areas to compensate

- The proposed Oak Grove substation was added on the southwest side of the Quad Cities

- The proposed Grimes substation was added on the northwest corner of Des Moines

- Central Iowa details were added, which have an important impact on wind generation placed there

The above changes are referred to as the MISO 2008 Base Case, characterized by the fact that it models expected wind penetration levels in 2008. The additional Iowa wind capacity was already modeled in the original MISO planning case, and totaled 819 MW and has been related back to the wind region-rankings. An additional 1065 MW of wind capacity was in the MISO queue at the time of this writing, but was not modeled in the case.

As observed from Figure 3.2, the highest average wind speeds are in the northwest region of the state which designated the study region for this project. To reduce the overall size of this region, further siting criteria were applied based on the proximity of the site to transmission. An important assumption was made at this point: It was decided that to maintain cost feasibility for the interconnecting utilities, MidAmerican and Alliant, all new wind generation would be connected at 69 kV and 161 kV lines and substations. However, this interconnection may be more cost effective for utilities wanting to use the new wind generation directly in their systems. To effectively transport large amounts of wind generation, interconnecting at 345 kV or higher may provide significant savings when sending power across the country. The main goal of connecting to the 69 kV and 161 kV was to maintain reliability in the existing transmission system with no transmission reinforcement.

To create a feasible study region the 69 kV up to 161 kV transmission one-line was overlaid on the average wind speed map seen in Figure 3.4. By assuming that any new wind generation would be located no further than 4 miles from an existing line, an 8 mile buffer was created around all transmission lines in the study area (see Figure 3.4). Then, by creating 20-mile intervals along all of the lines in the study area, 68 wind regions were created. The result of this process can be seen in Figure 3.5. The next step was to distinguish between regions in areas of similar average wind speed. To achieve this, the average elevation of a wind region was used as the critical criteria. The idea behind using elevation as a ranking methodology is that higher average elevation tends to provide a site with more consistent wind, as well as higher wind speeds. The results of this ranking process can be seen in Figure 3.6. It should be noted in Figure 3.6, sites colored red, orange, and yellow represent wind regions that show the highest potential to support new wind generation based on proximity to existing transmission, average wind speed, and elevation of the site. Sites colored cyan and blue represents sites that are still very desirable compared to the rest of the site, but do not show as much potential as those colored red, orange, and yellow.
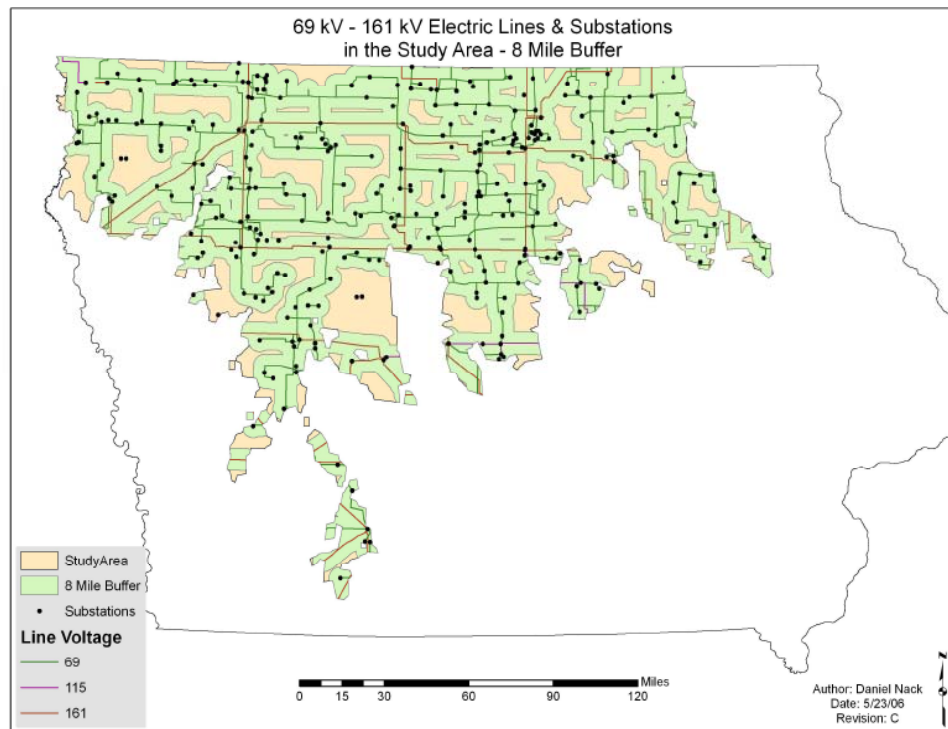
Figure 3.4: 69 kV – 161 kV Transmission with 8-mile buffer
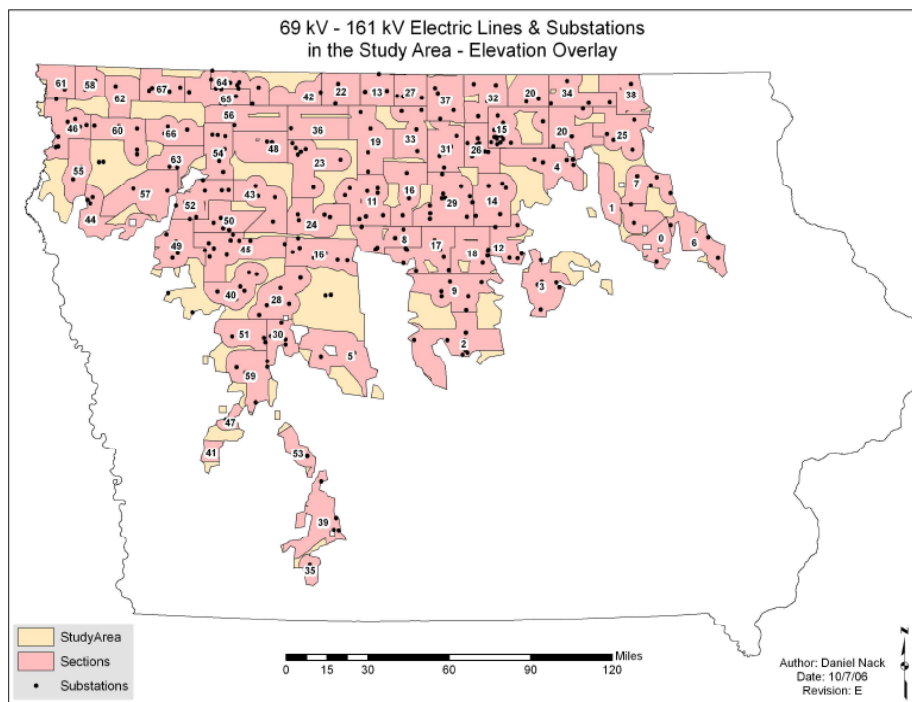
Figure 3.5: Transmission divided in 20-mile intervals
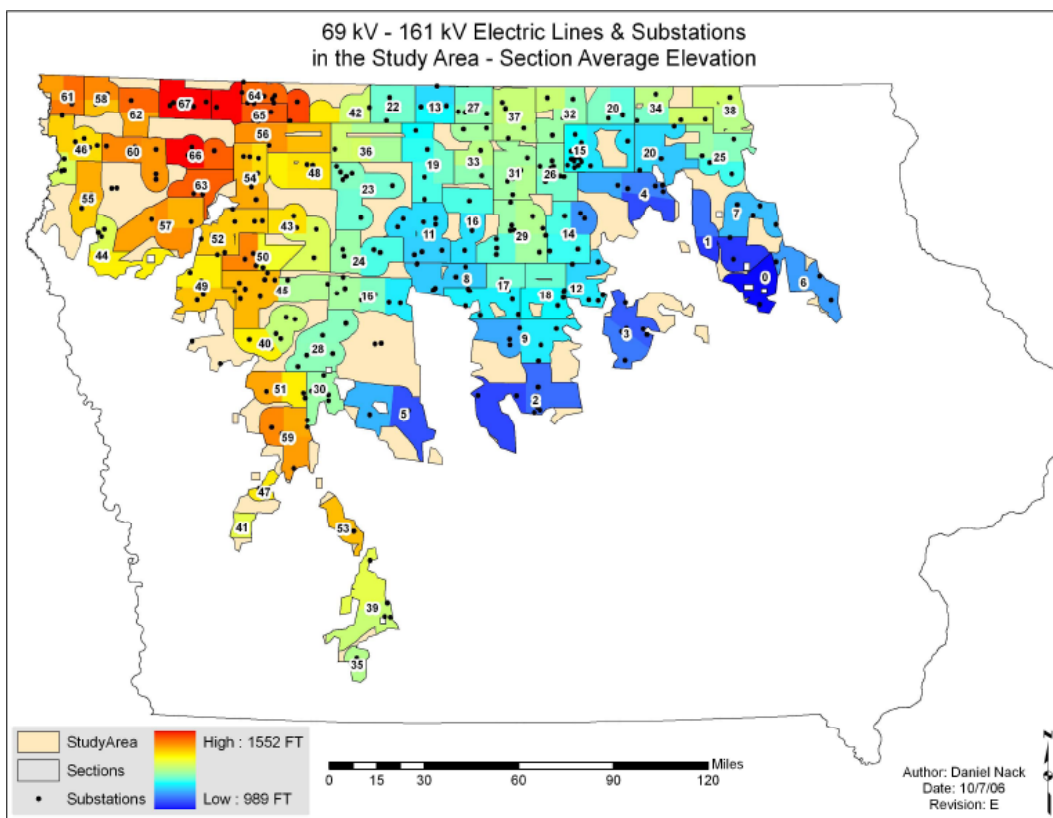
Figure 3.6: Fully ranked study region

Figure 3.6, became the basis of the static analysis and provided a systematic way to introduce wind generation into the state. The final issue addressed in the siting process was the spacing of turbines within a wind region. It was assumed that to maintain the viability of wind within a region, each turbine would require 60 acres of space to operate with full efficiency [10][11]. This factor does not play a role in determining the level of MW injection from each site, but rather limits generation based on the acreage available in each wind region.

Overall, this section developed a clear and systematic process for determining locations of viable wind generation sites. Using specific criteria, such as average wind speed, proximity to existing transmission, and average elevation a theoretical "queue" for adding generation to the power system was developed. Based on this "queue", any new generation can be studied using the power flow case provided by MEC and AE.

Substation Identification

Based on the results of the previous section a systematic power flow analysis was conducted to find the maximum allowable MW injection into the existing Iowa transmission system. The first step in this process was to identify substations within each of the 68 ranked wind regions and correlate them with the power flow file. This process was one of the most challenging steps in determining additional wind generation in the state. The only resources available to identify substations were PDF one-line files from MEC and AE, and each substation needed to be visually identified. However, these files often varied in scale and in particular, the naming of the substation. Abbreviations and full names differed from the one-lines to the power flow file making it extremely difficult to identify substations in a particular wind region. As a result, only 22 of the 68 wind regions and 44 substations were used in the static analysis.

Addition of New Generation

To add realistic data to the power flow file, in terms of reactive and active power, the choice of wind turbine was important. In the static study it was assumed that GE 1.5 sle

model turbines were used. This particular turbine is a doubly-fed induction machine model that allows the control of the production of reactive power, and effectively allows control of the power factor from a farm (the modeling and concepts behind this machine will be discussed later). This means that each individual turbine can be run at leading, lagging, or unity power factor [12]. In the static analysis it was assumed that the turbines .95 lagging, as a conservative estimate. Next, based on the active power of the farm the reactive power capability was determined using the following formula.

$$Qsub = Psub \tan\{\cos^{-1}(pf)\} \tag{3.2}$$

The next step in the process was to begin adjusting the power flow file to accommodate the new wind generation from the identified wind regions while maintaining the power balance for the entire system. The data provided by MEC and AE, was in the PSS/E software format. This program is widely used throughout industry and provides a robust power flow analysis.

Adjusting Existing Generation

After matching the substation from the transmission one-line to the appropriate substation number in the power flow file active and reactive power were connected to the substation as a new machine. In order to add wind generation in a particular region and maintain power balance, it is necessary to reduce existing generation in the same region and/or reduce transfers into that region. Tom Vilsack, the former governor of Iowa, had expressed an objective to increase power exports from the state. To be consistent with this objective, as wind generation was increased, generation was decreased only at units outside the state. The external areas selected to reduce generation were as follows:

- ComEd units in area 363
- Xcel units in area 600
- NPPD units in area 640
- OPPD units in area 645

These areas represent regions to the east, west, and north of Iowa and desirable regions to export power from the state. Each of the external area generation compensated 25% of any increase in wind generation in Iowa. In the PSS/E program, this was achieved using the interchange control facility. For example, if 100 MW of generation were to be added into the AE area, the interchange levels would be reduced by 25 MW in area 363, 600, 640, and 645, while the MEC area would remain unchanged.

Contingency Analysis

Each instance of new generation in a wind region required a contingency analysis to analyze the effects of the new generation in two steps. Step 1 focused on the local limitations that arose due to the addition of new generation, generally 3-5 circuits from the source of the new generation. This was followed by a system wide analysis in Step 2 necessary due because the system wide- effects were generally inconsequential in Step 1 since all violations were contained very near to the new generation. The process and results of the Step 1 and 2 analyses can be seen in the following sections. In each of these cases the thermal limitations of the transmission system were of particular issue. The reasoning behind this is that any voltage violations were easily correctable through the use of capacitor banks, a relatively inexpensive correction feature. As a result, the goal behind the Step 1 and 2 analyses were to relieve all thermal violations as a result of new wind generation.

Step 1: Maximum Wind Penetration Limited by Local Transmission Constraints

In Step 1, wind penetration levels were increased to the point where local transmission capability was exhausted. The term "local transmission" refers to the 69 and 161 kV transmission facilities near to the bus where MW injection was being increased; typically, this was within 3-5 circuits away. Normal limits were enforced, and for selected contingencies emergency limits were enforced. A limiting branch was determined as the most heavily loaded circuit within the local transmission system. This limiting branch was opened, the power flow was run, and a contingency branch was determined as the branch having the largest MW loading increase. The result of this procedure led to the identification

of the most heavily loaded branch (the limiting branch) together with the contingency (the contingency branch), which most severely loads the limiting branch following occurrence of that contingency.

With the limiting branch closed a contingency analysis was run for each case of additional wind penetration, where the selected contingency that was set always included the contingency branch identified by the procedure described above. If any contingency resulted in a violation, the level of wind penetration was reduced. This procedure was followed for each wind region.

For each wind region, the wind penetration was increased to a level where a normal or contingency violation occurred and then reduced according to the procedure described above. The results of cases A-T, each corresponding to a specific wind region, are provided in Appendix A. Each successive test case models additional wind penetration for a particular wind region (or combination of wind regions) together with the wind penetration added in previous test cases. Appendix A lists, for each test case, the wind region (or wind regions) studied under that test case, the substation (or substations) to which the additional wind generation (for that test case) is connected, the additional wind penetration for that test case (identified based on whether it is in the MEC or the AE area), the contingency causing the limitation, the limiting branch following the contingency, and the MEC and AE net export. Table 1 provides a summary of the total wind penetration added to each area along with the new levels of MW export.

Table 1: Summary of Step 1 Analysis

AREA	NEW GENERATION	NET EXPORT
MidAmerican Energy (Area 635)	1235 MW	892 MW
Alliant Energy (Area 331)	380 MW	81 MW

Step 2: Additional Limitations due to System-Level Transmission Constraints

The Step 2 analysis utilized the Case T power flow case, which models additional wind penetration of 1615 MW. Case T represents the maximum wind penetration based on

the Step 1 analysis and limited by local transmission constraints. This step was necessary to understand the system-wide effects of the additional wind generation. As mentioned in the Step 1 analysis, the contingency event for the new generation was constrained locally. Therefore, the effects of increased export from the state were not being observed. In order to achieve a complete picture of the effects of the new generation, a second contingency analysis was run.

In the Step 2 analysis, a set of 41 NERC level C contingencies cases provided by MEC and AE were run using the automatic AC contingency analysis feature in PSS/E. Following the successful completion of this analysis additional contingencies were investigated based on the following methodology. Branches that saw an overall increase in loading of 5% due to the 1615 MW additional wind penetration and that were loaded beyond 50% of the rated load were identified. These branches were designated Significantly Affected Elements (SAE), and became the basis of the additional analysis. Each SAE was opened individually to create an N-1 contingency event. By monitoring the loading of all elements in the MEC and AE areas, any violations due to the contingency event were identified. Violations were eliminated by reducing the wind penetration levels at buses most significantly affecting the post-contingency overload. This procedure reduced the generation in each area as given in Table 2, bringing the total increase in MW injection in the Iowa system to 1435 MW.

Table 2: Summary of Step 2 Analysis

AREA	ADJUSTED NEW GENERATION	ADUSTED NET EXPORT
MidAmerican Energy (Area 635)	1090 MW	746 MW
Alliant Energy (Area 331)	345 MW	46 MW

A table summarizing details of this analysis is provided in Appendix C.

Summary of Static Analysis

The results of the static increased the penetration level from 8.55% to 20.47%. This is based on the data from the MISO 2008 base case where 819 MW of wind generation existed prior to the start of this study. The total generation for MEC and AE was a combined 9576.1 MW. With the results of the static analysis, an additional 1435 MW of wind generation was added to the system resulting in a total generation level of 11011.1 MW. This is a significant increase in penetration, and represents what the Iowa transmission system is capable of handling at its current state. This number is very fluid and can vary based on many factors such as planned projects for current generation or increases in transmission capability. Another issue that may play an important role in determining a maximum penetration level in Iowa is the development of wind generation outside of the state. Significant wind generation projects are being planned in the Dakotas and Minnesota, with these states looking to be involved in exporting generation to the east coast of the United States [2]. This will affect the transmission capability of the state and may reduce the penetration level unless there is transmission reinforcement. Also, this value does not included projects that are currently in the MISO queue for the state.

Based on the MISO queue data for new generation, all proposed wind farms for the state were mapped back to the corresponding wind regions developed through this study. This data was tabulated and is given in Appendix D. Listed along with each item in the MISO queue, is the corresponding wind region, the proposed summer peak of that generation, and the limit in MW of the wind region. This information therefore allows identification of those wind regions for which the wind levels proposed exceeds the capacity of the transmission system modeled in the 2008 power flow case used in this study. These wind regions are highlighted in yellow on the right-hand side of the table.

In the aggregated, the current MISO queue calls for an addition of 3117.2 MW to the Iowa system by the year 2010, far exceeding the 1435 MW of transmission capacity identified in this study. Sites that are planned well into the future may utilize new transmission to accommodate the maximum level of wind generation that is planned in the queue, i.e. nameplate value, or can follow the limits set forth in this study as a basis for new MW injection.

CHAPTER 4: DYNAMIC MODELING OF WIND TURBINES

To appropriately model wind turbines for dynamic simulations the turbine needs to be divided into a series of subsystems. Each subsystem controls an important aspect of the wind turbine and distinguishes the type of turbine that is being modeled. Certain subsystems are specific to the type of turbine, while others are general for all wind turbines. The wind turbine is broken down into the following subsystems:

- Aerodynamic subsystem
- Mechanical subsystem
- Generator subsystem
- Wind turbine control subsystem

This chapter will describe how fixed speed generator (FSG) or doubly-fed induction generator (DFIG) wind turbine are different at the subsystem level and how the subsystems are combined to create a dynamic model of each wind turbine. Much of the differences in the two turbine types can be attributed to the physical design of the two machines. The FSG and DFIG wind turbines can be seen in Figures 4.1 and 4.2 respectively.
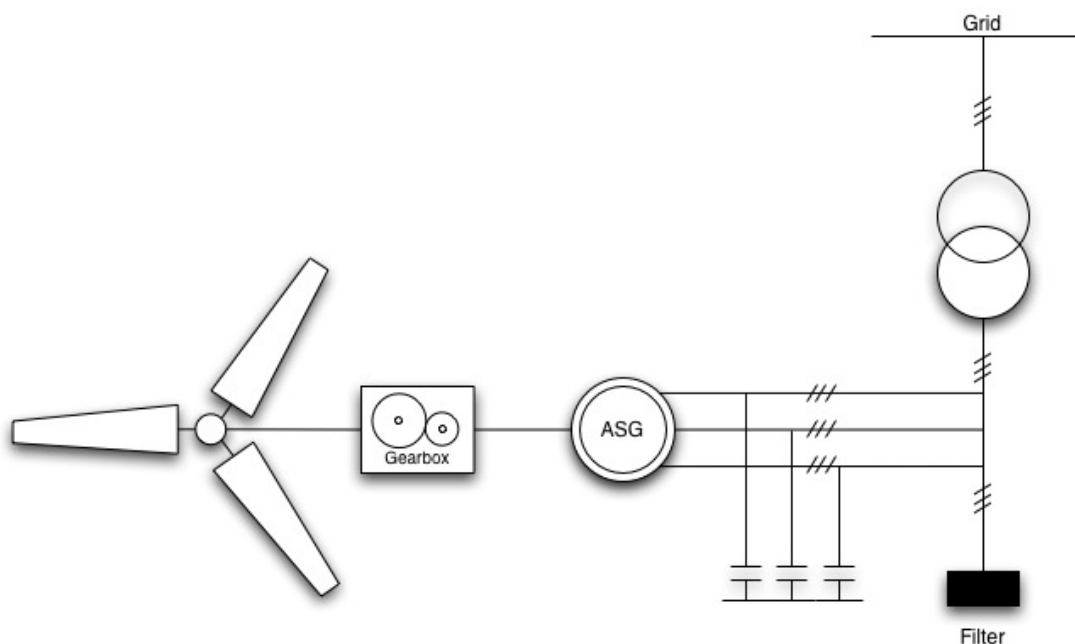
Figure 4.1: Block diagram of FSG wind turbine
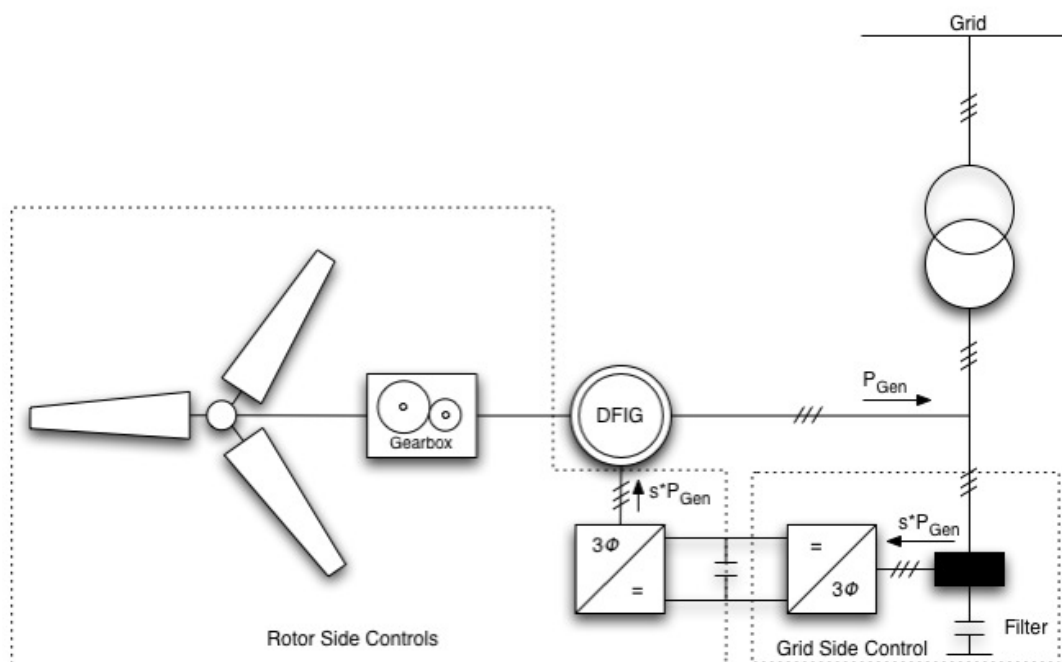
Figure 4.2: Block diagram of DFIG wind turbine

In the FSG the blades of the machine are coupled directly to the induction generation through a gearbox, the stator of the generator is connected to the electricity grid while the rotor is short-circuited. In a DFIG the turbine blades are decoupled from the machine to allow for speed control, and the electricity grid is fed from both the stator and the rotor through a power converter. The discussion of each subsystem will further highlight the differences in the two turbines.

Aerodynamic Subsystem

Kinetic Energy Present in Wind

The aerodynamic subsystem of wind turbines describes how turbines extract the kinetic energy present in the wind. The level of kinetic energy present is given as a generic function for all types of wind turbines. It is achieved by determining the energy available in the area covered by the rotating blades of the turbine, given as the following function (4.1):

$$P_{wind} = \frac{1}{2} \cdot \rho_{air} \cdot A \cdot v_{wind}^3 \qquad (4.1)$$

In (1), P_{wind} is the energy available in the cross-sectional area swept by the blades A, at wind speed v_{wind} at air density ρ_{air}. It is important to note in (4.1), P_{wind} assumes that all of the available kinetic in the wind is extracted. Physically, this means that all the wind is absorbed by the turbine and converted into mechanical energy. This would mean that no wind passes through the blades of the turbine. However, this is not the case as the Betz Limit defines the maximum level of energy extractable from the wind [13]. The Betz Limit states that at any instant the maximum percentage of energy extractable from the wind is 59 %. The Betz Limit is the basis for the level of extraction efficiency; it is defined by the turbine characteristics, and is given as the performance coefficient of the turbine (C_p). C_p is defined as the fraction of the energy extracted from the wind for a given wind speed. As a result the mechanical energy seen by the electrical system of the turbine is given as (4.2):

$$P_{mech} = C_p \cdot P_{wind} \qquad (4.2)$$

Up until this point the energy extracted has been a generic function that is not specific to any type of turbine. However, in (4.2), C_p is a unique function that is determined by specific turbine characteristics.

The Performance Coefficient, C$_p$

The performance coefficient is a critical value in the power production of wind turbines. It can be referred to two locations on the wind turbine;

1. *From blades at the hub of the wind turbine.* C_p is generally not given from this location as it neglects many of the mechanical losses that occur in the rotor shaft and in the gearbox that couple the mechanical and electrical systems of the turbine.

2. *With respect to the electrical power seen at the generator.* This value of C_p includes the mechanical losses and is given as a non-linear function of the tip speed ratio λ and blade pitch angle β.

To further understand the performance coefficient, it is important to expand on the concepts of the tip speed ratio and the blade pitch angle. The tip speed ratio is value that relates the rotational speed of the turbine blades with the wind speed. Based on the definition of the tip

speed ratio λ is expressed as (4.3). Here ω_{Rot} is the angular rotational speed, R is the radius of the blade and V_{Wind} is the wind velocity.

$$\lambda = \frac{\omega_{Rot} \cdot R}{V_{Wind}} \tag{4.3}$$

The blade pitch angle β is the angle at which the turbine blades encounter the wind. Adjusting β allows for a minimal level of control over the turbine's rotational speed. Using these the tip speed ratio and blade pitch angles, manufacturers determine the performance coefficient of the turbine for the varying pitch angles and what the turbine is capable of achieving. Figure 4.3 is an example of a performance coefficient plot for the GE 1.5 sle turbine. From Figure 4.3, it can be seen that for all of the blade pitch angles, there is an optimal range for the tip speed ratio. The optimal ratio λ_{opt} generally falls between 8 to 9, and is based on the manufacturers design. λ_{opt} will vary with the design of the turbine, relying on the number of blades and the structure of the rotor and shaft of the turbine. Further information on the optimal tip speed ratio can be found in [14].
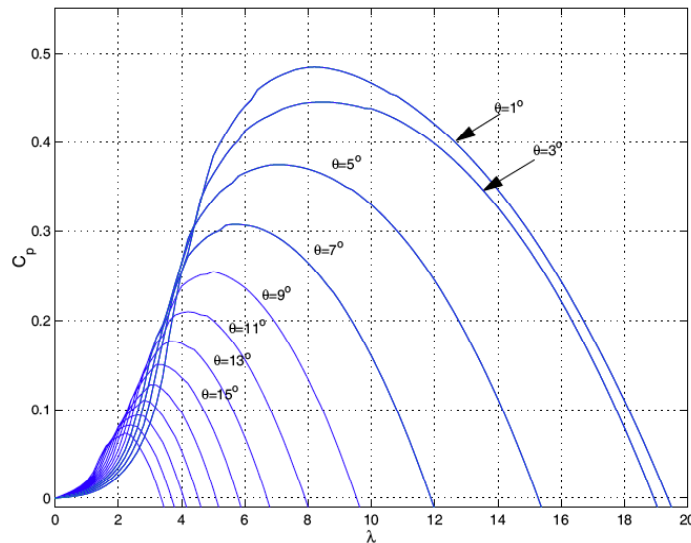
Figure 4.3: Performance coefficient plot for GE 1.5 sle wind turbine. In this plot λ is tip speed ratio while θ is equivalent to β the blade pitch angle [15].

Controlling λ_{opt} is a key factor in optimizing power output from a wind turbine. As seen in (4.3), controlling λ_{opt} requires control of the rotational speed of the turbine blades. In FSGs there is no speed control, and the only means of optimizing the tip speed ratio lie in the

control of the blade pitch angle. This provides a minimal level of control as in FSGs the time constants required to adjust the blade pitch angle are very long, and it is difficult to adjust β when the wind speeds change rapidly. As a result, FSGs are often designed based on wind characteristics of the region they will be installed in. This is done to match the rotational speed of the turbine with the most likely wind speed seen in the region. This results in the turbine operating in the region of λ_{opt} more often. In DFIGs, both blade pitch control and speed control are utilized which allows for the DFIG to achieve λ_{opt} for varying wind speeds, thus increasing power production. The concept of speed control will be discussed later and blade pitch control will be described in further detail. In dynamic simulations, the non-linear nature of C_p is represented as a complex polynomial function or more often through the use of tables. Using tables, allows for the varying values of C_p to be matched to the tip speed ratio for different pitch angles. This representation of the performance coefficient as a function of λ and β allows for the mechanical power to be delivered to the electrical system that is determined as (4.4):

$$P_{Mech} = \frac{1}{2} \cdot \rho_{air} \cdot A \cdot v_{wind}^3 \cdot C_p(\lambda, \beta) \tag{4.4}$$

This is the final output of the aerodynamic system and the structure. The mechanical subsystem can now be discussed.

Mechanical Subsystem

The mechanical subsystem represents the inertias of the rotating masses of the blades, the shaft and a gearbox that drive the generator, and finally the generator rotor itself. Figure 4.4 depicts the individual inertias of a wind turbine. The inertias of the blades and generator are H_{turb} and H_{gen} respectively, while K_{tot} represents the total staff stiffness. In a DFIG, the inertia of the blades is decoupled from the rest of the machine and as a result it is not utilized by the machine. This is due to application of additional control systems in the DFIG that will be discussed in later.
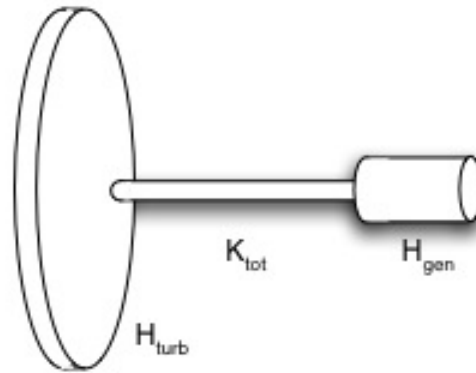
Figure 4.4: Two mass model of a wind turbine.

The inertia is of particular importance in the representation of FSGs in simulation. In most simulations programs the mechanical sub-system of the FSG is represented as a single, "lumped", inertia connected to the shaft of the induction generator. Representing the individual inertias is important in the modeling of FSGs [16]. In representing the FSG with a lumped mass inertial model, the voltage in the system will recover quickly, often with little or no electric power oscillations. It has been shown in [16], this representation is not truly accurate. Simulations in [16] show that representing the FSG as a fifth-order model with the shaft-stiffness and two inertias accounted for will provide varied results versus the lumped mass representation. The terminal voltage of the wind farm will show increased electric power oscillations. The lumped mass model will show the terminal voltage recover after a fault, but the same may not be true for the two mass model. Chapter 5 will discuss the availability of these models and identifies issues that will need to be addressed in the future as wind studies expand.

Generator Subsystem

The generator is the key factor in differentiating types of wind turbines. There are generally two types of generators that are used for dynamic modeling of wind turbines. The first is the use of an induction machine and the second is through the use direct-drive synchronous machine. This thesis will discuss the modeling of turbines using induction machines only as these are the most common installations today.

Induction Machine Modeling

The induction machine is an alternating current (AC) machine, where the rotating device is powered through induction. In an induction machine there is an alternating current in both the rotor and stator of the machine. The stator of the machine is connected to the three-phase system, while the rotor is short-circuited internally or the slip rings are connected to an external circuit. When balanced three-phase currents are applied at frequency f_s the stator windings produce an electromagnetic field that rotates at (4.5):

$$n_s = \frac{120 \cdot f_s}{p_f} \tag{4.5}$$

In (4.5) n_s is the rotational speed of the stator in revolutions per minute (RPM), while p_f is the number of poles of the machine. The rotation of the stator produces an electromagnetic field that induces a rotation in the rotor. The induced rotational speed of the rotor is given as n_r. For motor operation, n_r is determined by the torque required by the load being driven. For generator operation, n_r is determined by the prime mover. Using this value, the slip, s, of the machine can be calculated as (4.6):

$$s = \frac{n_s - n_r}{n_s} \tag{4.6}$$

The slip is the difference between the rotating field of the stator and the rotational speed of the rotor. Using the slip, the frequency of the rotor is given as (4.7):

$$f_r = s \cdot f_s \tag{4.7}$$

Generally, a mechanical load will be applied at the rotor and be driven via the transfer of electromagnetic torque by the stator. This type of induction machine acts as a motor, and the rotational speed of the rotor is less than the stator $n_r < n_s$. In the case of a wind turbine, the rotor of the induction machine is coupled to the rotating shaft of turbine blades. This drives the rotor at a speed greater than the rotor $n_r > n_s$. This allows the machine to act as a generator to supply power the connected three-phase system.

The Fixed Speed Generator Wind Turbine

The FSG consists of a squirrel cage induction machine where the blades of the turbine are coupled to the rotor of the induction machine using a gearbox. The gearbox allows the

rotor to rotate at the appropriate speed to provide generation to the three-phase system. The voltage equations are given in the *d-q* reference frame, found in [17]:

$$\left.\begin{aligned}
v_{ds} &= -R_s i_{ds} - \omega_s \psi_{qs} + \frac{d\psi_{ds}}{dt} \\
v_{qs} &= -R_s i_{qs} + \omega_s \psi_{ds} + \frac{d\psi_{qs}}{dt} \\
v_{dr} &= 0 = -R_r i_{dr} - s\omega_s \psi_{qr} + \frac{d\psi_{dr}}{dt} \\
v_{qr} &= 0 = -R_r i_{qr} + s\omega_s \psi_{dr} + \frac{d\psi_{qr}}{dt}
\end{aligned}\right\} \tag{4.8}$$

In (4.8) *v* is the voltage, *R* is the resistance, ψ is the flux, and *s* is the slip. All values are given in per unit quantities. In an FSG, the rotor currents are short-circuited thus the rotor voltages are equal to zero. Using (4.5) and (4.6), the slip of the machine is calculated as (4.9):

$$s = 1 - \frac{p_f \omega_r}{2\omega_s} \tag{4.9}$$

Since the machine acts as a generator, the current leaving the machine is defined positive. In (4.8), the flux linkages can be calculated using the machine parameters for the mutual (*m*), leakage (σ), rotor (*r*), and stator (*s*), inductances (*L*). They are given as (4.10):

$$\left.\begin{aligned}
\psi_{ds} &= -(L_{s\sigma} + L_m)i_{ds} - L_m i_{dr} \\
\psi_{qs} &= -(L_{s\sigma} + L_m)i_{qs} - L_m i_{qr} \\
\psi_{dr} &= -(L_{r\sigma} + L_m)i_{dr} - L_m i_{ds} \\
\psi_{qr} &= -(L_{r\sigma} + L_m)i_{qr} - L_m i_{qs}
\end{aligned}\right\} \tag{4.10}$$

By substituting (4.10) in (4.8), the following voltage equations are in (4.11) are obtained. In (4.11), the stator transients are neglected.

$$\left.\begin{aligned}
v_{ds} &= -R_s i_{ds} + \omega_s \left[(L_{s\sigma} + L_m)i_{qs} + L_m i_{qr}\right] \\
v_{qs} &= -R_s i_{qs} - \omega_s \left[(L_{s\sigma} + L_m)i_{ds} + L_m i_{dr}\right] \\
v_{dr} &= 0 = -R_r i_{dr} + s\omega_s \left[(L_{r\sigma} + L_m)i_{qr} + L_m i_{qs}\right] + \frac{d\psi_{dr}}{dt} \\
v_{qr} &= 0 = -R_r i_{qr} - s\omega_s \left[(L_{r\sigma} + L_m)i_{dr} + L_m i_{ds}\right] + \frac{d\psi_{qr}}{dt}
\end{aligned}\right\} \tag{4.11}$$

The electric torque can now be calculated as (4.12):

$$T_e = \psi_{qr} i_{dr} - \psi_{dr} i_{qr} \qquad (4.12)$$

Next, the swing equation of the machine is (4.13):

$$\frac{d\omega_m}{dt} = \frac{1}{2H}\left(T_m - T_e\right) \qquad (4.13)$$

In (4.13), H is the inertia of the induction machine combined with the mechanical inertia of the blades and rotor, and T_m is the mechanical torque from the blades of the turbine. The calculation of H is described later in this thesis.

The Doubly Fed Induction Generator Wind Turbine

The DFIG is modeled using the same equations as the fixed speed generator with one important difference: In modeling the voltage equations of the DFIG, the rotor voltages are no longer short-circuited. As a result, they must be included in equations describing the machine dynamics (4.14).

$$\left. \begin{aligned} v_{ds} &= -R_s i_{ds} - \omega_s \psi_{qs} + \frac{d\psi_{ds}}{dt} \\ v_{qs} &= -R_s i_{qs} + \omega_s \psi_{ds} + \frac{d\psi_{qs}}{dt} \\ v_{dr} &= -R_r i_{dr} - s\omega_s \psi_{qr} + \frac{d\psi_{dr}}{dt} \\ v_{qr} &= -R_r i_{qr} + s\omega_s \psi_{dr} + \frac{d\psi_{qr}}{dt} \end{aligned} \right\} \qquad (4.14)$$

In (4.14) the rotor voltages must be calculated and included as part of the generator model. Since, the rotor is no longer short-circuited, the DFIG connects the generator back to the grid through the use of a power electronics converter. The concepts behind this converter will be discussed later. Using the same substitution from (4.10) the following voltage equations are derived in (4.15).

$$
\left.
\begin{aligned}
v_{ds} &= -R_s i_{ds} + \omega_s \left[(L_{s\sigma} + L_m) i_{qs} + L_m i_{qr} \right] \\
v_{qs} &= -R_s i_{qs} - \omega_s \left[(L_{s\sigma} + L_m) i_{ds} + L_m i_{dr} \right] \\
v_{dr} &= -R_r i_{dr} + s\omega_s \left[(L_{r\sigma} + L_m) i_{qr} + L_m i_{qs} \right] + \frac{d\psi_{dr}}{dt} \\
v_{qr} &= -R_r i_{qr} - s\omega_s \left[(L_{r\sigma} + L_m) i_{dr} + L_m i_{ds} \right] + \frac{d\psi_{qr}}{dt}
\end{aligned}
\right\}
\qquad (4.15)
$$

By controlling the slip in (4.9) the DFIG can operate as a variable speed machine. This means that it can draw power from both the rotor and the stator operating at both super-synchronous and sub-synchronous speeds. This design allows for optimal power production from the machine for a large variation of wind speeds.

Wind Turbine Control Systems

Wind turbines incorporate significant levels of control to produce optimal power during the time they are online. Optimal power production is achieved differently in both the FSG and DFIG. Incorporating this control provides advantages and disadvantages for each wind turbine and will be discussed in this section. The first issue that will be examined is the inertial response of the FSG and DFIG. Although this is not truly a control system the concepts behind it are critical in developing the control systems in both turbines, in particular the speed control of the DFIG. Next, the blade pitch control system will be examined; this system is common to both the FSG and DFIG and is utilized in the same manner in both turbines. Finally, the reactive power control capabilities of the DFIG will be discussed.

Inertial Response of the FSG and Speed Control of the DFIG

The inertia of a machine is an important characteristic that determines the ability of a machine to respond to frequency changes in the system. If a contingency event occurs and the system incurs a loss of generation the system frequency will fall due to the generation load imbalance. The level of spinning inertia in the system, summed across all of the generating machines, will govern the rate of the frequency decline. The inertial characteristic is particularly important when approaching the problem of interconnecting significant levels of wind generation into a transmission system. If the new wind generation is displacing

traditional generation, the level of spinning inertia may decrease significantly if the installations are predominately DFIGs. This is due to the unique structure of the DFIG where the turbine blades are decoupled from the electrical machine to provide active and reactive power control. However, if the wind installations are using FSG turbines, the spinning inertial reserve may be preserved. This section will detail how the each turbine provides an inertial response to the system namely through natural use of the FSG and how through an inertia emulating control loop inertia can be theoretically extracted from a DFIG.

Fixed Speed Generator Wind Turbine Characteristics

In a fixed speed generator wind turbine (FSG) the inertia constant is determined like any other induction machine. The speed of the wind plays no part in determining the level of inertia energy extractable from the machine. For a given drop in frequency the machine responds by decelerating at a rate determined by its moment of inertia and all masses connected to the rotor shaft (i.e. the turbine blades). The moment of inertia will vary based on the turbine blade design as well as the current pitch angle. Generally, FSGs have inertia constants in the range of 3 – 5 s, resulting in an ability to respond to fast frequency changes.

The design of the FSG has the blades coupled directly to the rotor of the induction machine, which is connected directly to the 3-phase system. This scheme requires the machine to operate at the fixed speed of the system. The disadvantage of the FSG arises in its ability to operate at varying wind speeds. Since the time constants for changing the pitch angles of the blades are very long, due to the direct coupling to the rotor, FSGs have a difficult time responding to sudden variations in wind speed. As a result, power surges are often seen for large gusts of wind. This characteristic requires that FSGs be connected to a strong power system that can handle these sudden changes. This design allows for only one control aspect to be incorporated into the FSG, the pitch angle of the turbine blades. This is the only system that will allow for the control power production in an FSG, and will be discussed further in this thesis.

Doubly-Fed Induction Generator Wind Turbine Characteristics

In a doubly-fed induction generator wind turbine (DFIG) the inertia constant may be emulated through a variety of control schemes. Since the design of a DFIG requires the rotor be decoupled from the 3-phase power system, the mechanical inertia of the blades cannot be utilized in a DFIG WT that is connected to the system. It has been shown in various simulations that the addition of a control loop in the converter allows the DFIG WT to compensate for the low level of inertia present in the DFIG itself. Through control, the inertia of a DFIG can be at a level comparable to a FSG [18], [19], [20], [21], [22], and [23]. However, it is important to note that the DFIGs available on the market today do not utilize this control. Therefore, all controls in DFIGs described in this thesis are theoretical. This disadvantage is generally offset, by the ability of the DFIG to provide increased levels of power production efficiency due to its ability to handle the variability of the wind and the improved levels of voltage control. Since, the rotor is decoupled from the system it can operate at varying speeds and provide both active and reactive power to the system. This allows for the increase of in levels of output power for lower wind speeds as well as increased output at higher speeds when FSG WTs may not operate. Also, large gusts of wind can be absorbed in the DFIG design, and stored as kinetic energy in the machine when inertial control is present. The application of this control and its relation to system frequency response will be discussed in Chapter 5.

Calculation of Inertia Present in the Wind Turbine

The inertial characteristics are not unique to a particular turbine, but general across all types. The main goal is to identify the energy stored in the rotating mass of the turbine blades. This is given generically for any rotating mass as the following equation:

$$E = \frac{1}{2} J \omega_m^2 \tag{4.16}$$

Where J is inertia of the machine and ω_m is the rotational speed. This needs to be converted in the inertia constant used in power systems. That is achieved as follows:

$$H = \frac{J \omega_m^2}{2S} \tag{4.17}$$

Here, H is the inertia constant and S is the nominal apparent power of the machine. Following this conversion, the specific value of J needs to be identified for the blades of a wind turbine. The inertia of a given body is:

$$J = \sum m_i r_i^2 \qquad (4.18)$$

Where m_i is the mass of object i and r_i is the radial distance for the inertia axis. This equation is related back to a wind turbine by identifying the mass [13]middle of each blade, generally 1/3 of the turbine radius r, and the mass of each individual blade, m_b. This results in the following equation (note m_r represents the mass of the blade and rotor structure and is equivalent to $3m_b$):

$$J = 3m_b \left(\frac{r}{3}\right)^2 = \frac{1}{9}m_r r^2 \qquad (4.19)$$

Now, by substituting (4.19) into (4.16), the energy stored the in rotor and blade structure is achieved:

$$E = \frac{1}{18}m_r r^2 \omega_m^2 \qquad (4.20)$$

Here, $r^2 \omega_m^2$ is defined as the tip speed. After identifying the inertia constant of the mechanical structure, the generator rotor inertia needs to be identified. Generally for a typical induction machine this is given as H in the range of .4 - .8 s . In FSG turbines, the inertia identified in (4.19) is utilized in frequency response, however for DFIGs supplementary control must be applied to achieve an inertial response. The application of the inertia in frequency control will be discussed in Chapter 5 as well the additional DFIG control schemes.

Pitch Control System

The main control scheme utilized in nearly every wind turbine available today is blade pitch control. By control the pitch angle of the turbine blades a nominal level of control can be established for the turbine's power output. The reason this control is nominal at best is due to the inherent variability of wind; if the wind speed is fluctuating very quickly, i.e., wind speed changes of less than a few seconds, blade pitch control can respond and the power will vary greatly out of the turbine. However, if the wind speed change is on a slightly

larger time scale, with several seconds, the blade pitch angle can be adjusted to produce optimal power for the given wind speed. Optimal power production is achieved in the turbine based on controlling the blade pitch to match the C_p curve, of the turbine.

By utilizing the blade pitch and generator torque as the two control variables a basic version of speed control described in the previous section is created for the wind turbine. This control in general is the only level of control available on FSG wind turbines [23], [24], and [25]. As a result FSGs are often designed to interact with specific characteristics of the region they are installed in, i.e., their optimal rotor speed and tip-speed ratio are designed based on the average wind speeds of a region. DFIGs combine the blade pitch control with the speed control described in the previous section. These two levels of control allow the DFIG to operate over a greater range of wind speeds in conjunction with the variable speed machine [24], [25], and [26].

Voltage Control System

Voltage control is only possible in the DFIG wind turbine. Since the FSG structure requires a large level of reactive power consumption, the only methods of control available in the FSG are achieved using capacitor banks or SVCs. The DFIG's design using a power electronics converter to couple the rotor back to the power grid allows for the implementation of voltage control. This section will discuss the basics behind this control however it will not develop any detailed theory behind the concept. This is done since voltage control in the DFIG is well established and is available in many commercial turbines, GE, Enercon, Clipper, Suzlon, and many others [27], [28], and [29].

Voltage control in the DFIG is usually achieved in the power electronics converter that couples the rotor of the induction generator back to the power system grid. Figure 4.5 shows the design of the DFIG with the converter in place.
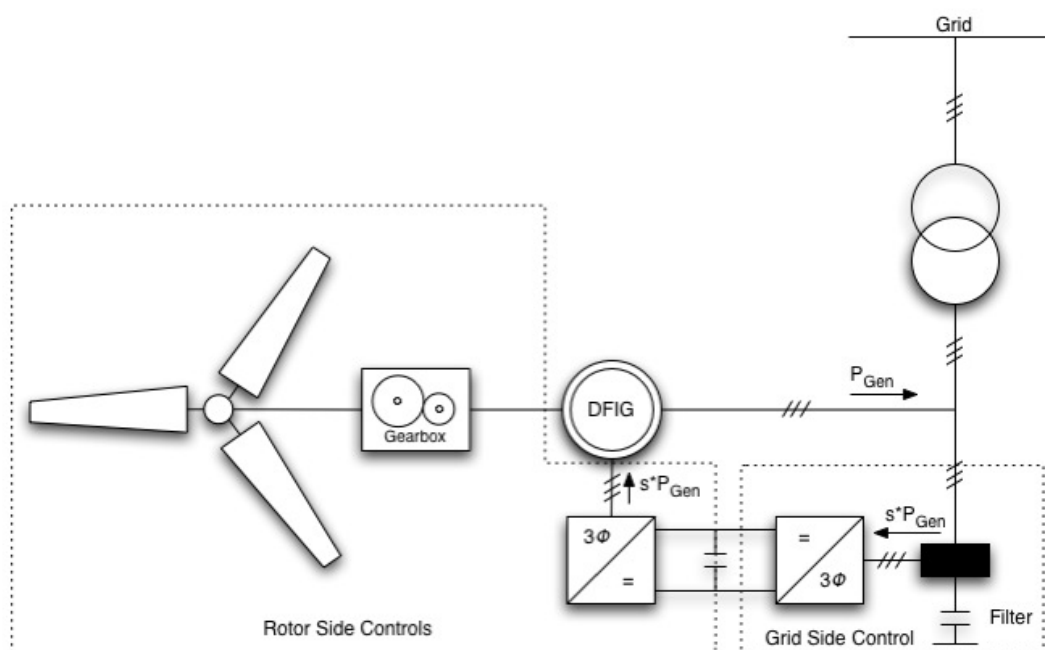
Figure 4.5: DFIG design with power electronics converter connecting machine back to the grid.

The control of reactive power is achieved by controlling the rotor current in the converter circuit. Control of the reactive power allows voltage control to be applied in one of two methods; control of the terminal voltage at the collector bus or control of the power factor out of the wind farm. In essence, the DFIG is combining the advantages of an induction machine and a synchronous machine in its voltage control capabilities. The main disadvantage of the DFIG arises in its inertial response capabilities as well as the complex levels of control that are applied in the reactive power control schemes.

CHAPTER 5: FREQUENCY RESPONSE AND THE EFFECTS OF INCREASED WIND PENETRATION

This chapter will first discuss the issues associated with frequency response in an electricity system and how it would change with the introduction of wind generation. Secondly, it will provide simulation results that reflect the effects of increased wind generation on frequency response. To build up a solid foundation in the concepts and effort needed to model wind turbines dynamically a smaller test system was used. The results presented in this chapter are all completed using a 6-bus test system. This system is shown in Figure 5.1. In addition to providing the effects of wind generation on system frequency response, this chapter will also detail the necessary requirements to accurately model the DFIG and FSG in PSS/E.
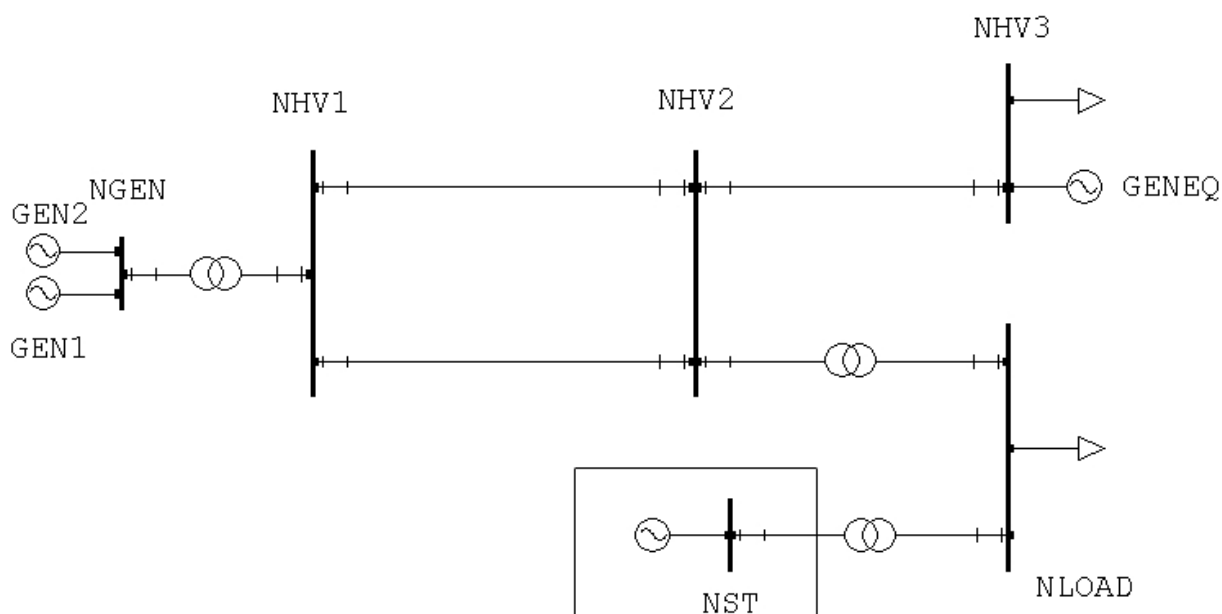
Figure 5.1: 6-bus test system used for dynamic simulations.

Frequency Control and Active Power

The frequency of a system is the rotational speed of machines (generators, motors, etc.) that constitute the system or operating area. Control of system frequency is a crucial aspect in the operation of a power system. In order to maintain a near constant frequency, it is necessary to maintain a balance between the generation and load present in the system. If

the system suffers a loss of generation and cannot supply the load present in the system, frequency will decline and could eventually lead to load shedding, generation disruption, or damage to many machines that are designed to operate around a very specific frequency range. If there is an excess of generation, the frequency will increase and the system will lose synchronism, once again leading to many of the same problems of under-frequency. The balance between load and generation is achieved through a variety of control schemes and can range on the order of less than one second to over a period of several days and is referred to as frequency control. This section will discuss the time frames associated with the different methods of control and how they apply to wind generation in the power system.

Compensating for Imbalance Following a Loss of Generation Event

To understand how wind power influences frequency response, the different levels of control applied in a power system immediately following a loss of generation event or loading imbalance and how conventional machines react to the event, must be discussed. Frequency control immediately following an event is applied generally in three time frames and is referred to as primary frequency [30]:

- Proximity Effect ($t = 0^+$)
- Inertial Response ($0^+ < t < t_g$ seconds)
- Governor Response (t_g seconds $< t < t_f$ minutes)

The responses from each of these phenomena are critical in mitigating any power imbalance sensed in a power system. The proximity effect describes how machines electrically nearer to a load change, ΔP_L, will provide a larger level of compensation in response to the imbalance. By reducing a network to its internal generator nodes the following is achieved [30]:

$$\Delta P_{ei} = \frac{P_{Sik}}{\sum_{j=1}^{n} P_{Skj}} \Delta P_L, \quad \text{for } i = 1, 2, 3, \ldots, n \tag{5.1}$$

(5.1) describes how machine i will react to a given load change ΔP_L at $t=0^+$ based on the synchronizing power coefficient (5.2):

$$P_{Sik} = \frac{\partial P_{ik}}{\partial \delta_{ik}}\bigg|_{\delta_{ik0}} = |E_i||E_j|\{B_{ik}\cos\delta_{ik0} - G_{ik}\sin\delta_{ik0}\} \tag{5.2}$$

From (5.2) it can be observed that a machine will react to the load change based on two factors in the synchronizing power coefficient:

- First, machines that have a higher transfer susceptance, B_{ik}, will provide a greater share of the compensation.
- Second, the smaller the difference in the internal angle, $\Delta\delta_{ik}$, the more a generator will compensate for the given load change.

The proximity effect occurs regardless of machine size or rating and since in the instant following the load imbalance the rotor angles cannot move instantaneously due to the mechanical limitations of the machine, the energy stored in the inertia of the rotating masses cannot be immediately applied to the loading change. The effects of the stored energy in the rotating masses are utilized in the time after the events of the proximity effect, through the inertial response.

The inertial response will occur in the time frame following the load imbalance, $t=0^+$ and until governor action begins at $t=t_g$. Following a loading increase or generation decrease, the system will suffer and overall deceleration during the time period for the inertial response. The mean deceleration for the system will be given as:

$$\frac{d}{dt}\frac{\Delta\overline{\omega}}{\overline{\omega}_R} = \frac{-\Delta P_L}{2\sum_{i=1}^{n}H_i} \tag{5.3}$$

(5.3) gives the average deceleration across the system, individual machines will responds differently based on their individual inertias. The individual response is given as:

$$2H_i\left[\frac{d}{dt}\frac{\Delta\omega_i}{\omega_R}\right] = -\Delta P_{ei} \tag{5.4}$$

By substituting (5.3) into the bracketed terms in (5.4) the following result is obtained:

$$\Delta P_{ei} = \left[\frac{H_i}{\sum_{i=1}^{n}H_i}\right]\Delta P_L \tag{5.5}$$

In (5.5) for a given load change, a machine will respond in proportion to their inertia, meaning the larger the inertia the larger the response. The inertial response of machines, will follow the proximity effect, and occur after a slight transient period, usually on the order of a few seconds. If the system has no turbine governor action, the inertial response will determine the final steady-state frequency following the load change. However, if turbine governors are present they will not have a significant effect in frequency mitigation until a few seconds following the event, around 2 seconds.

With the presence of turbine governors, a power system can apply another level of control and correct the generation-load imbalance following a contingency event. Turbine governor control is generally applied through the use of a speed-droop controller. The droop control will correspond to a 5% drop in the speed of the turbine, due to an increase in loading. As a result, the change in per unit mechanical power at the generator can be given as a function of the change in frequency (speed) and the R_u, the per unit regulation in $\frac{rad}{N \cdot m \cdot s}$.

$$\Delta P_{miu} = \frac{-\Delta f_u}{R_u} \tag{5.6}$$

From (5.6), calculating the individual change in the individual machine base can be given as:

$$\Delta P_{mi} = \frac{-\Delta f_u}{R_u} S_{Bi} \tag{5.7}$$

Then by making a similar substitution for the per unit frequency:

$$\Delta P_{mi} = \frac{-\Delta f}{60 R_u} S_{Bi} = C S_{Bi}, \text{ where } C = \frac{-\Delta f}{60 R_u} \tag{5.8}$$

Next, the summation of the mechanical power change at all the machines in the system will yield the change in loading suffered by the system:

$$\sum_{i=1}^{n} \Delta P_{mi} = C \sum_{i=1}^{n} S_{Bi} = \Delta P_L \tag{5.9}$$

Finally solving (5.9) for C, a substitution can be made in (5.8) that will provide the contribution of each machine with turbine governor control in response to a generation-load imbalance.

$$\Delta P_{mi} = \frac{S_{Bi}}{\sum\limits_{i=1}^{n} S_{Bi}} \Delta P_{L}$$

(5.10)

From (5.9), the contribution of each machine will be based on its rating. In essence, the larger the machine the more the generator will pick up for the given disturbance. Based on this discuss, the sequence or hierarchy in which the machines in a system will react to a loading disturbance has been determined. Now, the control action at the individual machine will be explored. The droop characteristic of an individual machine can be represented using the following block diagram. In Figure 5.2, the change in frequency is fed into the droop control block. In the function in the block, K represents the machines rating in comparison to the system base, i.e. $K = \dfrac{S_B}{S_{sB}}$. So in accordance with (5.10), the droop control will allow the machine to compensate for the load imbalance based on its size.
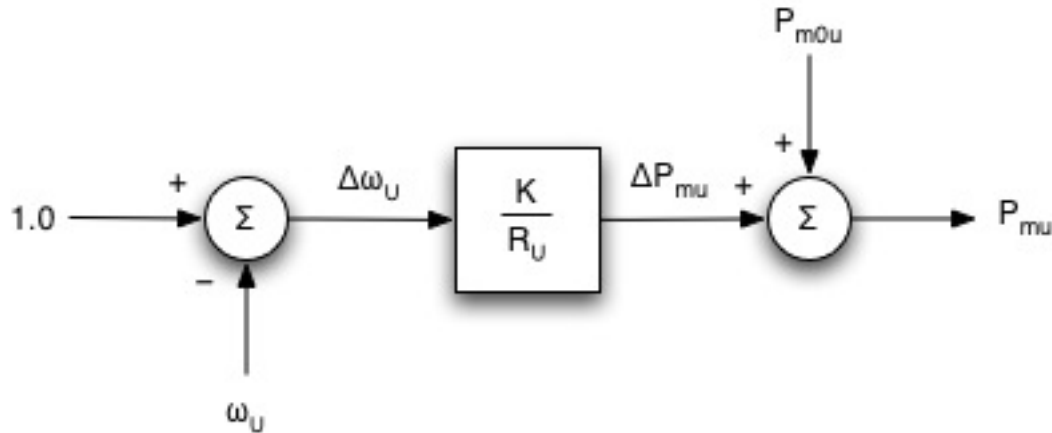
Figure 5.2: Droop control for a steam turbine governor [30].

Overall, these three control time frames are all applied immediately following a loss of generation or load imbalancing event and are important mitigating factors in maintaining system frequency. When wind generation is present in the power system, the type of wind turbines present and the penetration level of the wind generation will play important roles in determining the system frequency response. As previously mentioned, an inertial response is naturally present in the FSG that is lacking in the DFIG. This will allow the FSG to respond as a conventional synchronous machine during the inertial response time-frame of primary

frequency control. The DFIG however will operate as normal and will not contribute any support during primary frequency control. As a result an inertial response must be emulated in a DFIG through a series of control loops

DFIG Inertial Response Implementation

Due to the variability of the resource, an inertial response is the only method of primary frequency control available in wind turbines. The ability to respond to a load balance is naturally present in an FSG but in a DFIG, the inertial control is implemented through two hierarchical control loops. This is due to the fact that the mechanical and electrical dynamical systems operate at very different time scales. The electric system dynamics are much faster than the mechanical system dynamics. As a result the lower loop of control is implemented to control the electrical generator and converter. This allows for the control of the active and reactive power generated by the wind turbine. The higher level of control is applied to the mechanical system and used to control the blade pitch angle and speed of the blades. The lower level of control is applied at the converter and is common through out power system [18], [19], [20], [21], [22], and [23].

Speed Control Implementation

The mechanical control, in particular the speed control is how the DFIG differs from the FSG. The speed control loop is present in many commercially available turbines today, namely GE, Enercon, Mitsubishi, and others. Through the implementation of speed control, the optimal level of power can be extracted by the turbine for varying wind speeds. The primary task of speed control is to keep the tip speed ratio of the wind turbine at the optimal level. This is achieved through the following control implementation. By using the steady-state generator speed as the reference value (reference value identified from manufacturer power curves), a speed control loop can be developed. As a result, for low wind speeds the generator is kept at a low fixed speed and for high wind speeds, i.e., those above the rated value of the wind turbine, the blades are progressively pitched to maintain the optimal level of power generation. The blade pitch control will not be discussed here as it has little effect on the inertial response of DFIGs.
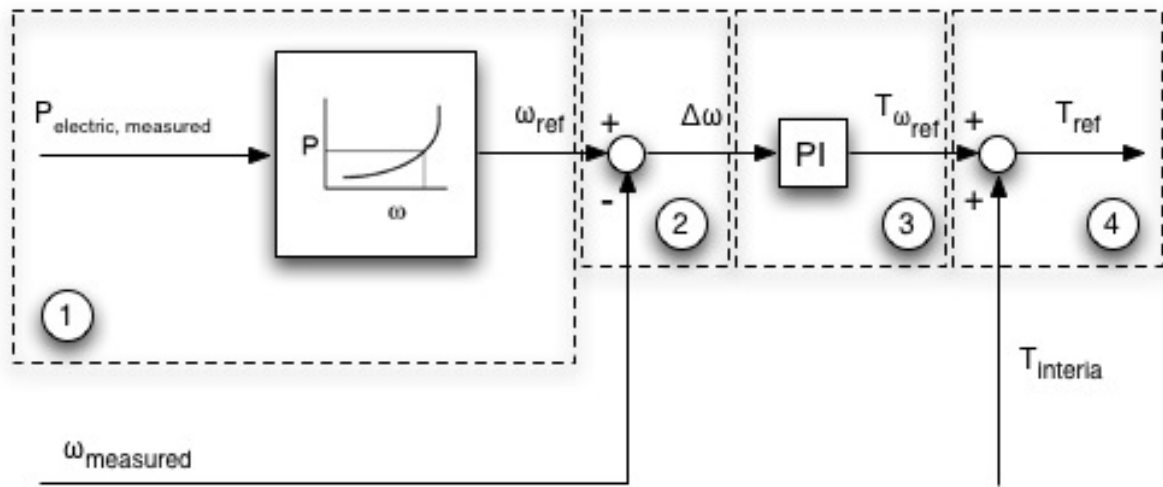
Figure 5.3: Speed Controller [18], [19], [20], [21], and [22]

The implementation of the speed control can be seen in Figure 5.3. There are several important characteristics within the control.

1. This is the generator reference speed, ω_{ref}, identified from the predefined *P-ω* characteristics of the machine.

2. Here the error between the measured speed and reference speed is calculated as $\Delta\omega$.

3. The error is then sent into a PI controller, resulting in a torque speed reference value $T_{\omega,ref}$. This value is due to the imbalance between the turbine torque and generator torque that will result in an accelerating or decelerating torque until the desired speed is reached.

4. The last portion of the control, T_{ref} arises as a result of a combination of $T_{\omega,ref}$ (the speed controlled torque) and $T_{inertia}$, an additional inertia response torque term. This term is achieved through the use of a second control loop and is where the theoretical inertial response loop is applied.

Inertial Response Control Implementation

As seen from Figure 5.3 to emulate inertia in a DFIG, the speed control relies on an inertial response torque term. This term is generally achieved using one of the following two control implementations. The first method seeks to emulate the inherent behavior of a synchronous machine. By taking the derivative of the kinetic energy available at any speed, ω_m, the power that can be extracted is given as follows:

$$P = \frac{dE_k}{dt} = J\omega_m \frac{d\omega_m}{dt} \qquad (5.11)$$

Next the combined inertia constant, H, is substituted in for the moment of inertia, J. This value was derived from (4.16) – (4.20). As a result the following equation, where ω_m is the grid frequency, is derived:

$$\frac{P}{S} = 2H \cdot \frac{\omega_m}{\omega_s} \cdot \frac{d\left(\omega_m / \omega_s\right)}{dt} \qquad (5.12)$$

Next, using per unit quantities, (5.12) can be referred to as follows:

$$\overline{P} = 2H \cdot \overline{\omega} \cdot \frac{d\overline{\omega}}{dt} \qquad (5.13)$$

Finally from (5.13), the per unit torque is given as:

$$\overline{T} = 2H \cdot \frac{d\overline{\omega}}{dt} \qquad (5.14)$$
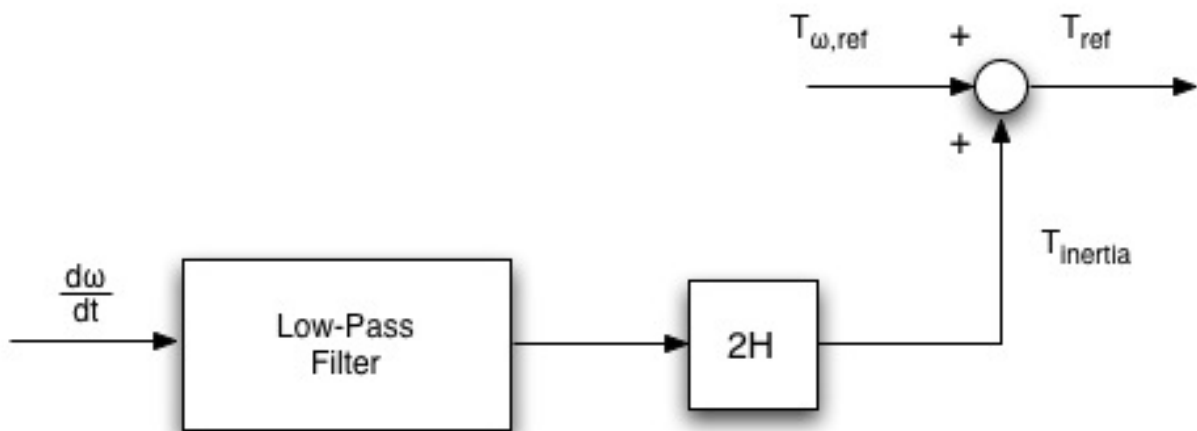
Figure 5.4: Inertia Controller [18], [19], [20], [21], and [22]

This results in the control loop shown in Figure 5.4. Here to minimize the impact on the mechanical drive train loads, the rate of power injection was modified by adding a first order (low-pass) filter. This leads to two events: first, there is a reduction in the rate of electromagnetic torque, and second, there is also a reduction in the magnitude of the peak torque. This represents the $T_{interia}$ that is combined with the speed control reference torque in Figure 5.3.

The second method to achieve the inertial response torque term is through the use of proportional control. In this method, the torque term is calculated based on the absolute deviation from the nominal system frequency. This is given as:

$$T = k_p \left(\omega_o - \omega_{measured} \right) \tag{5.15}$$

In (5.15), ω_o is the nominal speed and k_p is the proportional constant. This type of control is known as droop control and can be seen in Figure 5.5. It is equivalent to the primary frequency control that is applied to conventional synchronous generators. Once again, the droop control results in the inertial response torque term that is added to the speed controlled torque term.
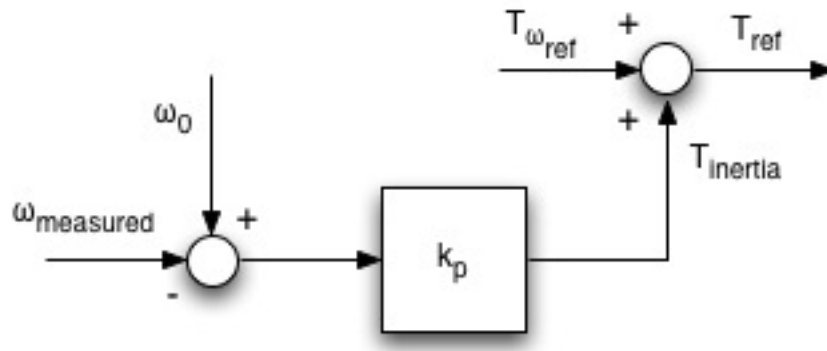
Figure 5.5: Droop Controller [18], [19], [20], [21], and [22]

As a result of both methods of inertial response control, the DFIG is able to utilize the mechanical inertia that is stored in the blades of the wind turbine. This allows the DFIG to act in a manner similar to the FSG with respect to the ability to handle changes in system frequency, but it also maintains the ability of the DFIG to operate at varying wind speeds,

allowing for larger levels of power generation. This control is very sophisticated, and as of now has not been implemented commercially on DFIG machines. Applying this control may be an option in the future and as seen in [18], [19], [20], [21], [22], and [23], the benefits may be substantial in maintaining greater levels of spinning reserve, however with the current demand for wind turbines today the control may be not be able to be implemented until further in the future. As a result, other options must be explored for maintaining spinning inertial reserve when large levels of DFIG generation are present in the system. These options will include some of the longer time frame control options and will be discussed in the following sections.

Regulation and AGC

The three methods of control discussed are examples of primary control that will be applied immediately after the load imbalance. Regulation is a control that is applied constantly to account for the minute-to-minute load fluctuations in the system. Regulation is vital since system loading is not constant and as it changes during from minute-to-minute, regulation is required to maintain the generation load balance in the system. As a result regulation is suited to deal with the unpredictable changes between load and generation over a small time period and is used to manage the tie-line flows and frequency between control areas. Regulation between control areas in the power system maintained primarily through the use of Area Generation Control (AGC).

Unlike the governor response to a load variation, AGC manages the small load perturbations and regulates the frequency between control areas to a specified nominal value [17]. AGC is achieved by maintaining the scheduled interchange values between control areas by controlling the output of selected generators in the system. In a system with a significant level of wind penetration, the regulation capability of the AGC might be significantly impacted and could required additional regulation capacity, however this will greatly depend on how the wind generation is integrated into the power system. If the wind farms interconnections are very sparse and include many small farms operating throughout the power system regulation cost may increase [31], [32]. This will be due the large level of

variability associated with each individual farm and the lack of correlation from one farm to another.

Through aggregation the large level of variability of a single turbine can be reduced considerably, i.e. larger farms of many interconnect wind turbines operating at many different speeds will be less variable than the output from a single turbine [31], [32]. This variability can be further reduced if the farm is interconnected into a control area with sufficient regulation capability [31], [32]. In fact, the increased cost of regulation is often negligible when the interconnecting farms are sufficiently large and placed in the appropriate control environment [33]. Essentially, since the regulation time frame is on the order of minutes, the changes in large wind farms are not very severe in comparison to the changes over long periods.

Load Following and Unit Commitment

Due to resource's inherent variability, regulation is an operation that is well suited to control the fluctuations of any interconnected wind generation. However, two longer time frames aspects of generation-load balance, load following and unit commitment, present greater challenges in systems with large penetration levels of wind generation. Load following occurs over a range of around 10 minutes to a few hours. By predicting the system loading during this period system operators attempt to maintain system capacity at the loading levels predicted for the next time horizon [32]. Figure 5.6 shows the time period over which regulation and load following occur.
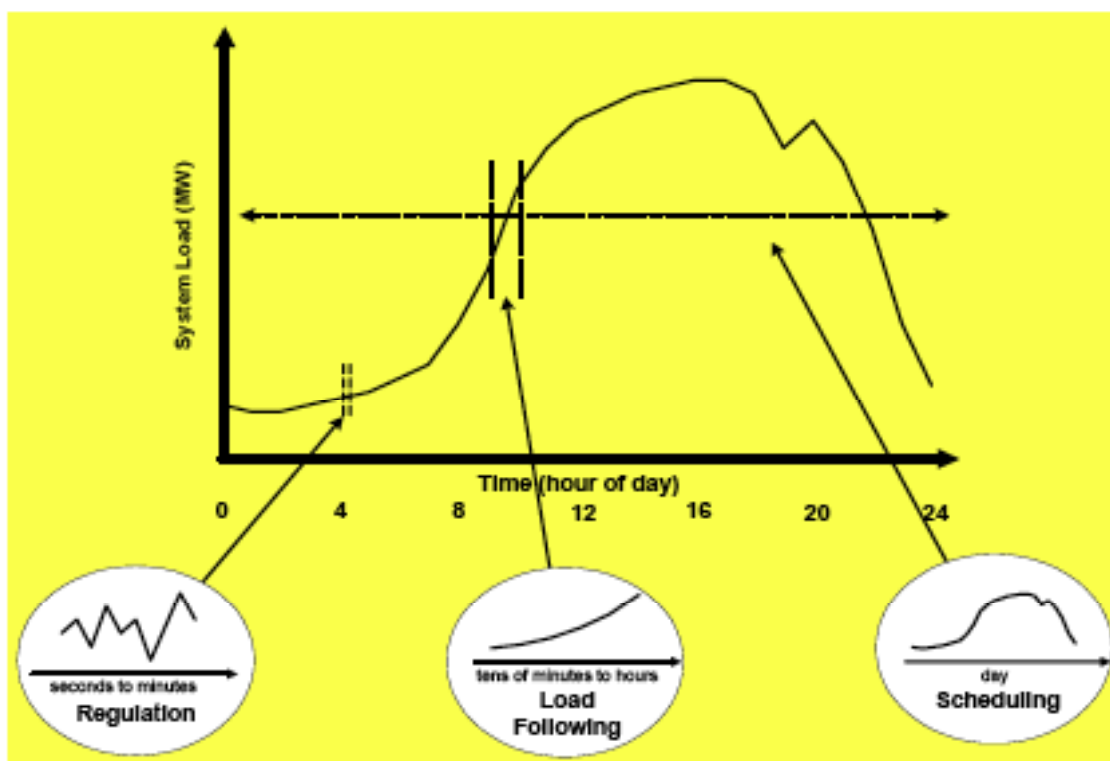
Figure 5.6: Generation-load balancing time frames for regulation and load following [32].

As seen in Figure 5.6, load following will attempt to ramp up and ramp down generation capacity to match the predicted load for a given time period. However, if wind generation is introduced into the system the task of load following becomes significantly more complicated. This is due to the increased error in wind forecasting as the time horizon increases. Figure 5.7 demonstrates the difficulty in predicting wind power production over longer period of time. Planning generation for a longer time horizon may introduce increased levels of error and require increased capacity to compensate for any short falls in prediction [32] and [34]. The difficulty is further exaggerated in the case of unit commitment which falls over a period of days. Unit commitment occurs when utilities schedule their generation levels based on the predicted load over several hours to a few days [32]. As a result, scheduling too much conventional generation on days when there are high wind speeds can increase cost, however scheduling insufficient levels of generation can also increase cost, requiring the utility to purchase electricity at high market prices. Load following and unit commitment are two crucial aspects that will need significant study in

order to accurately predict and schedule generation, as the penetration level of wind generation increases.
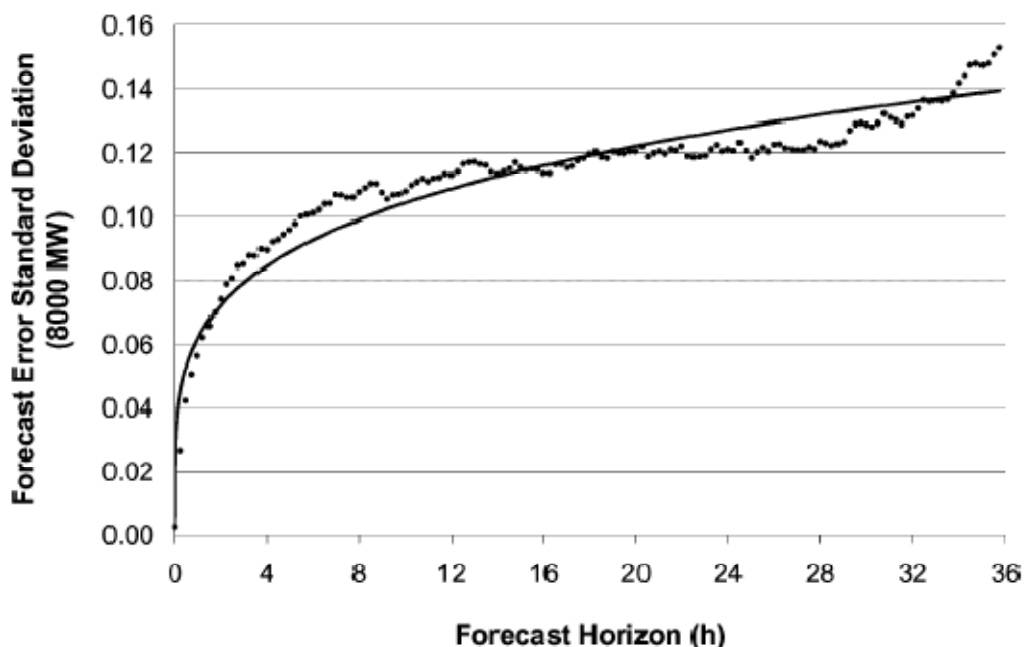
Figure 5.7: Forecast error in 8000 MW offshore wind farm [35].

PSS/E Dynamic Modeling Requirements

This section will focus on the primary control methods for frequency control using two types of wind turbines in a small, 6-bus test system. The goal was to explore what the effects of wind turbines are in a power system and how they affect the frequency control of the power system. As a result, simulations were performed in the PSS/E software platform. This section will detail the necessary requirement to model a wind turbine in PSS/E.

PSS/E provides a special external platform to incorporate different wind turbines into any system.   PSS/E Wind, the external platform, provides five wind turbine models in the standard package; the GE 1.5 MW and 3.6 MW turbine model, the Vestas V47 and V80 turbine model, and a generic WT3 DFIG wind turbine model. The GE models are both DFIG machines with WindVAR control [36]. The WindVAR control is the control scheme applied by the GE corporation for voltage control at a designated control bus at either a terminal

voltage value, e.g. 1.05 p.u. or at a designated power factor. The Vestas machines are both variable speed machines that use DFIGs, however they are not capable of voltage control. They are designed using the OptiSlip system, which controls the slip of the DFIG to produce optimal power for varying wind speeds [37]. The WT3 DFIG is a generic model of the DFIG with GE's WindVAR control implemented. The differences between the GE model and the WT3 will be discussed in the next section

PSS/E DFIG Modeling

Initially, the dynamic study in PSS/E was conducted using the GE 1.5 turbine model that was available in PSS/E Wind. During the course of this study the frequency of the system was observed at different DFIG penetration levels for the same loss of generation event. The event in the case of the 6-bus test system was the loss of the 100 MW conventional plant at bus NGEN. The goal of this study was to examine the frequency of the system based on the current specifications of DFIG machines today; in particular, since the DFIG decouples the blades and generator, there should be no inertial response from the DFIG farm for a loss of generation event. Based on this, as generation is reduced at conventional plants and increased at the DFIG farm, the system frequency should degraded during the event, i.e. the frequency dip should grow as more DFIG is introduced into the system. However, it was observed that this was not the case when the GE 1.5 model was used in the study. In fact, the system frequency improved as the DFIG penetration increased from 15% to 22.5%, these results can be seen in Figure 5.8.

Based on this result the power output of the DFIG farm was monitored for the same event at the two penetration levels, Figure 5.9. From Figure 5.9, it can be observed that the power output of the DFIG farm actually increases following the event. This would imply that the DFIG is "storing" kinetic energy and not producing the optimal level of wind generation for the given wind speed. However, based on the discussion of Chapter 4, this is not true, and unless inertial control is implemented, the DFIG should always be producing the optimal level of power for any given wind speed.

To resolve this phenomenon, the WT3 model was used in place of the GE 1.5. Along with replacing the model, the K_{PLL} constant was increased from 40 to 150. The K_{PLL}

constant governs the phase lock loop of the DFIG model, and was increased based on discussions with individuals at GE [38]. The results of these changes can be seen in Figure 5.9 and 5.10, where the power output and system frequency are compared between the GE 1.5 and WT3 models, respectively. Figure 5.9, compares the power output between the two turbine models, as observed, the power output from the WT3 turbine stays constant during pre and post-event conditions where as the power output from the GE 1.5 turbine increases post-event. Since this power increase is no longer present from the DFIG farm, the system frequency is lower when the WT3 turbine is used. Using this turbine, a more accurate representation of the system frequency and power production capability of the DFIG farm is achieved. As a result, the WT3 wind turbine was used for all simulations involving DFIG machines.
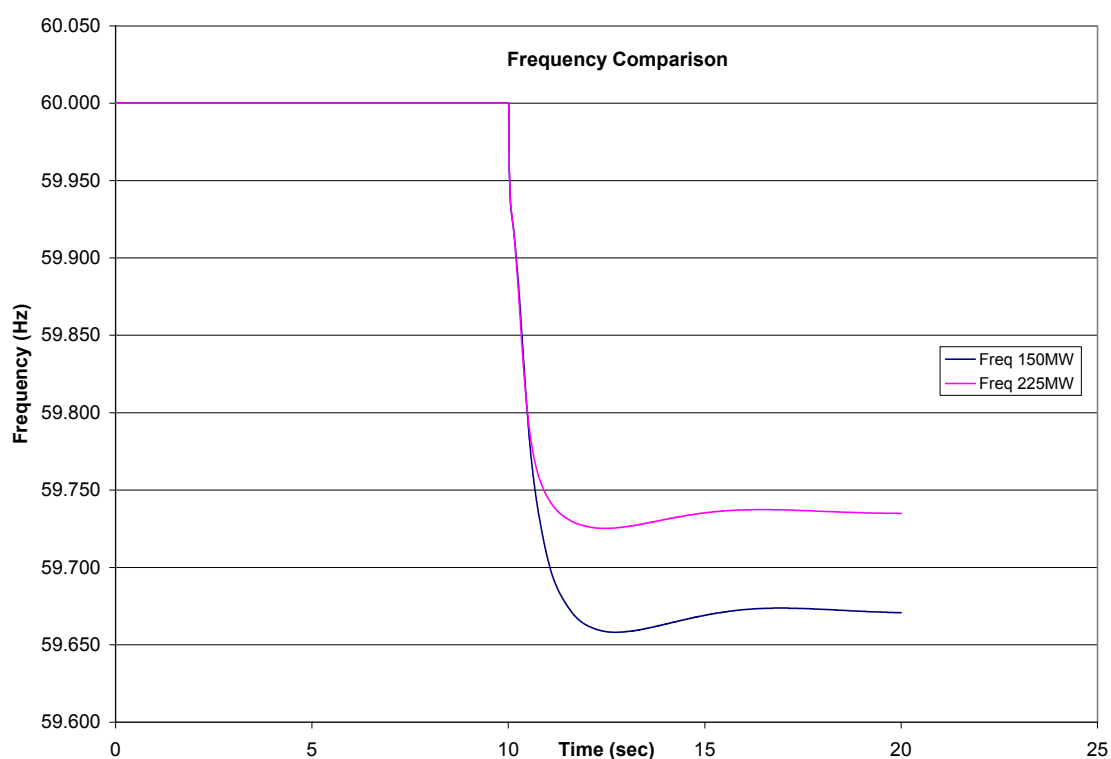
Figure 5.8: Frequency simulations at 15% and 22.5%. System frequency improves when more DFIGs are present in the system
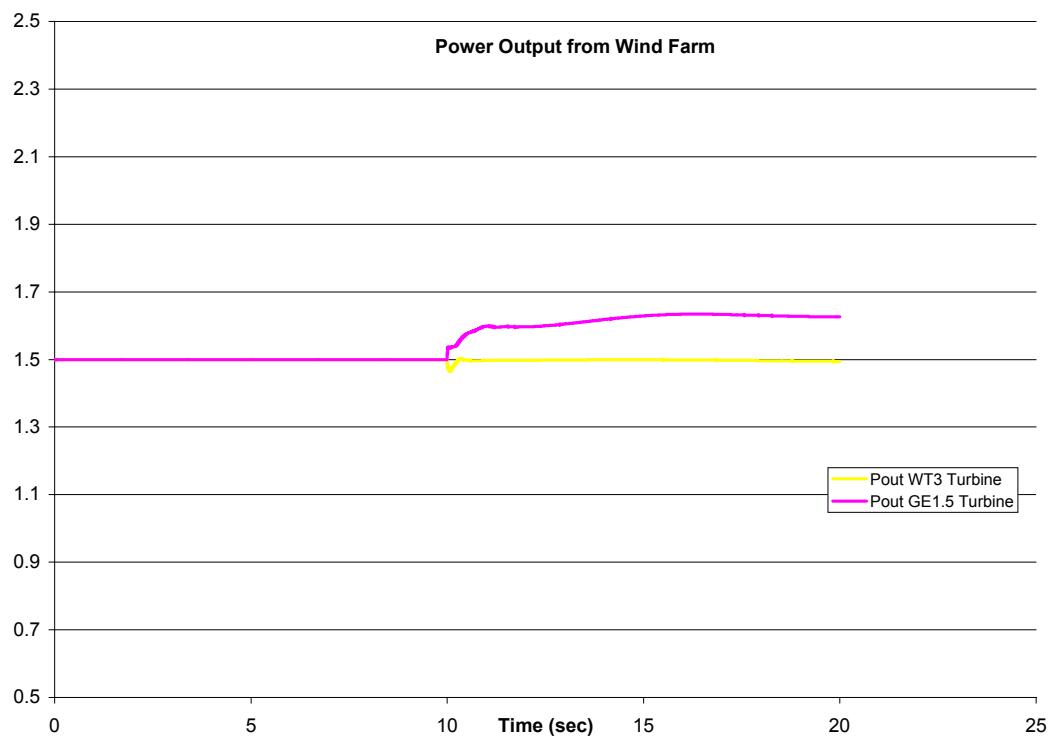
Figure 5.9: Power output from DFIG farm for GE 1.5 wind turbine and WT3 wind turbine. Power increases post-event in GE 1.5 wind turbine.
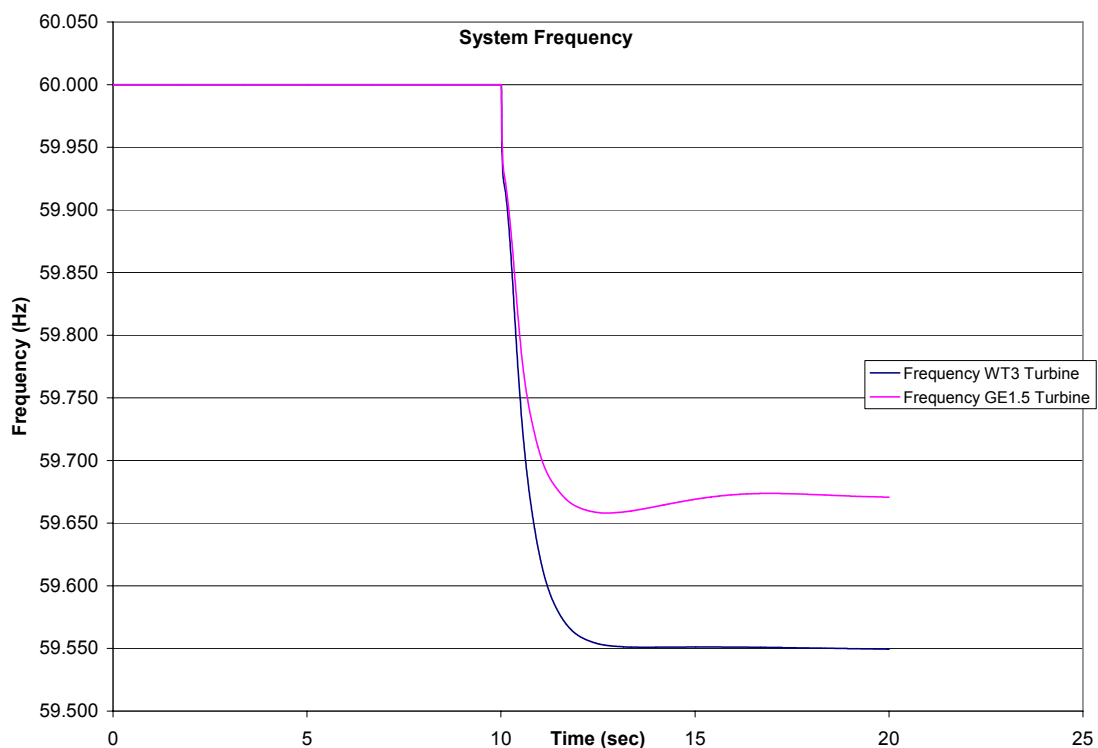
Figure 5.10: Frequency simulations for GE 1.5 and WT3 wind turbines. Frequency dip is larger when WT3 wind turbine model is used for simulation.

PSS/E FSG Modeling

In the PSS/E model library there is no representation of FSG wind turbine. As a result, the following substitution was necessary. From the standard model library, an induction generator, CIMTR1 [39] was used with the appropriate generator constraints [17]. Based on the instructions provided in the PSS/E user manual, the induction generator was represented as squirrel induction generator [40]. A lumped inertial constant was placed on the shaft of the machine to represent the inertia of the blades, shaft, and rotor. This is not truly representative of the FSG, the lumped mass model neglects oscillations that may occur due to the many inertias rotating in the turbine (see Chapter 4 for further explanation. However, it allows for the correct representation of the reactive power consumption while providing a natural inertial response for a loss of generation event. Future studies may want to contact manufacturers of FSG wind turbines to obtain proprietary models that will detail the oscillations in the turbine and provide more accurate results. This study will use the modified induction generator for all dynamic simulations using FSG wind turbines.

Results of Dynamic Studies

This section will present the results of the dynamic frequency simulations run on the system in Figure 5.1. Before the results are presented the initial conditions of the system will be discussed as well as the test scenarios. This will include how generation and load were varied in the system, as well as how the wind penetration levels were changed from one simulation to another.

Initial Conditions and Test Scenarios

For the 6-bus test system given in Figure 5.1, the effects of wind generation needed to be examined in a variety of conditions. Several conditions were altered and the results were monitored. In particular the primary frequency control ability of the system was monitored for two conditions.

1. The influence of unit decommitment versus load increase was investigated. This meant that as wind generation was added to the system, conventional generation was decommitted. For example, if 100 MW of wind generation was added to the system, the maximum generating capacity of a designated generator was decreased by 100 MW. In the case of the 6-bus test system, this designated generator was unit 2 at the NGEN bus. Next, rather than decommitting generation, loading was increased to accommodate the new wind generation. Similar to the generation decommitment scenario, if 100 MW of wind generation was added, load in the system was increased by 100 MW. The purpose behind these simulations was to examine the effect of wind generation on the system's spinning inertial reserve. This issue will be discussed in the next section.

2. The influence of turbine type on primary frequency control. For these simulations, the ability of the DFIG and the FSG to respond to a loading imbalance was observed at three penetration levels, 15%, 22.5%, and 30%. The purpose behind these simulations was to determine the ability of the turbine to responds to a loading imbalance under varying operating conditions.

Results of Dynamic Simulations for Frequency Response

For the first set of simulations the effect of DFIGs on system frequency was explored. First, 150 MW of DFIG wind generation was connected at bus NST and two separate sets of initial conditions were applied to the system. First, with the 150 MW of generation connected, the maximum power production capability of machine 1 at bus NGEN was reduced by 150 MW from 400 MW to 250 MW. This decommitment of generation reduced the level of inertia present in system. Next rather than decommitting generation, the loading in the system was increased by 150 MW. This meant that the inertia present in the system was the same as in the base case scenario, where there was no wind generation present. Using these two scenarios, a loss of generation event was applied to the system in the form of the drop of a 100 MW unit at bus NGEN at time t=1 second. The effects of this event can be seen in Figure 5.11. When generation was decommitted, the system frequency response degraded, meaning there was an increased dip versus the loading increase following the same

loss of generation event. This was expected since there was less inertia present in the system when the generation at bus NGEN was reduced.
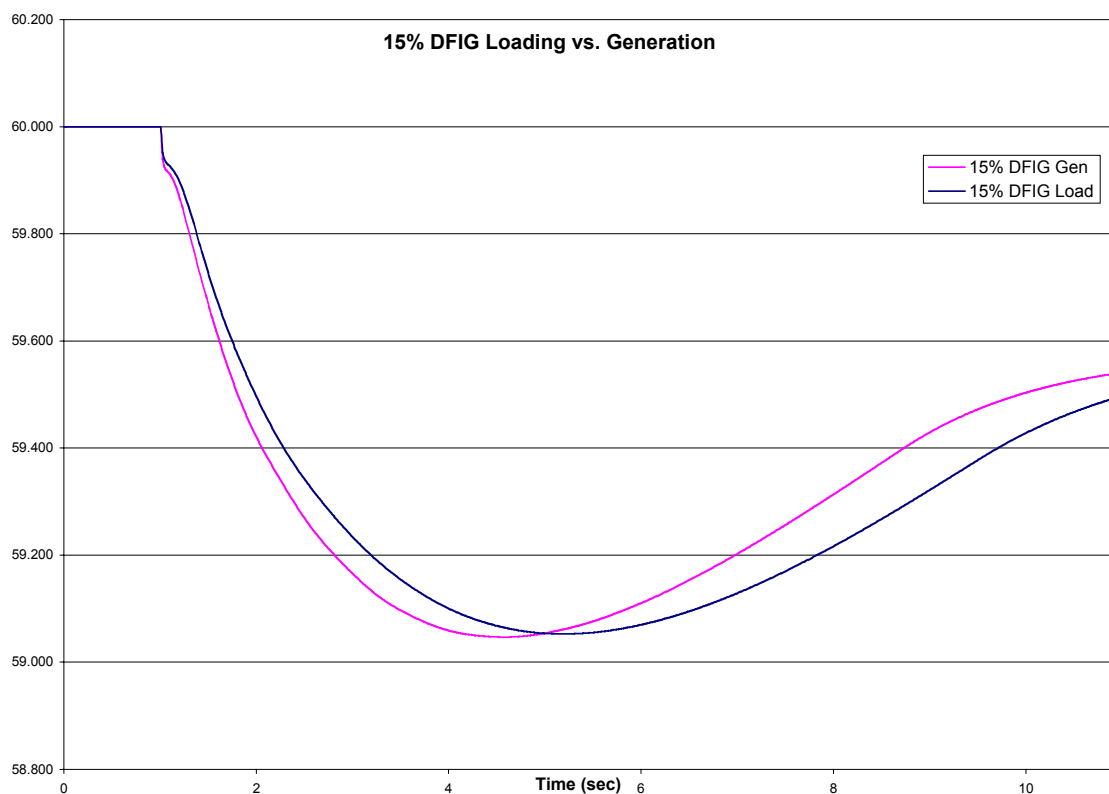
Figure 5.11: Frequency comparison for 150 MW (15%) of DFIG penetration. System frequency response is improved when load is increased compared to generation decommitment.

Following the simulations at the 15% penetration level, wind generation was increased to 225 MW or a 22.5% penetration level in the system and then to 300 MW or 30% penetration level. Simulations were run using the same two scenarios from the 15% penetration level. Generation was decommitted and load was increased by the corresponding penetration level to provide two simulations at each level. The results of these simulations can be seen in Figures 5.12 and 5.13 for the two system scenarios.
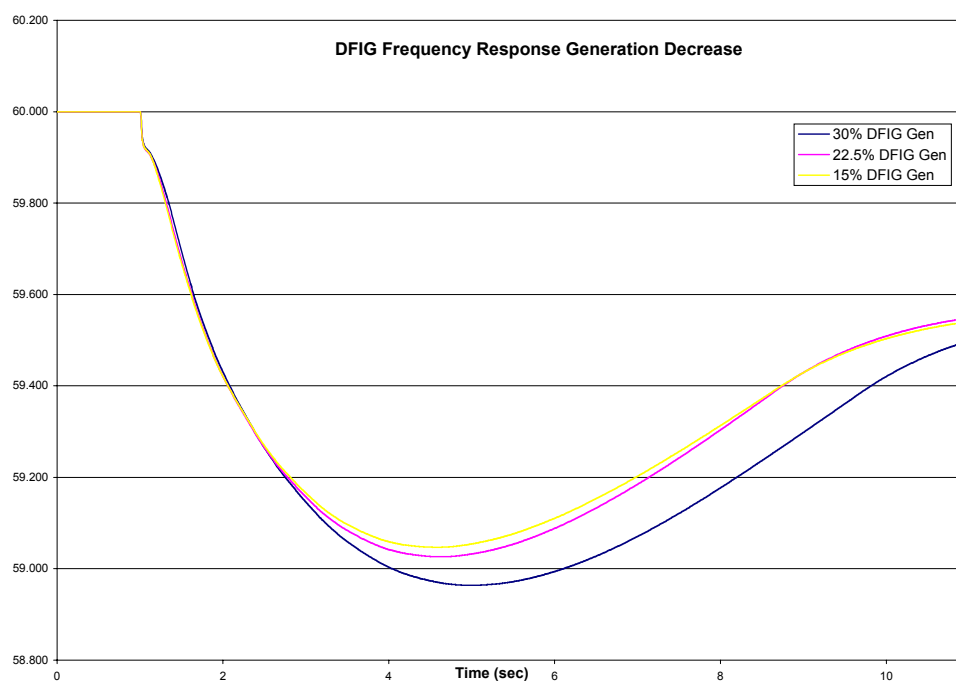
Figure 5.12: System frequency response at 15%, 22.5% and 30% penetration levels with a system generation decommitment. The system frequency further degrades as more DFIG wind generation is added to the system
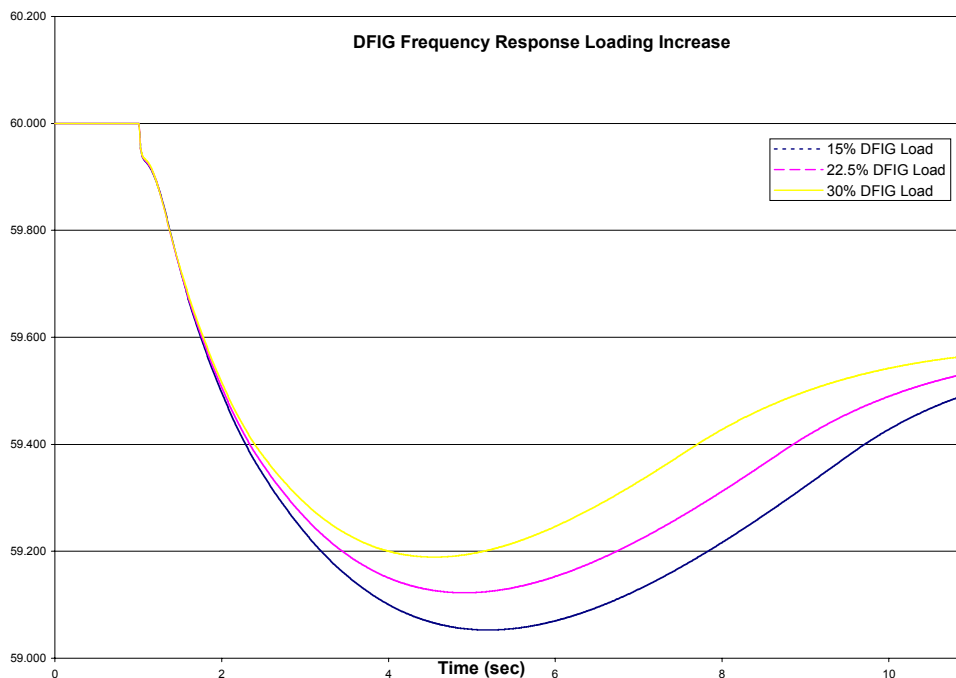
Figure 5.13: System frequency response at 15%, 22.5%, and 30% penetration levels with a system loading increase. The system frequency further improves as more DFIG wind generation is added to the system.

Figures 5.12 and 5.13 demonstrate how important the overall level inertia present in the system is to the system's frequency response. Figure 5.12 shows that when generation is decommitted as the level of DFIG penetration increases the system frequency degrades. Since DFIGs provide no inertial support the total level of inertia present in the system decreases when DFIGs are added and conventional generation is decommitted, as a result the frequency response is progressively worse as the DFIG penetration increases. In Figure 5.13, the response is dramatically different, in each of these cases, rather than decommitting generation the system loading was increased maintaining the power balance in the system. As a result, the inertia in the system is the same for all cases. When the DFIG penetration is increased the frequency response of the system improves since there is more generation present and there is a larger level of inertia capable of responding to the loss of generation event. This would suggest that if a system operator desired to increase the wind penetration in a system using only DFIGs, they should be wary of decommiting conventional generation in order to accommodate the new wind generation as the system frequency could suffer during a loss of generation event. A full comparison of the various system frequency responses can be seen in Figure 5.14.
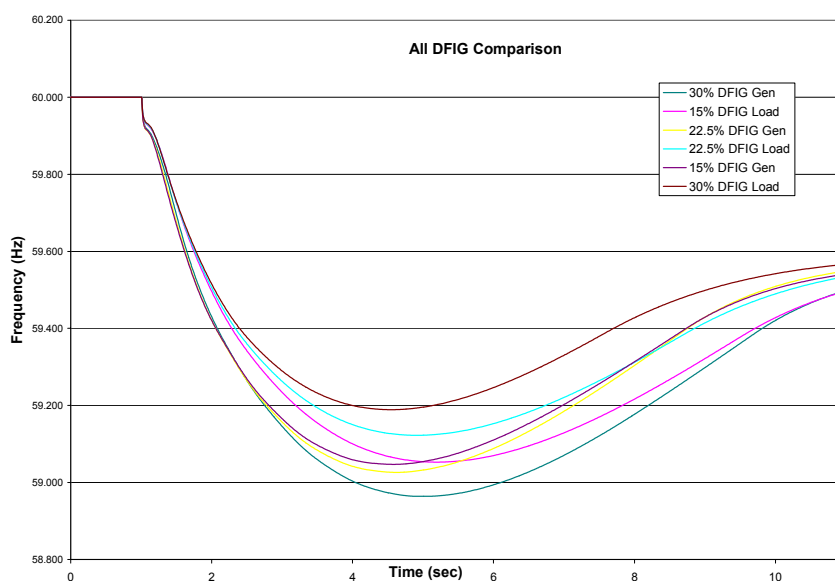
Figure 5.14: System frequency response for 15%, 22.5% and 30% DFIG penetration levels. Frequency dip is most severe at 30% penetration level with generation decommitment, when system inertia is at a minimum.

To establish a relationship between the frequency response and penetration level of DFIG turbines, the nadir or minimum in the frequency was observed during each trial. They are described in Table 5.1.

Table 5.1: Frequency Nadir Achieved for Loss of Generation Event

DFIG Scenario	15% Generation Decommitment	22.5% Generation Decommitment	30% Generation Decommitment	15% Loading Increase	22.5% Loading Increase	30% Loading Increase
Frequency Nadir (Hz)	59.047	59.026	58.964	59.053	59.122	59.189

Plotting the results of Table 5.1 provides a linear relationship between frequency nadir and increased wind penetration levels with loading increases. There is a non-linear relationship for increased wind penetration levels with generation decommitment, however the result can be extrapolated into a linear relationship. The results can be seen in Figure 5.15. This means that if the new wind generation is balanced with new load, the system frequency nadir will improve at a rate of 0.009067 Hz for every 1% of new DFIG wind generation introduced to the system. Using linear regression to represent the trace of generation decommitment a rate of decrease was determined to be 0.005533 Hz for every 1% of new DFIG wind generation. The results achieved for the wind penetration level and nadir decrease or increase, are unique to the system used in the simulations. By observing the frequency nadir and carefully controlling the penetration levels of the new wind generation, similar results can be achieved for other electricity systems.

This constant value can provide insight into a systems behavior and generalize its reaction to large levels of new wind generation. For example, if this particular system were to achieve a 50% penetration of wind generation with a loss of 100 MW, one would expect for the generation decommitment scenario a nadir of 58.862 Hz. This value is very low and would create serious problems for machines and loads in the system. 100 MW is also a relatively small level of generation loss, as such large losses of generation would have greater impacts on the frequency nadir. Extrapolating such information from the simulations

provides valuable theoretical insight as to how the system may react at large wind penetration levels.
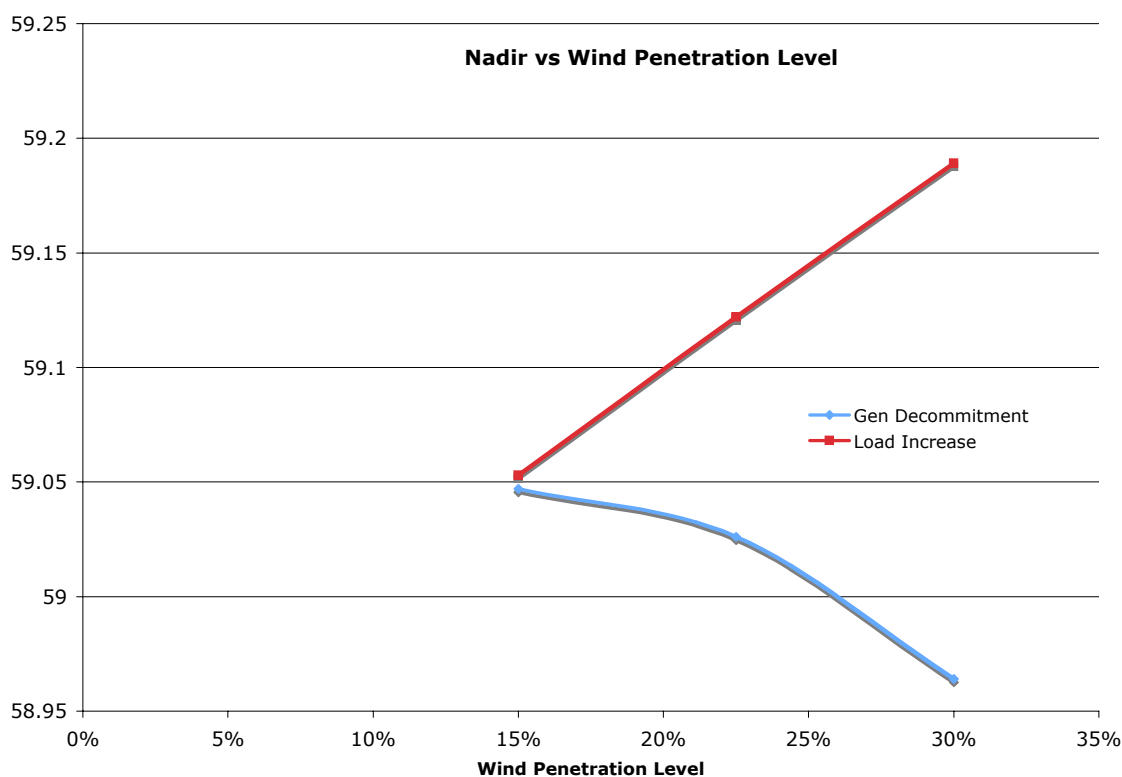
Figure 5.15: Frequency nadir plotted against wind penetration level for two system scenarios.

Following this set of simulations the DFIGs in the system were replaced with FSG wind turbines.

Since FSG wind turbines are capable of providing the system with inertia, the results are drastically different in comparison to the DFIG simulations. As a result, Figure 5.16 shows the system's frequency response as FSG penetration increases. The system frequency remains nearly constant as penetration increases. This is due to the fact that the FSG turbine can provide inertial support and as a result the overall level of inertia remains very close to the base case value as the FSG grows. However, the increased presence of inertia with the FSG turbines provide an improved response in comparison with the DFIG machine, Figures 5.17, 5.18, and 5.19.
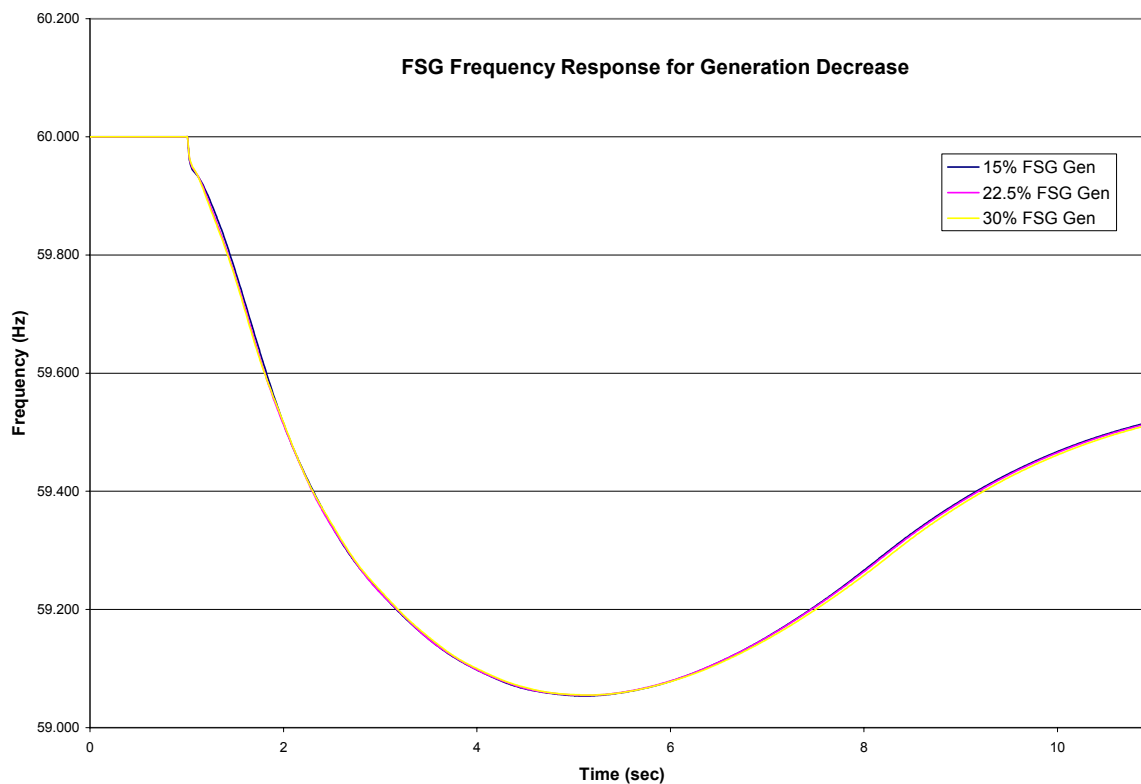
Figure 5.16: Frequency response at 15%, 22.5% and 30% for FSG wind turbines with generation decommitment. Increased penetration of FSG wind turbines improves the system's frequency response.
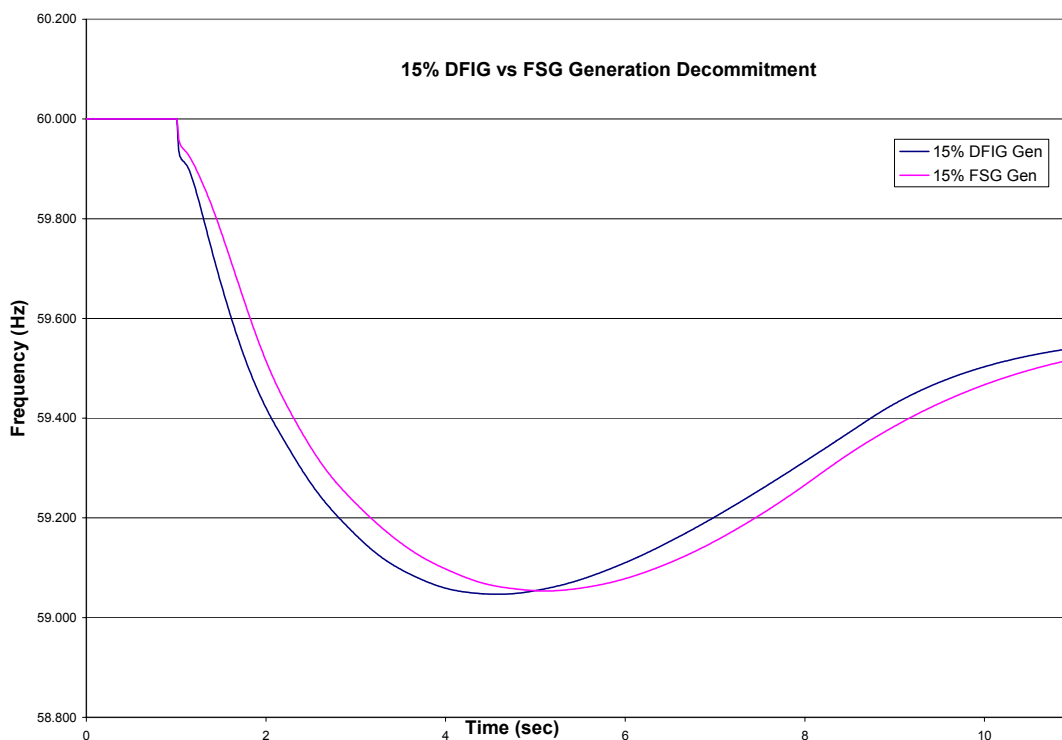
Figure 5.17: Frequency response at 15% for FSG and DFIG wind turbines with generation decommitment, showing the impact of turbine type on the system.
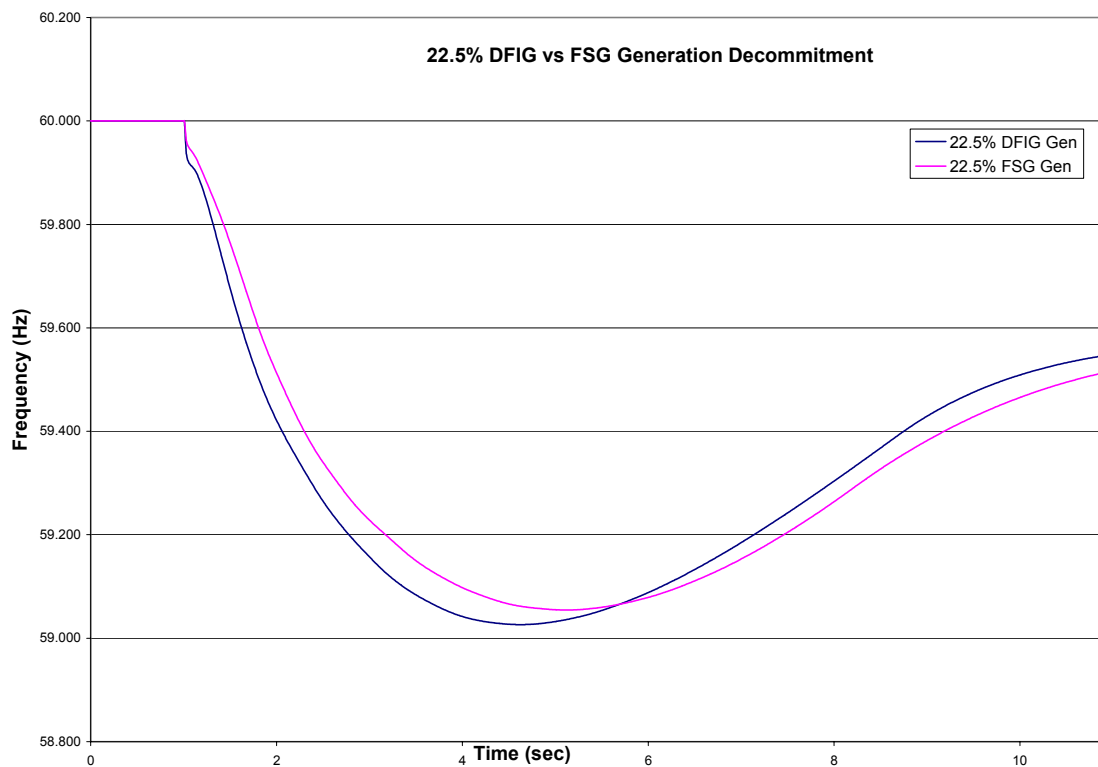
Figure 5.18: Frequency response at 22.5% for FSG and DFIG wind turbines with generation decommitment, showing the impact of turbine type on the system.
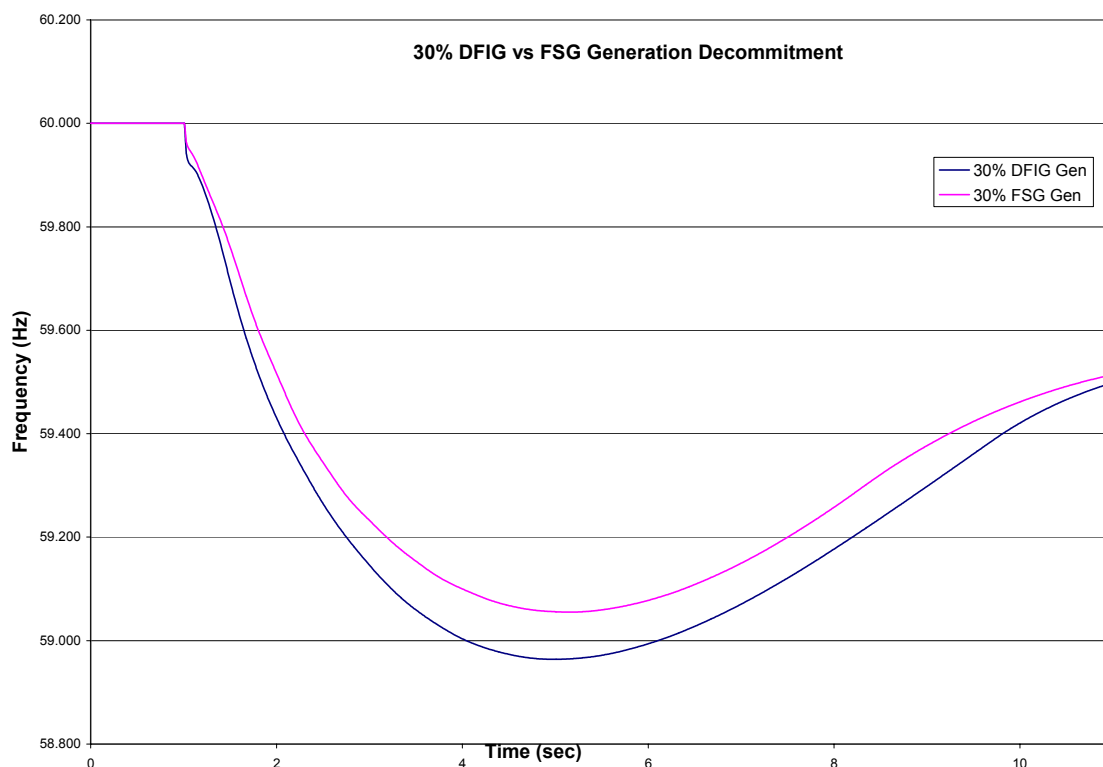
Figure 5.19: Frequency response at 30% for FSG and DFIG wind turbines with generation decommitment, showing the impact of turbine type on the system.

Using the same procedure as in the DFIG simulations, the next set of simulations on the FSGs increased the loading in the system to accommodate the new wind generation rather than decommiting the generation at a conventional plant. Figure 5.20 provides the frequency response plots for the system as the penetration level of FSGs is increased. As seen in the DFIG simulations with loading increases, the frequency improves as the presence of the FSGs in the system increase. In fact, the response is improved over the same levels of DFIG penetrations, Figure 5.21. This can be seen in the relationship between frequency nadir and FSG turbine penetration, Table 5.2
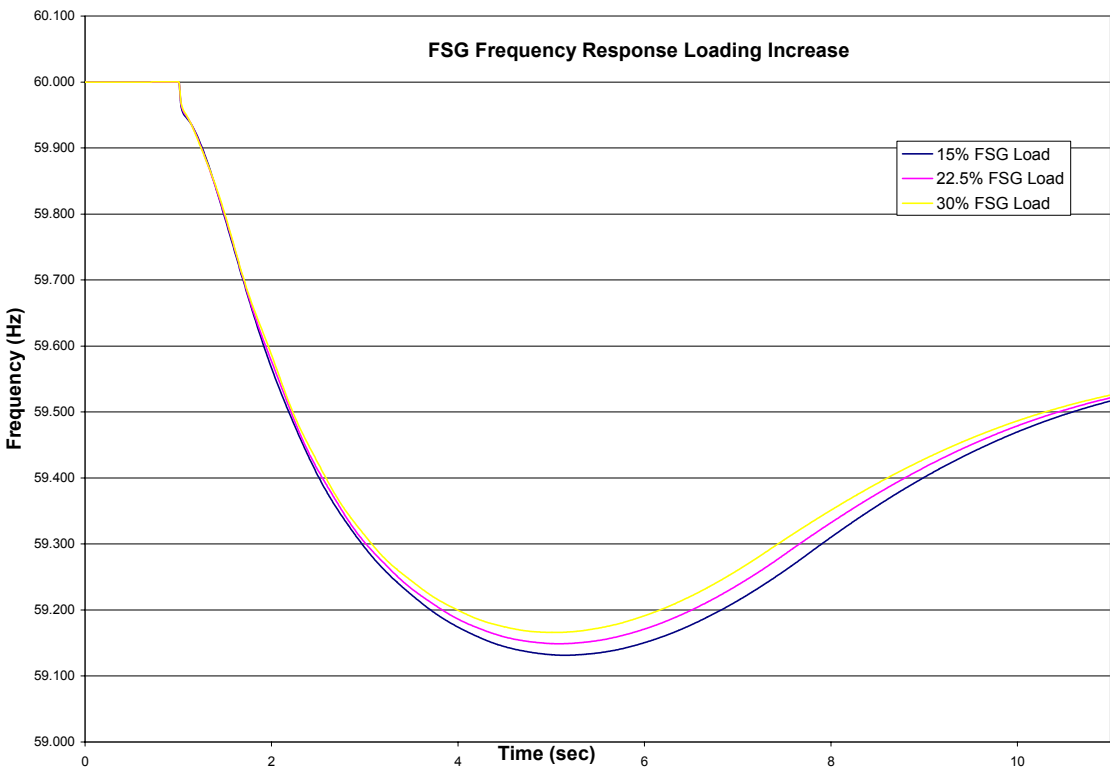
Figure 5.20: Frequency response at 15%, 22.5%, and 30% for loading increases in the system. Frequency improves as FSG penetration increases due to the increased level of inertia in the system.
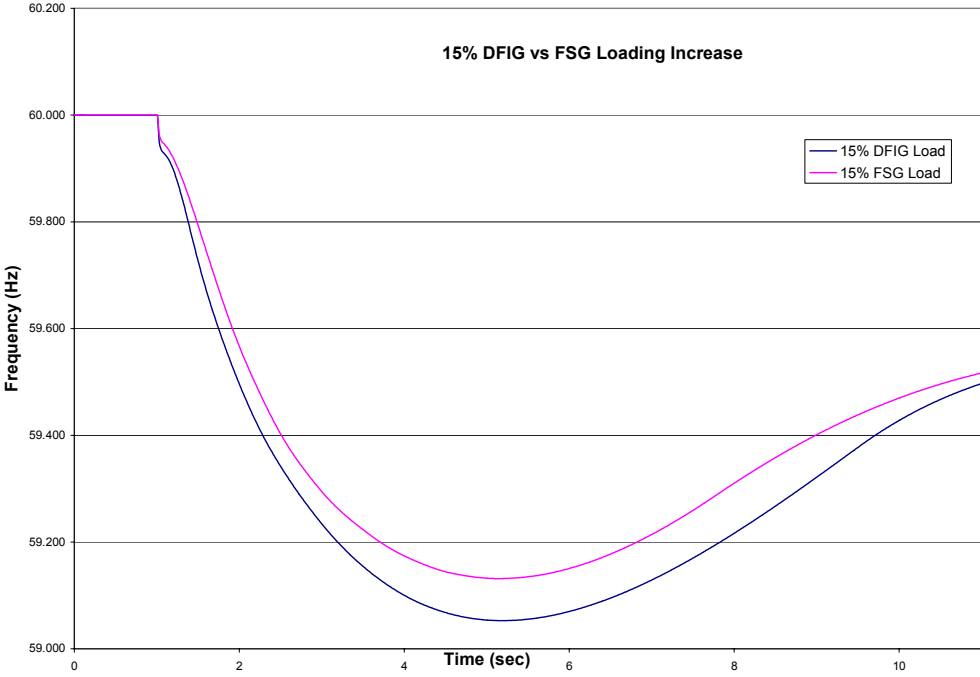
Figure 5.21: Frequency response comparison at 15% for DFIG and FSG wind turbines. There is an improved response with FSG turbines.

Figure 5.22 plotted the resulting nadir against the varying penetration levels of FSG turbines to see if there was a relations ship between the increase in wind penetration and the minimum frequency achieved following a loss of generation event.   Table 5.2 shows the resulting nadirs at their corresponding penetration levels.   Once again a nearly linear relationship is established for the increase in wind penetration and nadir achieved during the loss of generation event.   When generation is decommited and FSG wind penetration increases, the nadir remains constant. However, when generation is kept constant and system loading is increased to accommodate the new FSG generation, the nadir increases at a rate of 0.004267 Hz for every 1% penetration increase.

Compared to the rate achieved for DFIG penetration increases with loading increases it is less, however the minimum frequency achieved is increased in the case of FSG wind turbines. Similar to the DFIG, the results for the FSG can provide insight into how the system frequency will change as penetration increases or decreases. Due to the FSG's ability to provide an inertial response frequency is almost always positively affected.

Table 5.2: Frequency Nadir Achieved for Loss of Generation Event

FSG Scenario	15% Generation Decommitment	22.5% Generation Decommitment	30% Generation Decommitment	15% Loading Increase	22.5% Loading Increase	30% Loading Increase
Frequency Nadir (Hz)	59.054	59.055	59.055	59.132	59.169	59.196
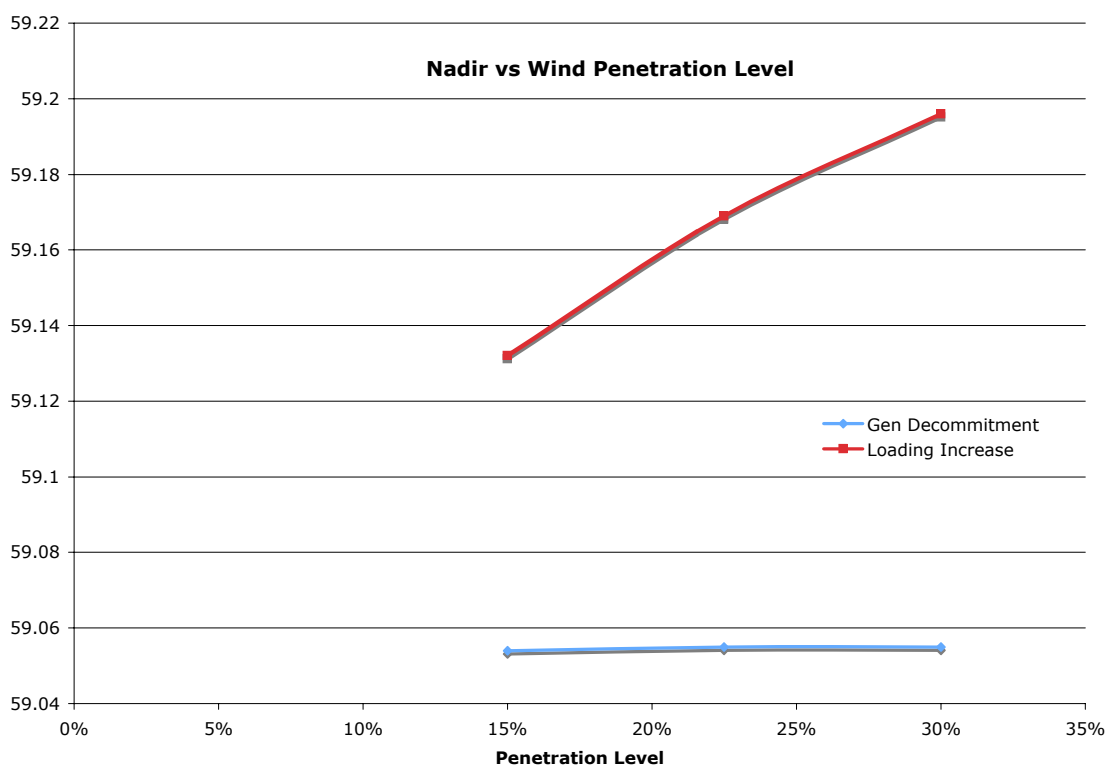
Figure 5.22: Frequency nadir versus FSG wind penetration increases.

Overall, the series of simulations show that frequency improves in either one of two ways; First, generation commitment or decommitment plays a significant role in determining the system's frequency response. By decommitting generation, the overall level of inertia is reduced, and more stress is placed on synchronous units in the system. Without, adequate levels of support from the synchronous machines in the system the frequency falls significantly and the system would require additional inertial support. Secondly, turbine type plays an important role in determining the systems frequency response. Through the simulations, it can be observed that the inertia present in the FSG wind turbine improves system frequency response when compared with the simulations when DFIG wind turbines are present in the system. The improved response can be attributed to increased presence of inertia in the FSG wind turbines, as that was the major difference between the two simulations.

CHAPTER 6: VOLTAGE SIMULATIONS AND SOFTWARE COMPARISON

The purpose behind this chapter was to develop an understanding of the voltage capability of the DFIG and FSG. This was done in order to examine what the trade-off would be for a utility if they were to focus exclusively on the frequency aspect of wind turbines. DFIGs and FSGs present as natural opposites in their ability to cope with frequency and voltage. In DFIGs voltage control is integrated system and the purpose of the turbine is to incorporate voltage regulation in conjunction with power production. In creating the ability for voltage regulation the DFIG loses its inertial response. Chapter 5 demonstrated some of the theoretical concepts for frequency control but they are not as yet available on any of the commercial turbines available today. The FSG on the other hand, has a natural inertial response, but no ability to control voltage. This chapter will provide an overview of the voltage regulation capability of both turbines along with a comparison with another software platform for dynamic simulation, Eurostag.

Results of Dynamic Simulations for Voltage Performance

Following the completion of the dynamic studies involving the frequency response turbines, simulations that explored the voltage performance of the turbines types were run. Rather than exploring the inertia response obtained from the two types of turbines, the goal of the voltage stability simulations was to examine the reactive power production capability of the DFIG. As detailed in Chapter 4, the DFIG's decoupled structure allows for the implementation of voltage control. In the case of these simulations the control of the DFIG was applied in the form of terminal voltage control at the collector bus of the wind farm. The FSGs were modeled as induction generators with capacitive compensation as to allow the power factor at the collector bus to be 0.95 inductive. As mentioned in Chapter 4, this model of the FSG does not represent the true nature of the turbine. Only the reactive consumption of the FSG is represented in the lumped mass model, to accurately represent the turbine, a higher order model needs to be incorporated into the simulations. Due to the limited

availability of turbine models, the lumped mass model was used for the voltage simulations as well.

To explore the voltage stability of the turbine types, two aspects of the voltage were monitored as the penetrations of DFIGs and FSGs were varied through out the system. First, the terminal bus voltages were monitored as DFIGs and FSGs were added to the system and secondly, the minimum voltage dip of the system during a line faulting event was observed. The fault applied at the 380kV line between bus NHV1 and NHV 2 as indicated in 6.1 and was a $0.2j$ impedance fault applied for 150 ms or 9 cycles in accordance with FERC Order 661 [41].
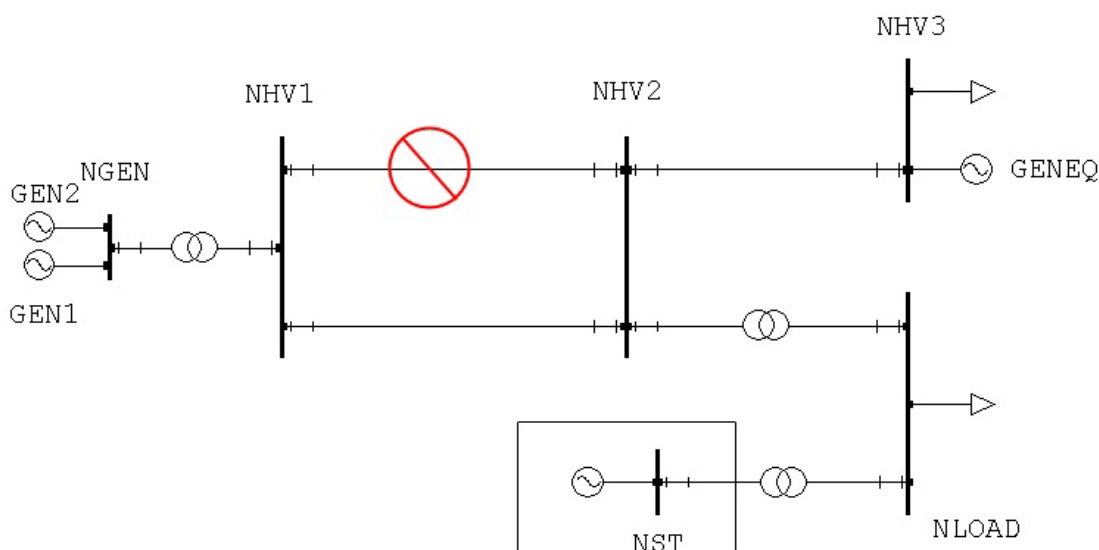
Figure 6.1: Location of fault applied to the 6-bus test system

Before the faulting simulations were run, the impact of wind turbines on steady state conditions was observed. As seen in Table 6.1, the presence of DFIGs improved terminal voltages during steady state conditions. Average voltages in the system increased as the penetration of DFIG turbine increased, rising from 0.94065 at 15% DFIG penetration to .944767 at 30% DFIG penetration. The difference in average voltage was more pronounced when the DFIGs were replaced with FSG wind turbines. At the 30% penetration level the average voltage dropped to 0.91785 when FSGs were installed in the system. This begins to highlight the differences in voltage impact the two types of turbines have; FSGs negatively impact the voltage of the power system with their large reactive consumption requirements,

whereas DFIGs utilized in the appropriate manner can raise voltage levels across the system. Even though there is capacitive support at the FSG bus the voltages are lower when compared to the same penetration level of DFIGs. Since there is no voltage control applied at the FSG bus, as the size of the farm grows the size of the capacitor bank or SVC must grow as well. This means that FSG farms will require additional support to maintain nominal voltage levels whereas the DFIG farms will be able to provide the necessary support and maintain the appropriate voltage levels on their own.

Table 6.1: Terminal Voltages for Varying Penetrations of DFIGs and FSGs

BUS	1	2	3	4	5	6	Average
15% DFIG	1.000	0.9466	0.9377	0.9366	0.9330	0.8900	0.94065
15% FSG	1.000	0.9411	0.9240	0.9228	0.9140	0.8665	0.928067
22.5% DFIG	1.000	0.9472	0.9406	0.9370	0.9376	0.8961	0.943083
22.5% FSG	1.000	0.9392	0.9192	0.9153	0.9079	0.8594	0.9235
30% DFIG	1.000	0.9485	0.9424	0.9358	0.9410	0.9009	0.944767
30% FSG	1.000	0.9367	0.9131	0.9060	0.9004	0.8509	0.91785

Following the steady state voltage analysis, the faulting simulations were run for the same 6-bus test system. In Figure 6.2, the terminal voltage at the wind turbine interconnection bus, NST, can be seen following the application and clearing of a fault at the 15% penetration level for both DFIGs and FSGs. From Figure 6.2, it can be observed that both types of turbines can handle the application of the fault and can recover to the appropriate voltage level following the clearing of the fault.

Following the simulation at 15%, the penetration level of the wind turbines was increased to 22.5%. The results of the same faulting simulation can be seen in Figure 6.3. Here, the results are following the trends described by the steady-state simulations as well as the first dynamic simulation. The voltage level is lower when the penetration level of FSGs

is increased and the recovery following the clearing of the fault is significantly slower. The opposite is true for the increasing penetration level of DFIGs; the voltage is increased and the recovery following the clearing of the fault is not significantly changed. Figure 6.4 shows the results at the 30% penetration level, here the voltage race for the FSG is degraded the most and takes longer to recover to the pre-fault conditions.
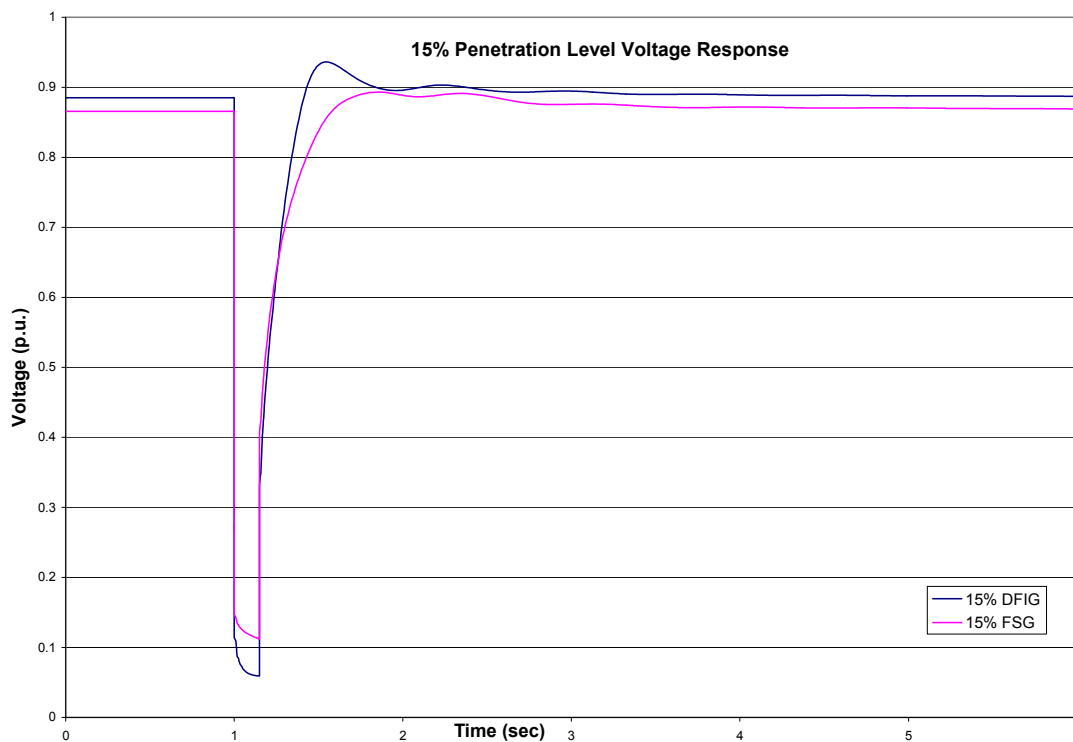
Figure 6.2: Voltage simulation at 15% penetration level. DFIG presence indicates a slightly faster recovery.
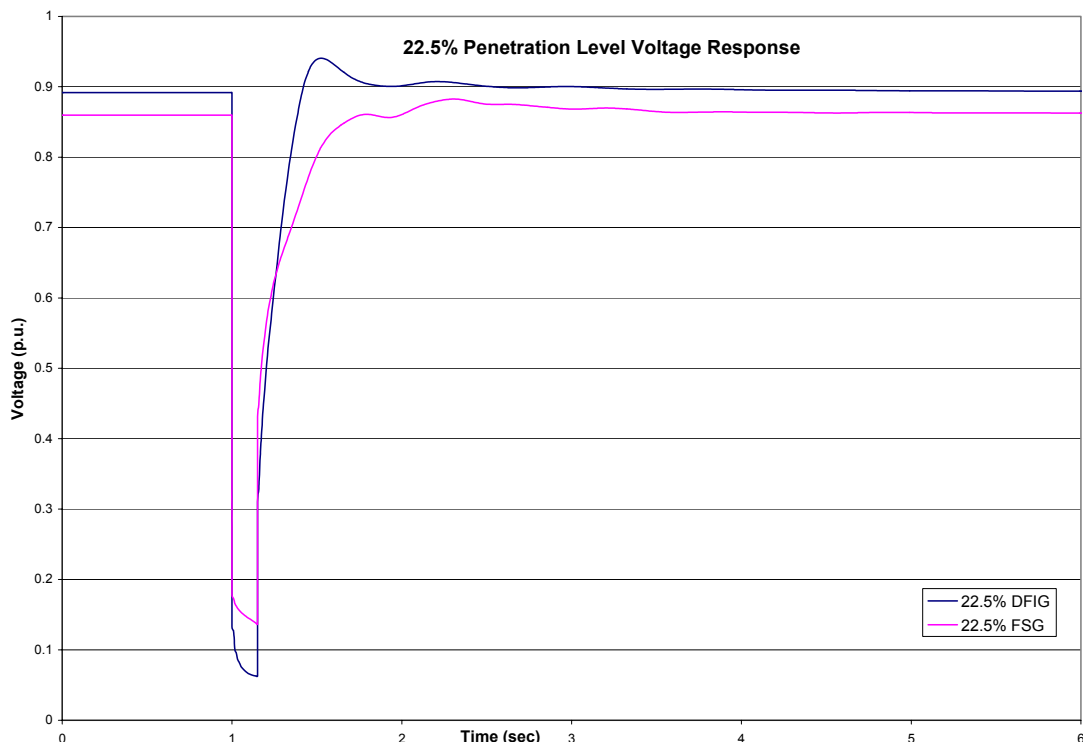
Figure 6.3: Voltage at 22.5% penetration level. The FSG response is degraded over the 15% penetration level while the DFIG response improves
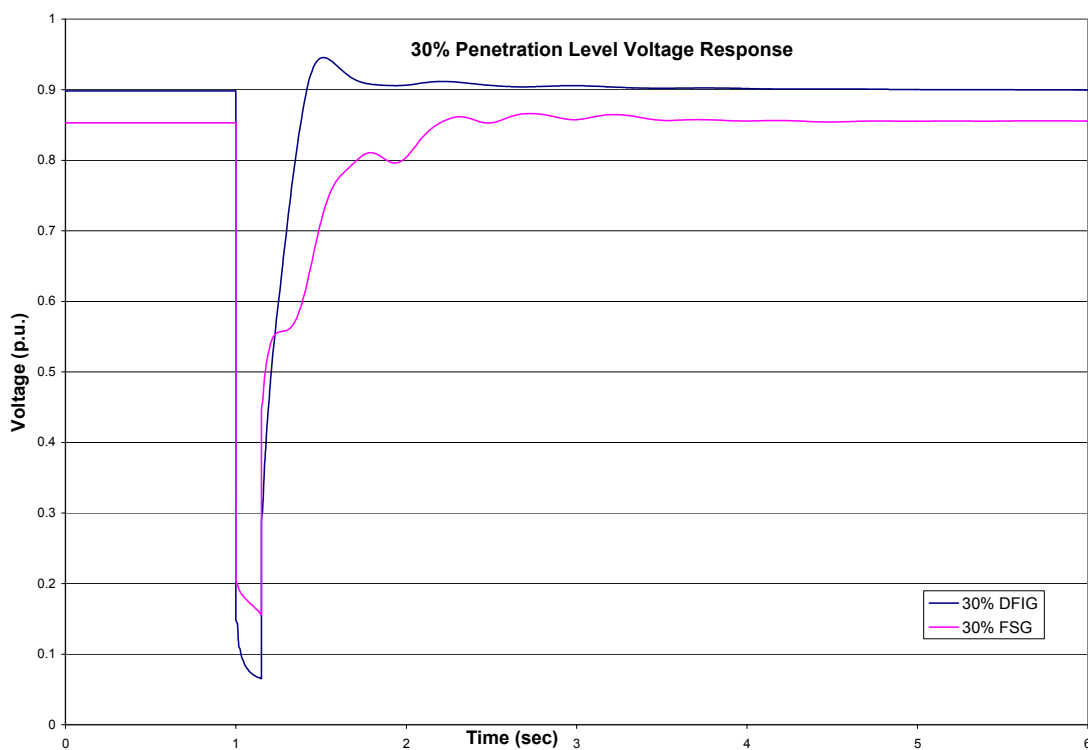
Figure 6.4: Voltage simulation at 30% penetration level.

In Figures 6.2-4, the voltage recovery is improved as the penetration level of the DFIG wind turbine increases; however the dip is not improved in comparison the FSG turbine. For the simulation in Figure 6.5 the size of the fault was increased from 0.2j to 0.02j and as a result shows the consequence of increasing the severity of the fault.

The DFIG is able to recover to the nominal voltage following the clearing of the fault, where as the FSG is not. The DFIG is able to recover to a nominal voltage due to its ability to produce the necessary reactive support in response to the fault. The FSG must rely on the capacitive support at the connector bus for the farm. In cases when the faults vary greatly FSGs may have difficulty in responding to all scenarios due to the rather static nature of capacitive support The DFIG can act independent of the capacitive support and allow the wind farm to ride through the fault and recover to a nominal voltage
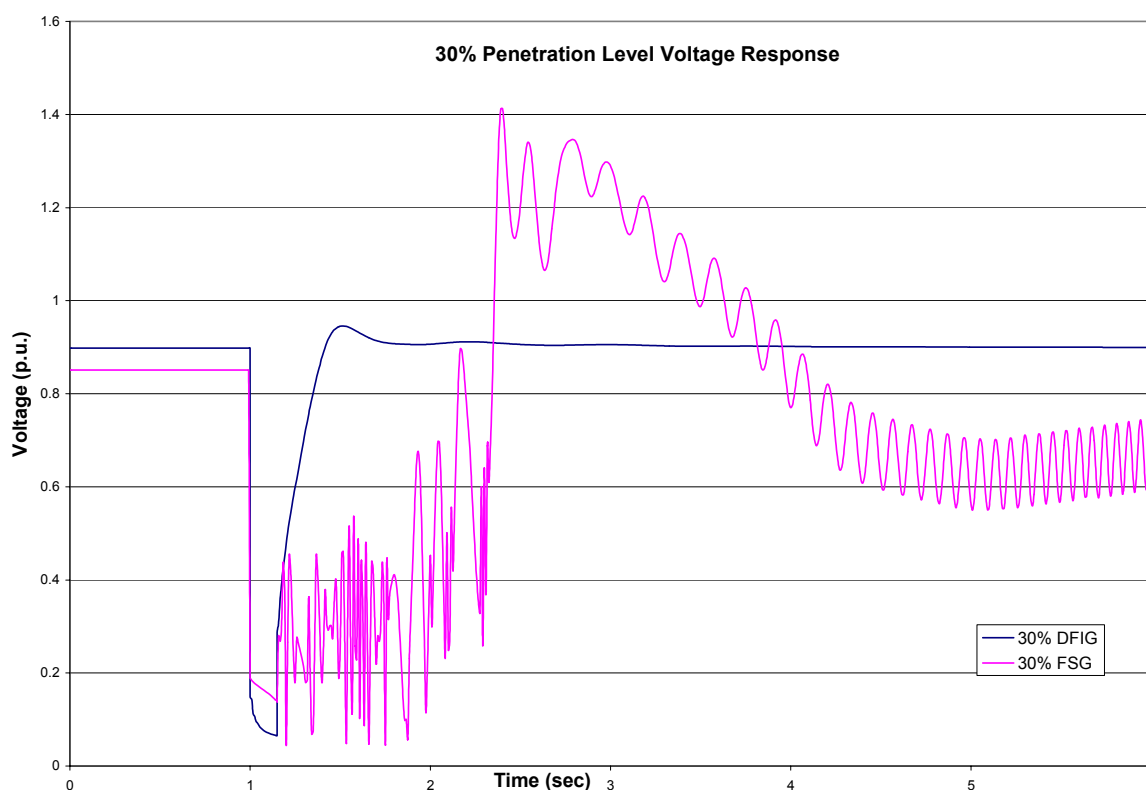
Figure 6.5: Voltage simulation with increased fault size

In general, adding DFIGs not only improves the terminal voltage response but the average bus voltages as well. This is directly due to the DFIG's ability to produce reactive power allowing for voltage control. In a strongly connected system, where maintaining appropriate voltage levels is greatly desired, DFIGs present a logical option for any new wind generation introduced to the system. Their ability to provide local voltage control along with improved steady-state voltages across the system may provide increased voltage support during contingency events. FSG turbines may cause voltage concerns if they are interconnected into the system. These simulations provide only the base characteristics of the FSG, a more complex model is required display the true nature of these turbines, however it can be readily observed that the larger the penetration level, the greater the recover following the faulting event. System operators must carefully consider the nature of the system and proceed accordingly based on the characteristics exhibited by both the DFIG and FSG.

DFIG and FSG Modeling in Eurostag and Comparison to PSS/E

The DFIG machine is Eurostag is present in the standard model library, following the instructions in the Eurostag tutorial, the turbine can be modeled in the test system [42]. This model exhibits the correct behavior during loss of generation events and was used in all simulations involving Eurostag.

The FSG model in Eurostag is represented in a similar manner that in PSS/E. An induction generator is coupled to a large mass representing the blades of the turbine. Like PSS/E this is a lumped mass model, and was the only model available for simulation. Inquiries should be made for FSG model availability for any future studies

The next set of simulations were completed in Eurostag. The results can be seen for a 15% and 30% penetration levels of DFIGs and FSGs in Figure 6.5 and 6.6. Similar to the results from PSS/E the case when the wind turbines are represented as FSGs shows an improved frequency response compared to the case where DFIGs are present. This is consistent with equation 5.1 and the concepts behind the issue of inertial response.
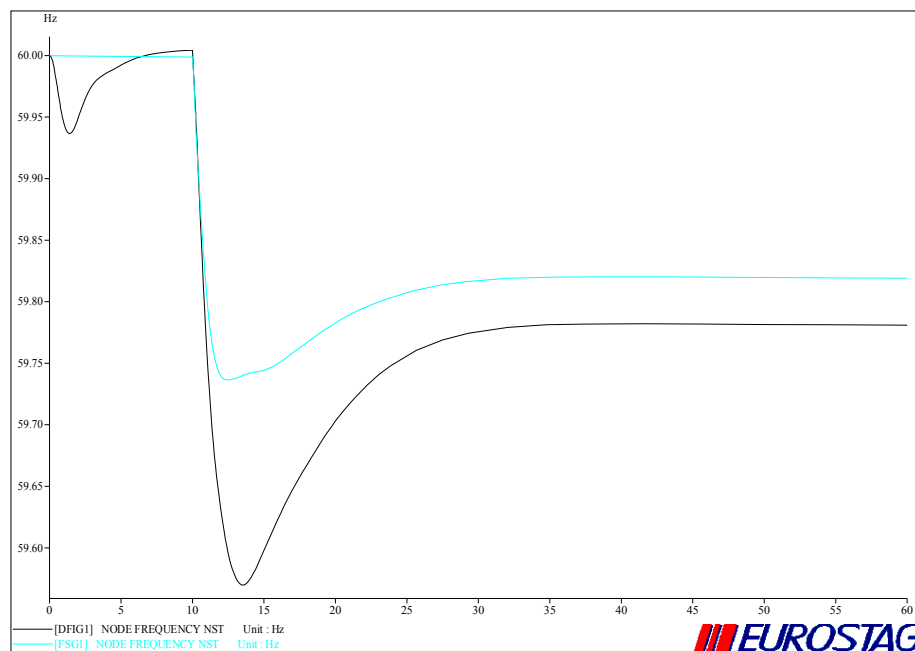
Figure 6.5: Frequency response plot for 15% penetration level for DFIG (Black) and FSG (Blue) from Eurostag.
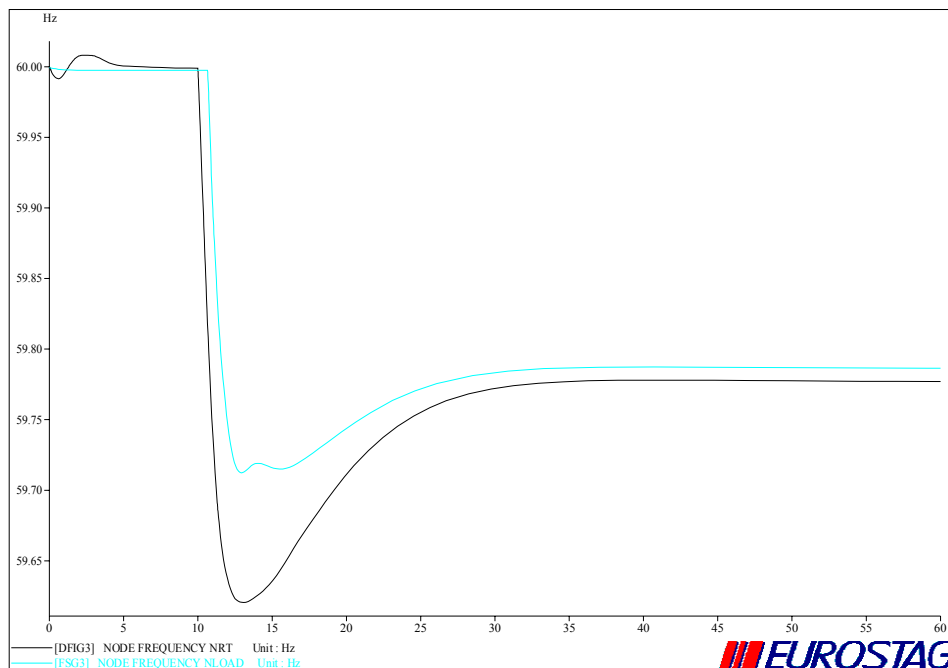
Figure 6.6: Frequency response simulations 30% penetration level for DFIG (Black) and FSG (Blue) from Eurostag.

Figure 6.7 shows the results of the 15% penetration simulation in Eurostag. The results are similar to the characteristics displayed in the PSS/E simulations; the FSG voltage is lower and takes slightly longer to recover to the pre-fault condition.
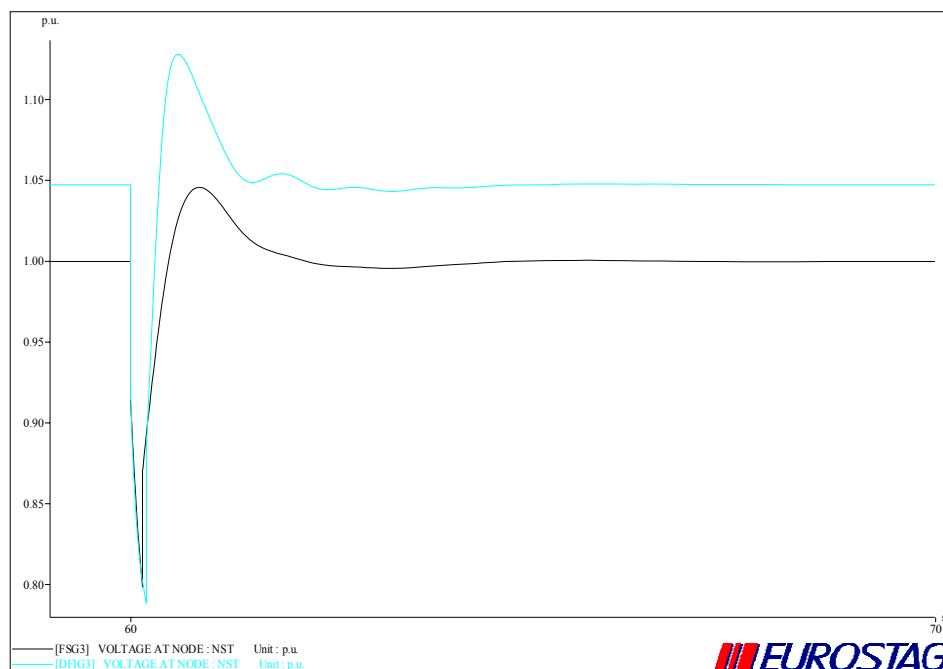
Figure 6.7: Voltage simulations at 15% penetration level in Eurostag.

The results provide similar results to those seen from PSS/E however the goal was not to analyze the differences in the results but what are the qualitative differences between the two programs. Both programs are useful tools in conducting dynamic simulations of power systems, however the size of the system is a large factor in choosing the appropriate software package. PSS/E is designed to accommodate large power systems that contain many thousand buses. For example, the system used in the static simulations in Chapter 3 was over 43,000 buses. With the appropriate dynamic data, dynamic studies can be completed on this in relatively short periods of time.

The main disadvantage of PSS/E arises in its ability to analyze the individual characteristic and individual components of the machines in the system. Many of the wind turbine models a considered proprietary software and it is very difficult to manipulate or alter the control systems in these turbines. Knowledge of Fortran is required to create user-models and can often be tedious process. However, many utilities use PSS/E to run simulations and

there is a vast database of models available for the users. These models are easily incorporated into PSS/E and require no conversion to a readable format. Since PSS/E is such a widely used program, the same model may not be available for Eurostag and often the PSS/E model must be converted into the equivalent Eurostag model. There is a feature in Eurostag that will try to determine the equivalent model, however if it fails, the model must be constructed manually.

A distinct difference between Eurostag and PSS/E is seen in the flexibility of the software; Eurostag is much more malleable and the machine models can be altered in detail, i.e. there is access to the control systems and increased interaction between machines and those control systems. Rather than using a programming language, the machines interact through the various control systems through the use of macro-blocks. This allows for combining various systems and machines in a much easier fashion compared to the rigid structure of PSS/E. This is advantageous when the user desires to explore individual characteristics of the machine or create their own control systems. Eurostag also allows for the easier extraction of simulation results. In PSS/E the desired observables, i.e, the system characteristics for study, must be pre-selected, Eurostag compiles all of the observables into a single output file. This output file is loaded into a separate post-processor program and does not require the user to pre-select the output channels. All the information from voltage to frequency is contained within this file. This is a particularly advantages feature when several values are wished to be observed.

A user must determine the appropriate software platform based on the characteristics of the system, what they wish to observe, and the length of the desired simulation. PSS/E is a preferable option if the system is large, i.e. many thousands of buses, and the simulation time is relatively short, with 2-3 minutes. Eurostag can be considered if the size of the system is small, under 100 buses, and can run longer simulations 5-10 minutes on the smaller system. Users may find Eurostag cumbersome and unwieldy if they wish to observe large systems. Overall, each program presents a differing set of advantages and disadvantages; the user must decide what needs to be observed and proceed on the selection based on the qualities presented here.

CHAPTER 7: CONCLUSION AND SCOPE FOR FUTURE WORK

Establishing fundamental basis and understanding of wind generation and turbines is crucial in future projects involved with wind. This thesis provided that foundation in first developing a systematic process to analyze an electricity system's static capability to accommodate large levels of wind generation. By identifying locations suited to support wind and completing the appropriate security studies a maximum level of MW injection was identified based the characteristics of the existing transmission system.

Second, it was able to assess the system's dynamic frequency response for two common types of turbines. Using a test system, insight can be provided for how the electricity system would respond in Iowa and across most of the United States; even with significant penetrations of wind generation the type of turbine will not greatly hinder the ability of system to respond to a load-generation imbalance. Since there is significant support and large losses of generation are very rare in the system wind turbines will most likely not have a significant impact on frequency in very short time frames. The challenge with will arise in the forecasting of wind in longer time horizons, i.e. load following and unit commitment. It will be crucial to accurately schedule conventional generation with the predicted levels of wind generation and develop strategies to respond to events when those predictions are off. Along with exploring wind forecasting, the voltage capabilities of the turbines should also be further explored. These two areas will provide critical information on how wind generation can be utilized fully in the future across the nation.

Static Assessment of Increased Wind Penetration

Overall, this thesis has provided an in-depth analysis of the steps required to integrate wind generation in a power system from both the static and dynamic aspects. Before beginning a static assessment of a power system under increased wind penetration levels several assumptions concerning the system must be made:

1. *Wind turbine MW output*: Wind turbine MW output is lower than its rating most of the time, a fact captured by 20-40% capacity factors. Estimation of wind farm MW generation levels for simulation studies may be based on probability densities of MW

generation levels of wind farms in the same region. In the absence of such data, assuming a 100% capacity factor is prudently conservative, since wind farms may generate at capacity from time to time. For steady-state analysis, one can avoid this issue by identifying maximum MW injection rather than maximum wind capacity.

2. *Wind turbine reactive capability*: DFIGs may produce or absorb reactive power and so may result in improved voltage control at the transmission level. FSG are generally required to install capacitors to bring substation power factor close to unity. These facts suggest assumption of 1.0 power factor is appropriate for steady-state analysis.

3. *Performance violations*: Complete steady-state analysis requires assessment of both thermal violations and voltage magnitude violations. A simplifying assumption eliminates assessment of voltage violations on the basis that they are generally less expensive to address than thermal violations.

4. *Loading*: Studying multiple loading scenarios is most rigorous, but time limitations often requires selection of only one or just a few. In the U.S., a summer peak loading scenario generally corresponds to most thermally stressed loading on the transmission system. During the winter season, however, wind speeds are generally at the highest, while the loading of the system is lower than in the summers. For steady-state analysis, where maximum MW injection is desired, a study based on a summer peak loading is most appropriate. Unit commitment patterns occurring during peak or off-peak conditions of one of the other three seasons may result in a different choice for dynamic analysis.

5. *Wind turbine type*: The type of wind turbine to be used needs to be assumed. Different models of turbines have different properties. This is especially important in deciding between an FSG and a DFIG. DFIGs have the ability to produce both active and reactive power, and there are several models where the power factor of the turbine can be controlled. The ability to provide reactive power support is not available in FSG wind turbines. The selection of turbine type will affect power system simulations in both steady-state and dynamic analyses. Recent trends suggest assuming all new wind turbines are DFIG is most appropriate.

6. *Interconnection voltage*: Interconnections of large-scale wind farms may occur at the lower transmission voltage levels, i.e., 69 to 230 kV, or at the higher voltage transmission

levels, i.e., 345 kV and above. The assumption on interconnection needs to be based on the overall goal of the utility or group installing the new wind generation. Connecting at lower voltages incurs lower interconnection costs; however, connecting at higher voltages will decrease losses and thus operational costs if the wind power is to be exported to distant load centers.

7. *Substation*s: It is important to decide whether the construction of new substations will be required to accommodate the new generation. Often an existing substation may be expanded to accommodate the new wind farms, incurring significant savings if the interconnection circuit length is not too long. A reasonable assumption is that existing substation will be utilized if the interconnection circuit length is less than 10 miles.

8. *Maximum MW injection per location:* One may assume a location's MW injection is limited only by the transmission system. However, this may be overly conservative. To account for the influence of economics on decisions to site wind farms, one may assume that wind farms will be developed only within a certain distance, e.g., 4 miles, of existing transmission. Such an assumption, together with typical wind farm land requirements, can provide reasonable upper bounds on MW injection per substation.

9. *Redispatch:* As wind penetration levels are increased, existing thermal generation must be redispatched to accommodate. Reasonable options here include the following:

    a. Local redispatch: Here, the assumption is the wind power is used to supply local load, displacing existing local generation.

    b. External redispatch: Here, the assumption is the wind power will be exported from the control area where it resides, displacing existing external generation. Here, one must identify the control areas that will import the wind power and the units within that control area that will be redispatched.

10. Key to either approach (a) or (b) is whether existing units will be decommitted or not. Steady-state analysis is affected by decommitment via the elimination of a unit's reactive supply. Dynamic analysis is affected by decommitment via this effect together with elimination of a unit's inertia.

The above assumptions provide the necessary information to begin a static analysis. To complete the analysis several steps need to be taken:

1. *Select study region*: First a study region needs to be defined. The study region will be the based on examining the wind patterns of the region. Generally, the areas with the highest average wind speeds are selected. This is often broken down into monthly, daily, and diurnal studies of average wind speeds. By determining where the wind speeds are consistently high, reliable locations for generation can be identified.

2. *Rank regions:* Wind generation is added systematically to the system by identifying the most economically attractive locations. This is done splitting the study region to ranked sections, based on average wind speed, proximity to existing transmission and finally the elevation of the site. Elevation is used as a ranking factor, due to the fact that areas of higher elevation have a correlation to higher wind speeds. This allows for two distinctions; first, by identifying substations in these sections an idea on the potential of the section to support the most productive wind farms is discerned. Second, it establishes a systematic queue of sections for adding wind generation into the system. By proceeding through the established queue, generation can be added to the system until all sections are exhausted. This portion of the analysis is completed using a power flow case of the system, modeled with the new wind generation. In considering the new wind injections, detailed contingency analyses should be completed along with the power flow analysis. These analyses can be completed using the appropriate power flow software platform.

3. *Local contingency analysis*: It is important to perform the contingency analysis on two levels; first, to examine the local thermal limits of the transmission due to increased generation at the new site. This contingency analysis will yield a result based on the constraints of circuits near new generation, usually 3 – 5 circuits away from the site of injection. The level of maximum penetration based on local limitations can be determined for all locations of new wind farms. Following the identification of this initial penetration level, a broader system-wide analysis can begin.

4. *System contingency analysis:* By looking at all of the transmission lines in a system, and determining those most significantly affected by all of the new wind generation, a more refined penetration level can be determined. In the case of this study, any transmission line loaded beyond 50% of its thermal limit that saw a 5% increase in loading as a result

of new wind generation, was designated a Significantly Affected Element (SAE). By using each SAE as an N-1 contingency event, wind generation is then stepped down until all violations are relieved. This allows for the identification of the maximum wind penetration level based on the thermal limits of the existing transmission system. It is should be noted that this penetration level is purely thermal, and does not attempt to relieve voltage violations by adjusting wind generation. This is based on the Assumption 3, that most voltage violations are easily relieved using capacitive correction.

Following these steps will allow for an in-depth assessment of a system's maximum wind penetration level based on thermal limitations. Static analysis will provide valuable insight into a system's limitations and which locations are suitable for new wind generation. Although the analysis process is very basic, significant work and planning must go into the static study. It is vital to incorporate all available information concerning system characteristics to wind patterns in order achieve the most accurate results. Based on these results, the study can move toward the dynamic assessment of wind turbines.

Using the process developed for a static assessment, an analysis of the 2008 MISO Summer base case was completed. This assessment showed that the under the existing transmission conditions the system could accommodate 1435 MW on new wind generation.

Dynamic Assessment of Turbine Types

In this thesis, the dynamic study was not completed on the same system used in the static analysis. Rather, the dynamic study provided a broader look at the phenomena associated with two particular turbine types, the Fixed Speed Generator wind turbine and the Doubly-Fed Induction Generator wind turbine. Frequency response to a loss of generation event was the main concern of this study, and as a result the concepts concerning inertial response were discussed in great detail. By establishing the fundamentals of the calculation of inertia in wind turbines, this thesis was able to assess how it could be utilized in a power system following a loss of generation event. Using a 6-bus test system a generalized set of characteristics associated with each turbine was developed for various operating conditions.

1. *Increased DFIG penetration:* DFIG penetration can both positively and negatively affect the system's frequency nadir during loss of generation events depending on how power balance is maintained in the system.

   a. *Generation Decommitment:* If as DFIG penetration grows, power balanced is maintain by decommiting existing conventional generation the system's frequency response will degrade due a reduction in the level of spinning inertia. Increased DFIG penetration will result in a lower nadir for the system's frequency for a loss of generation event.

   b. *Loading Increase:* If loading in the system is increased rather than decommiting generation as DFIG wind generation is introduced to the system, the system's frequency response will improve. This occurs since the system's inertia is preserved as new generation is added. The increased inertia allows for the frequency nadir to be arrested quicker and the minimum value reached during the loss of generation event is greater than the generation decommitment scenario.

2. *Increased FSG penetration:* FSG penetration will generally not negatively impact the system's frequency nadir during a loss of generation event.

   a. *Generation Decommitment:* Generation decommitment will not have the same impact on the system frequency if the wind penetration increases are completed using FSG wind turbines. The increased presence of inertia in these turbines will keep the frequency nearly constant as wind penetration increases in the system.

   b. *Loading Increase:* If the new wind generation is accommodated by increasing the system loading, the frequency response is improved as new wind generation is added to the system. The response is improved in comparison to the same penetration levels of DFIG wind turbines. Since the FSG turbines are now providing the system with inertia, the response is quicker in comparison with the DFIGs and the system is able to arrest the minimum frequency level.

Based on the results of the frequency analysis, the FSG turbine provides the greatest advantage to the power system in increasing its ability to responds to loss of generation events. The inertia that the FSG contributes to the system will benefit the frequency stability

and improve the response, however it should be noted that in conjunction with this improved response there would be a trade off in the system's voltage stability. By completing a dynamic voltage analysis the goal was to provide basic insight into what the two turbines contribute in terms of system voltage stability. From a voltage aspect the two turbines will act as follows:

1. *DFIG turbines:* DFIGs are capable of providing voltage support through a power electronics converter. In a strongly interconnected system, DFIGs will maintain or even improve the voltage levels during steady-state conditions. For dynamic simulations, the DFIG will provide a faster recovery to the pre-fault conditions and improved voltage levels at the buses across the system.

2. *FSG turbines:* FSGs have no available control schemes for voltage regulation and consume large levels of reactive power. As a result voltage levels are generally lower at system buses for steady-state conditions. Dynamic simulations show a slower response and degraded voltage outputs as the penetration levels of FSGs increase.

The idea behind this analysis was to establish what a system operator might give up in order to achieve an improved frequency response. The two turbines are not ideal, but understanding what is necessary to model the two turbines in power system will provide future user and system operators insight into incorporating wind generation into power systems.

Along with providing generalized assessment of turbine types, this thesis also detailed how to set up dynamic simulations in PSS/E and Eurostag. Using the appropriate dynamic models can greatly influence the results of the simulations and the proper steps and precautions must be taken to ensure the most accurate results. This thesis also detailed the advantages possessed by the two programs and the capability of each to handle large-scale simulations over varying periods of time.

Scope for Future Work

The scope for future work in the area of wind turbine analysis is vast and will become more important as increased levels of wind generation are introduced to the power system. In the case of this project, a dynamic study of the wind penetration level identified from the

static analysis needs to be completed. This will allow for a true assessment of the maximum penetration level of wind generation in Iowa and will show how the system's dynamic frequency response and voltage stability change for different types of turbines and at different penetration levels.

In today's market new wind installations are predominately DFIG. This will undoubtedly have an effect on the system's frequency response. Studies can be completed on the effects of generation decommitment and loading increases as the new wind generation is introduced into Iowa. Creating the controls necessary to emulate inertia on the DFIG can also provide another avenue for study in system planning studies. Also, other avenues of inertial support can be explored, such as fly-wheel mechanisms or inertial reserves.

Wind generation will be a vital source of energy in the years to come and completing these analyses will be invaluable in understanding the abilities and limitations of the wind turbine.

CHAPTER 8: BIBILOGRAPHY

[1] C. Buckley, N. Scott, H. Snodin, P. Gardner, *Review of Impacts of High Wind Penetration in Electricity Networks*, 2005 Garrad Hassan Pacific Pty Ltd.

[2] EnerNex Corp., *Final Report – 2006 Minnesota Wind Integration Study Volume I*, 2006 EnerNex Corporation

[3] AWEA, Projects, Document Retrieved, June 1, 2006 [Online] Available: http://www.awea.org/projects/

[4] M. Luther, U. Radtke, W. R. Winter, *Wind Power in the German Power System: Current Status and Future Challenges of Maintaining Quality of Supply*, Editor: T. Ackermann, 2005 *Wind Power in Power Systems*

[5] *Study into the Impacts of Increased Levels of Wind Penetration on the Irish Electricity System: First Interim Report*, 2002 Garrad Hassan International

[6] H. Holttinen, P. Meiborn, C. Ensslin, L. Hofmann, J. McCann, J. Pierik, J. O. Tande, E. Hagstrom, An Estanquerio, H. Amaris, L. Soder, G. Strbac, B. Parsons, *Design and Operation of Power Systems with Large Amounts of Wind Power Production*, IEA Wind Collaboration.

[7] T. Gray. *Wind Power Technology and Siting Issues*, 2005 Wind Powering America All-State Summit

[8] Iowa Energy Center, Renewable Energy and Energy Efficiency; Research, Education and Demonstration, *Iowa Wind Maps July and December*, Photos Retrieved, No Date, [Online] Available: http://www.energy.iastate.edu/Renewable/wind/maps-index.htm

[9] Iowa Energy Center, Renewable Energy and Energy Efficiency; Research, Education and Demonstration, *Wind Energy Manual*, Document Retrieved, No Date, [Online] Available: http://www.energy.iastate.edu/Renewable/wind/wem/windpower.htm

[10]   Rochester Public Utilities, *Power services—Wind power FAQs*. Document Retrieved, April 2007, [Online]. Available: http://www.rpu.org/your_home/power_services/wind_power/faq/

[11]   U.S. Department of Energy, Office of Energy Efficiency and Renewable Energy. *Landowners' frequently asked questions about wind development*, Document Retrieved August 14, 2003 [Online]. Available: http://www.eere.energy.gov/windandhydro/windpoweringamerica/pdfs/wpa/34600_landowners_faq.pdf

[12]   GE Power, *GE Wind Energy. WindVAR: Unique VAR control technology*. Document Retrieved, 2004 [Online]. Available: http://www.gepower.com/businesses/ge_wind_energy/en/downloads/ge_windvar_brochure.pdf

[13]   H. Knudsen and J. N. Nielsen, *Introduction to the Modeling of Wind Turines*, Editor: T. Ackermann, *Wind Power in Power Systems*, 2005

[14]   M.A. Yurdusev, R. Ata, N.S. Cetin, *Assessment of Optimum Tip Speed Ratio in Wind Turbines Using Artificial Neural Networks*, Energy Vol. 31, 2006

[15]   W.W. Price, J.J. Sanchez-Gasca, *Simplified Wind Turbine Generator Aerodynamic Models for Transient Stability Studies*, PSCE 2006

[16]   V. Akhmatov, H. Knudsen, A.H. Nielsen, *Advanced Simulation of Windmills n the Electric Power Supply*, Electrical Power and Energy Systems Vol. 22, 2000

[17]   P. Kundur, *Power System Stability and Control,* McGraw-Hill, Inc. New York, 1994

[18]   G. Lalor, A. Mullane, and M. O'Malley, *Frequency Control and Wind Turbine Technologies*, IEEE Transactions on Power Systems, VOL. 20, NO. 4, November, 2005

[19]   G. Ramtharan, J. B. Ekanayake, and N. Jenkins, *Frequency support from doubly fed induction generator wind turbines*, IET Renewable Power Generation, VOL. 1, Issue 1, March 2007

[20]   J. Morren, J. Pierik, S.W.H. de Haan, *Inertial response of variable speed wind turbines*, Electric Power Systems Research 76 pp. 980-987, 2006

[21]   T. Thiringer, A. Petersson, T. Petru, *Grid Disturbance Response of Wind Turbines Equipped with Induction Generator and Double Induction Generator*, Power Engineering Society General Meeting, 2003 Vol. 3

[22]   G. Lalor, J. Ritchies, S. Rourke, D. Flynn, M. O'Malley, *Dynamic Frequency Control with Increasing Wind Generation*, Power Engineering Society General Meeting, 2004

[23]   J. Morren, S.W.H. de Haan, W.L. Kling, J.A. Ferreira, *Wind Turbines Emulating Inertia and Supporting Primary Frequency Control*, IEEE Transactions on Power Systems, Vol. 21, No. 1, 2006

[24]   Z. Lin, G. Qingding, *Adjustable-Pitch and Variable-Speed Control of Wind Turbines Using Nonlinear Algorithm,* Sixth International Conference on Electrical Machines and Systems, Vol. 1, 2003

[25]   E. Muljadi, C.P. Butterfield, *Pitch-Controlled Variable-Speed Wind Turbine Generation,* IEEE Transactions on Industry Applications Vol. 37, No. 1, 2001

[26]   A. Petersson, T. Thiringer, L. Harnefors, T. Petru, *Modeling and Experimental Verification of Grid Interaction of a DFIG Wind Turbine*, IEEE Transactions on Energy Conversion, Vol. 20, No. 4, 2005

[27]   E. Hau, *Wind-turbines Fundamentals, Technologies, Application, Economics*, Spring Inc, New York, 2000

[28]   M. Kayikci, J.V. Milanovic, *Reactive Power Control Strategies for DFIG-Based Plants*, IEEE Transactions on Energy Conversion, Vol. 22, No. 2, 2007

[29]   J.G. Slootweg, H. Polinder, W.L.Kling, *Reduced-order Modeling of Wind Turbines,* Editor: T. Ackermann, *Wind Power in Power Systems*, 2005

[30]   P.M. Anderson, A.A. Fouad, *Power System Control and Stability*, Wiley-Interscience, Hoboken, 2003

[31]   B.J. Kirby, *Frequency Regulations Basics and Trends*, Oak Ridge National Laboratory, 2003

[32]   B. Parson, M. Milligan, *Grid Impacts of Wind Power Variability: Recent Assessments from a Variety of Utilities in the United States*, National Renewable Energy Laboratory, 2005

[33]   J.C. Smith, E.A. DeMeo, *Wind Power Impacts on Electric Power System Operating Costs: Summary and Perspective on Work to Date*, American Wind Energy Associated Global WindPower Conference 2003

[34]   R. Doherty, G. Lalor, M. O'Malley, *Frequency Control in Competitive Electricity Market Dispatch*, IEEE Transactions on Power Systems, Vol. 20, No. 3, 2005

[35]   B.C. Ummels, M. Gibescu, E. Pelgrum, W.L. Kling, A.J. Brand, *Impacts of Wind Power on Thermal Generation Unit Commitment and Dispatch*, IEEE Transactions on Energy Conversion, Vol. 22, No. 1, 2007

[36]   GE Energy, *GE 1.5 Brochure*, Document Retrieved, September 2005 [Online] Available:

http://www.gepower.com/prod_serv/products/wind_turbines/en/downloads/ge_15_brochure.pdf

[37]   Vestas, *Vestas V52 Brochure*, Document Retrieved, September 2007 [Online] Available:

http://www.vestas.com/Admin/Public/DWSDownload.aspx?File=%2fFiles%2fFiler%2fEN%2fBrochures%2fproductbrochureV52_UK.pdf

[38]   Email conversation with GE Representative, November 11, 2007

[39]   *CIMTR1 Datasheet*, Appendix E, Program Operations Manual Vol. II, PSS/E, 2005

[40]   *Models CIMTR1 and CIMTR3*, Program Applications Guide Vol. II, PSS/E, 2005

[41]   Federal Energy Regulatory Commission, *FERC Order No. 661-A, Interconnection of Wind Energy,* Document Retrieved, December 12, 2005 [Online] Available:
http://www.ferc.gov/EventCalendar/Files/20051212171744-RM05-4-001.pdf

[42]   Eurostag, *Eurostag Tutorial*, Tractebel Engineering, Belgium. 2005

APPENDIX A: STEP 1 ANALYSIS (LOCAL LIMITING CONTINGENCIES)

Case	Wind Region	Substation	MEC ΔP (MW)	AE ΔP (MW)	Contingency		Limiting Branch		MEC Export (MW)	AE Export (MW)
					From	To	From	To		
A	67	ALLNDRF 69kV (34892)	0	40	ALLNDRF 69kV (34892)	SIBLEY 69kV (34893)	TRIBOJI8 69KV (34136)	FLYCLD8 69kV (34906)	-343	-259
B	65/64	MILFRDJ8 69kV (63732)	20	-	TRIBOJI8 69kV (34136)	MILFRDJ8 69kV (63732)	WISDOM8 69kV (63710)	MILFRDJ8 69kV (63732)	-323	-259
		MONTGMY8 69kV (34300)	-	20	MONTGMY8 69kV (34300)	FR LK TP 69kV (62876)	MONTGMY8 69kV (34300)	NEWPRAG8 69kV (34301)	-323	-239
		ORLEANS8 69kV (34689)	-	20	-	-	TRIBOJI8 69kV (34136)	ALLNDRF 69kV (34892)	-323	-219
					-	-	ORLEANS8 69kV (34689)	ORLNTAP8 69kV (34690)	-323	-219
		WAHPETN8 69kV (34681)	-	20	-	-	TRIBOJI8 69kV (34136)	ORLNTAP8 69kV (34690)	-323	-199
		CBBOSWT8 (34538)	-	25	-	-	CBBOSWT8 (34538)	MNTGMY8 (34692)	-323	-174
C	62	GEORGE 8 69kV (34540)	-	30	-	-	GEORGE 8 69kV (34540)	SHELDON8 69kV (64033)	-323	-144
D	60	HOSPERS8 69kV (63947)	10	0	RCKVALY8 69kV (64023)	SHELDON8 69kV (64033)	HOSPERS8 69kV (63947)	L1SXCTR8 69kV (66589)	-313	-144
		SHELDON8 69kV (64033)	75	0					-238	-144
E	51	CARROLL 69KV (63900)	50	0	ARISTAP8 (34650)	CRESTN8 (34653)	LORIMRR8 (34585)	SLAKEN 8 (34588)	-188	-144
		CARROLL 161KV (63901)	50	0	ARISTAP8 (34650)	CRESTN8 (34653)	LORIMRR8 (34585)	SLAKEN 8 (34588)	-138	-144
F	50	BVISTA 161 kV (63906)	50	-	-	-	HOSPERS8 (63947)	L1SXCTR8 (66589)	-88	-144
		Storm Lake North (64038)	50	-	-	-	HOSPERS8 (63947)	L1SXCTR8 (66589)	-38	-144
		LT SX 5 (63892)	50	-	LT SX 5 161kV (63892)	J3COVEY8 69kV (67125)	LT SX 5 161kV (63892)	LT MID 8 69kV (64617)	12	-144
		LT SX 8 (63893)	50	-					62	-144
		Rock Valley (64023)	50	-	-	-	HOSPERS8 (63947)	L1SXCTR8 (66589)	112	-144
		SAC 69kV (63910)	50	-	-	-	HOSPERS8 (63947)	L1SXCTR8 (66589)	162	-144
		SAC 161kV (63911)	50	-	-	-	HOSPERS8 (63947)	L1SXCTR8 (66589)	212	-144
G	44	LEMARST5 161kV (64000)	50	-	LT SX 5 161kV (63892)	LEMARST5 161kV (64000)	SAC 5 161kV (63908)	SACWIND5 161kV (63910)	262	-144
		LEMARS 5 161kV (64001)	50	-					312	-144
		LEMARS 8 69kV (64002)	50	-	-	-	LEMARST5 64000	LEMARS 5 161kV 64001	362	-144
		SAC CITY (64625)	50	-					412	-144
H	39	Summit Lake North (34588)	-	30	-	-	ARISTAP8 (34650)	CRESTN8 (34653)	412	-94
I	32	St. Ansgar (34367)	-	45	ADAMS 8 (34306)	N88INTER (34369)	GRAFTNT8 (34364)	STANSGR8 (34367)	412	-49

J	31	Garner Map Co. (34667)	-	15	-	-	GARNER 8 (34669)	HANCOCK8 (63727)	412	-34
		Klemme (34671)	-	15	GRRIVER8 (34643)	ELLSTNR8 (34644)	ARISTAP8 (34650)	CRESTN8 (34653)	412	-19
K	29	Williams Bros. (63759)	40	-	SWEAZY (63726)	WILLIAM8 (63759)	WILLIAM8 (63759)	WALL LK8 (64313)	452	-19
		Clarion (64223)	70	-	-	-	CLARION8 (64223)	ROWAN8 (64244)	522	-19
L	26	Wheeler Wood (34400)	-	5	-	-	HANLNTN8 (34376)	MT VALLE (69000)	522	-14
		Armour (34664)	-	15	-	-	GARNER 8 (34669)	HANCOCK8 (63727)	522	1
		Portland (34913)	-	10	-	-	HANLNTN8 (34376)	MT VALLE (69000)	522	11
M	23	Emmetsburg (64240)	15	-	-	-	HANLNTN8 (34376)	MT VALLE (69000)	537	11
		Emmetsburg East (64247)	5	-	-	-	HANLNTN8 (34376)	MT VALLE (69000)	542	11
N	20	Rudd Jct. (34412)	-	20	STANSGJ8 (34368)	DOUGLST8 (34374)	ADAMS 8 (34306)	N88INTER (34369)	542	31
O	18	Alden (34285)	-	25			GARNER 8 (34669)	HANCOCK8 (63727)	542	46
P	15	Sub B (64210)	50	-	TWNLAK (63773)	SB MFD8 (64211)	SB BFD8 (64210)	HAYES8 (64241)	592	46
		Sub M (64211)	30	-	-	-	SB BFD8 64209	HAYES8 (64241)	622	46
Q	14	Hampton 69kV (63730)	15	-	-	-	HANLNTN8 (34376)	MT VALLE (69000)	637	46
		Hampton 161kV (63731)	15	-	-	-	HANLNTN8 (34376)	MT VALLE (69000)	652	46
R	13	Elmore (34263)	-	15	-	-	BUFFCTR8 (34363)	WINNCO (69010)	652	61
		Humboldt Cent. (64225)	20	-	HUMBLTE8 (64226)	THOR8 (64238)	HOPE 8 (63720)	HMBLTTP8 (64224)	672	61
		Humbodlt East (64225)	20	-	HUMBLTE8 (64226)	THOR8 (64238)	HOPE 8 (63720)	HMBLTTP8 (64224)	692	61
S	8	Wall Lake 69kV (64312)	100	-	-	-	SWEAZY 63726	WILLIAM8 (63759)	792	61
		Wall Lake 161kV (64313)	100	-	-	-	WILLMSN8 (63729)	WALL LK8 (64313)	892	61
T	7	Tripoli (34435)	-	15	DONLDSN8 (34437)	OELWEIN8 (34438)	FRDBRGM8 (34434)	TRIPOLI8 (34435)	892	76
		Readlyn (34436)	-	15	-	-	DONLDSN8 (34437)	ORAN 8 (34456)	892	91

APPENDIX B: MEC ANALYSIS STEP 2 (SYSTEM LIMITING CONTINGENCIES)

Bus No.	Name	Bus No.	Name	Base Loading	Line Rating	Base Case Loading (%)	Case T Increase (MW)	Case T Loading (%)	Violation	Solution
34016	EMERY 5	64252	FLOYD 5	112.6	238	47.3	24.4	0.575630252	34376-69000	-5 MW @ 34400
34054	GR JCT 5	63771	DRAGER 5	9.1	165	5.5	79.2	0.535151515	None	-
34540	GEORGE 8	64033	SHELDON8	3.2	40	8	30.4	0.84	Bus Islanded	-
34669	GARNER 8	63727	HANCOCK8	15.1	28	54	11.4	0.946428571	Bus Islanded	-
63715	STM LKJ8	63907	BVISTA 8	8.3	36	23	14.1	0.622222222	None	-
63726	SWEAZY	63759	WILLIAM8	4.6	41	11.3	32.6	0.907317073	63726-64313	-20 MW @ 64313
63729	WILLMSN8	63731	HAMPTON8	3	41	7.4	20.1	0.563414634	None	-
63729	WILLMSN8	64313	WALL LK8	10.9	41	26.5	25.2	0.880487805	None	-
63734	WELSBRG8	63759	WILLIAM8	9.6	41	23.4	19.9	0.719512195	63726-63759	-30 MW @ 64313
63759	WILLIAM8	64313	WALL LK8	11	41	26.9	10.5	0.524390244	63734-63759	-20 MW @ 64210 -15 MW @ 64211
63771	DRAGER 5	63900	CARROLL5	24	165	14.6	79.1	0.624848485	Bus Islanded	-
63800	CBLUFFS3	65356	S3456 3	510.6	956	53.4	114.6	0.653974895	None	-
63889	PLYMOTH5	64000	LEMARST5	115.7	223	51.9	13.1	0.577578475	None	-
63893	LT SX 8	66593	J4IDAGR8	3.4	41	8.4	17.8	0.517073171	None	-
63893	LT SX 8	66597	J7PANMA8	5.9	41	14.3	18.4	0.592682927	None	-
63893	LT SX 8	67125	J3COVEY8	11.8	41	28.7	16.2	0.682926829	None	-
63908	SAC 5	63910	SACWIND5	56.5	170	33.3	61.4	0.693529412	None	-
63947	HOSPERS8	64033	SHELDON8	8.7	41	21.2	20.9	0.72195122	None	-
63947	HOSPERS8	66589	L1SXCTR8	12.7	41	31.1	20.7	0.814634146	None	-
64209	SB KFD8	64241	HAYES8	26.1	71	36.8	30.3	0.794366197	None	-
64220	WRIGHT 5	64312	WALL LK5	15.8	167	9.5	80.1	0.574251497	63729-64313	-20 MW @ 64313
64223	CLARION8	64244	ROWAN8	15.4	41	37.7	7.4	0.556097561	None	-
64224	HMBLTTP8	64226	HUMBLTE8	11.2	30	37.2	7.3	0.616666667	None	-
64239	FRANKLN5	64285	BUTLER 5	39.8	181	22	67.9	0.595027624	None	-
64239	FRANKLN5	64312	WALL LK5	22	167	13.2	63.4	0.511377246	None	-
64256	UNIONTP5	64285	BUTLER 5	32.9	181	18.2	68	0.557458564	None	-
64312	WALL LK5	64313	WALL LK8	21.4	83	25.8	27.5	0.589156627	None	-
64360	SB PIC 5	64662	PIC MID8	0	74	0	39.9	0.539189189	Bus Islanded	-
64363	SB PIC 8	64373	CORVL12G	0	37	0	19.9	0.537837838	Bus Islanded	-
64363	SB PIC 8	64374	CORVL34G	0	37	0	19.9	0.537837838	Bus Islanded	-
64363	SB PIC 8	64662	PIC MID8	0	74	0	39.9	0.539189189	Bus Islanded	-

APPENDIX B: AE ANALYSIS STEP 2 (SYSTEM LIMITING CONTINGENCIES)

Bus No.	Name	Bus No.	Name	Base Loading	Line Rating	Base Case Loading (%)	Case T Increase (MW)	Case T Loading (%)	Violation	Solution
34000	NIW 5	34010	HAYWARD5	58.9	200	29.4	44	0.5145	34376-69000	+25 MW @ 34285
34015	LIME CK5	34016	EMERY 5	85.3	200	42.6	50.3	0.678	None	-
34015	LIME CK5	34572	ADAMS_S5	49.1	194	25.3	50.4	0.512886598	None	-
34016	EMERY 5	64252	FLOYD 5	112.6	238	47.3	24.4	0.575630252	None	-
34020	HAZL S 5	34135	DUNDEE 5	59.5	167	35.6	25.9	0.511377246	None	-
34021	LANSINGW	69523	GENOA 5	133	223	59.7	18.8	0.680717489	None	-
34051	TOLEDO 7	34066	M-TOWN 7	36.5	77	47.5	6.9	0.563636364	None	-
34054	GR JCT 5	63771	DRAGER 5	9.1	165	5.5	79.2	0.535151515	None	-
34136	TRIBOJI8	34137	TRIBOJI5	44	84	52.3	7.9	0.617857143	Bus Islanded	-
34136	TRIBOJI8	34692	MNTGMY8	16.8	40	42	19.6	0.91	None	-
34200	CNTRVIL8	34573	N CENT8	30.8	48	64.2	2.6	0.695833333	None	-
34248	TRUMANM8	34249	TRUMAN 8	25.8	47	54.9	3.3	0.619148936	None	-
34248	TRUMANM8	34280	TRUMANT8	28.7	47	61	3.2	0.678723404	None	-
34250	LEWISVL8	62802	MADELIA	21.1	47	45	3.1	0.514893617	None	-
34280	TRUMANT8	61934	RUTLAND	31.6	36	87.8	3.3	0.969444444	None	-
34300	MONTGMY8	34301	NEWPRAG8	4.6	36	12.7	22.8	0.761111111	None	-
34301	NEWPRAG8	60936	NPRAG2T8	3.1	35	8.9	16.9	0.571428571	None	-
34306	ADAMS 8	34369	N88INTER	9.1	44	20.7	32	0.934090909	34270-34374	-40 MW @ 34367
34364	GRAFTNT8	34367	STANSGR8	3.3	47	7	28.7	0.680851064	None	-
34364	GRAFTNT8	34368	STANSGJ8	2.2	47	4.7	28.7	0.657446809	None	-
34367	STANSGR8	34369	N88INTER	9.1	47	19.4	32.1	0.876595745	None	-
34368	STANSGJ8	34374	DOUGLST8	3.3	47	7.1	42.9	0.982978723	34306-34369	-25 MW @ 64033
34370	RICEVIL8	34371	RICE 8	8.1	54	15.1	33.9	0.777777778	None	-
34370	RICEVIL8	34374	DOUGLST8	4.3	47	9.2	40.8	0.959574468	34306-34369	NONE
34376	HANLNTN8	69000	MT VALLE	19.2	25	76.9	4.9	0.964	Bus Islanded	-
34384	MCARMOR8	34396	EMERY N8	39.7	51	77.8	4.2	0.860784314	None	-
34540	GEORGE 8	64033	SHELDON8	3.2	40	8	30.4	0.84	Bus Islanded	-
34570	ADAMS_N5	69547	ROCHSTR5	68.4	200	34.2	33.8	0.511	None	-
34585	LORIMRR8	34588	SLAKEN 8	23.2	24	96.8	3.4	1.108333333	34650-34653	-30 MW @ 34588
34592	SLAKES 8	66569	CRESTON8	30.6	72	42.5	13	0.605555556	34585-34588	NONE
34650	ARISTAP8	34653	CRESTN8_	21.6	24	90.2	1.9	0.979166667	34643-34644	NONE
34669	GARNER 8	63727	HANCOCK8	15.1	28	54	11.4	0.946428571	None	-
34722	IOWA JCT	34723	SHARON T	21.1	40	52.7	2.8	0.5975	None	-

APPENDIX C: QUEUED GENERATION IDENTIFICATION

MISO Queue Num	MISO Queue Date	In Service Date*	Control Area	Wind Region	County	Max Summer Output ** (MW)	Study Limit ** (MW)
37061-02	11-Feb-03	31-Dec-06	ALTW	64/65	Dickenson	194	105
37404-01	29-May-02	15-Dec-03	ALTW	64/65	Dickinson		
38572-01	08-Aug-05	01-Oct-06	ALTW	64/65	Dickinson		
38595-01	31-Aug-05	31-Dec-06	MEC	51/59	Carroll	150	100
38708-03	22-Dec-05	31-Dec-07	MEC	51/59	Carroll		
37869-01	15-Jul-04		DPC	27/37	Winnebago	19.8	-
39014-01	24-Oct-06	31-Dec-10	ALTW	27/37	Winnebago	200	-
38862-01	25-May-06	01-Mar-08	ALTW	24/34/38	Mitchell	20	20
39063-03	12-Dec-06	01-Oct-10	ALTW	20/34/38	Howard and Mitchell	150	20
38695-01	09-Dec-05	01-Oct-06	ALTW	14/18	Franklin	200	55
38695-02	09-Dec-05	30-Sep-07	ALTW	14/18	Franklin		
38695-03	09-Dec-05	01-Oct-06	ALTW	14/18	Franklin		
37844-01	11-Aug-03	01-Jun-04	WAUE	60	O'Brian	150	85
38618-01	23-Sep-05	01-Oct-07	MEC	51	Crawford	34	100
38842-02	05-May-06	01-Oct-08	WAUE	51	Crawford		
37680-02	28-Feb-03	01-Dec-04	MEC	50	Buena Vista/Sac	661	350
37722-03	11-Apr-03	01-Dec-07	MEC	50	Pocahontas		
38616-01	21-Sep-05	30-Dec-06	MEC	50	Palo Alto		
38617-01	22-Sep-05	01-Dec-06	MEC	50	Pocahontas		
38946-01	17-Aug-06	31-Aug-11	CBPC	50	Palo Alto		
38623-01	28-Sep-05	01-Aug-06	ALTW	42	Emmet	50.4	-
36730-01	23-Jul-00	31-Dec-07	ALTW	32	Worth	280	45
38612-02	17-Sep-05	31-Dec-06	ALTW	32	Worth		
37698-01	18-Mar-03	01-Oct-03	ALTW	31	Cerro Gordo	88	30
38596-01	01-Sep-05	31-Dec-07	ALTW	31	Worth		
36770-01	01-Sep-00	01-Apr-01	ALTW	29	Hancock	430	110
37232-03	07-Dec-01	01-May-03	MEC	29	Wright		
38324-01	03-Dec-04	31-Dec-06	MEC	29	Wright		
38761-01	13-Feb-06	30-Jul-07	ALTW	29	Hancock		
38622-01	27-Sep-05	01-Sep-07	ALTW	20	Howard	176	20
39063-02	12-Dec-06	01-Oct-09	ALTW	20	Howard		
38518-01	15-Jun-05	01-Sep-06	ALTW	5	Greene	164	-
38957-01	28-Aug-06	01-Oct-07	ALTW	5	Guthrie		
38796-01	20-Mar-06	31-Aug-07	ALTW	2	Story	150	-

*The in service date represents the date originally proposed to have the generation installed. However, in the 2008 base case these projects are not yet in service.
** Entries highlighted in yellow are wind regions for which the proposed wind generation exceeds the capacity as identified in this study.